Investigating ASC-αSynuclein complex-triggered inflammatory responses in murine microglia

Karan Thakur

A thesis submitted to the University of Ottawa
in partial fulfillment of the requirements for the
Master's degree in Neuroscience

Department of Cellular and Molecular Medicine
Faculty of Medicine
University of Ottawa

ABSTRACT

Neuroinflammation is a fundamental hallmark of several chronic neurodegenerative diseases, including Parkinson's disease (PD), and is closely associated with microglial activation. PD is characterized by the progressive loss of dopaminergic neurons in the substantia nigra and the accumulation of misfolded α-synuclein (αSyn) protein aggregates in surviving neurons. A key signaling mechanism that activates chronic inflammation is based on NLRP3 inflammasome activation, which can occur via aggregated forms of amyloid-β (Aβ) and αSyn. The inflammasome adaptor protein, ASC, has an intrinsic ability to oligomerize and, upon cell death, is released as specks into the extracellular space. These ASC specks are recognized by microglia as 'danger signals', thereby driving inflammation and neurodegeneration. Recent evidence has suggested that extracellular ASC specks can bind Aβ, and that the internalization of ASC-Aβ complexes by microglia results in the amplification and perpetuation of pro-inflammatory responses. Moreover, studies on human samples and preclinical animal models of PD have established a link between αSyn aggregation, microglial NLRP3 inflammasome activation and neuronal cell death. However, the underlying molecular mechanisms that perpetuate chronic inflammatory responses are incompletely understood. In this study, I produced ASC-αSyn complexes and evaluated their effects on NLRP3 inflammasome activation using a mouse SIM-A9 microglial cell culture model. Examination of electron microscopic images revealed that αSyn was found in close proximity and clustered around ASC fibrils. I further demonstrated that ASC-αSyn complexes were capable of activating the NLRP3 inflammasome to a greater extent than ASC or αSyn alone. This was determined by an increased expression of the NLRP3 sensor at the protein level, augmentation of ASC speck formation and activation of caspase-1. In addition, ASC-αSyn

complexes triggered caspase-1-dependent interleukin (IL)-1β/IL-18 processing by SIM-A9 cells, resulting in increased release of IL-1β and IL-18 into their conditioned media. This study links ASC and αSyn to mechanisms that amplify pro-inflammatory responses, thereby promoting a state of chronic inflammation. Overall, these results reveal a role for ASC specks in perpetuating inflammation and point at the possible importance of ASC-αSyn complexes, as triggers, in the propagation and exacerbation of αSyn-linked pathology.

ACKNOWLEDGEMENTS

I would like to express my sincere gratitude to my supervisor, Dr. Jagdeep K. Sandhu, and co-supervisor, Dr. Michael Schlossmacher, for providing an opportunity to fulfill my dreams and allowing me to carry out this ambitious project. Your consistent guidance and unwavering support have encouraged me to be the best version of myself as a human and scientist throughout my Master's study, which was a challenging time in my personal life. To my thesis advisory committee, Drs. Wandong Zhang, Edana Cassol, and Hsiao-Huei Chen, thank you for providing insight as to how to improve my research and widen my perspectives.

To Dr. Christine Péladeau Ladouceur, your supervision and mentorship has been of immeasurable help from providing project suggestions to teaching me important techniques. Thank you for being patient with me since the start of my graduate studies and always being available for me. This project would not have been completed without your guidance.

To everyone at the Sandhu and Schlossmacher labs, thank you for your generosity and support in numerous ways to my make experience worthwhile. Each day was gratifying due to your presence.

To my mother and father, Swatiben and Jitendrakumar, I have the utmost gratitude for the values you have instilled in me and the life you have provided for me. I've had the opportunity to live out the dreams that you had, and I hope I have made you proud and continue to do so. You taught me to walk so one day I can run.

I would also like to deeply thank the following people for their contributions to this thesis. Michel Menard (National Research Council Canada; NRC) generously provided a vial of mouse SIM-A9 microglial cells. Dr. David Cai (University of Ottawa and NRC) produced human

recombinant ASC and supplied a substantial amount for the experiments performed in this thesis. Melisa Hewitt (NRC) assisted in the initial characterization and culturing of the SIM-A9 cells. Dr. Jyh-Yeuan (Eric) Lee (University of Ottawa) kindly allowed Dr. Péladeau Ladouceur and I to use his laboratory to prepare samples for EM. Dr. Martin Couillard (NRC) and the TEM Core Facility (University of Ottawa) allowed Dr. Péladeau Ladouceur and I to use their facilities and aided with some EM imaging. Dr. Gerard Agbayani (NRC) helped to perform the multiplex experiments. Klaudia Baumann (NRC) assisted with confocal microscopy imaging. Simple Western immunoassay experiments were performed by Ewa Baumann (NRC). All preparation of samples, data compilation and analysis were performed by me.

Thank you to the funders of this work, the Faculty of Medicine at the University of Ottawa, NRC Graduate Program, and Ontario Graduate Scholarship (OGS) Program. Your commitment to supporting trainees and research is commendable and deeply appreciated.

Lastly, I'd like to share a quote that has embodied my life and career: "He, who has a why to live, can bear almost any how" by Friedrich Nietzsche. This is a testament to demonstrating resiliency and perseveration during difficult times and underscores the importance of discovering a compelling reason to navigate the challenges we face in life.

TABLE OF CONTENTS

LIST OF ABBREVIATIONS

3D	Three-dimensional
AD	Alzheimer's disease
ANOVA	Analysis of variance
ASC	Apoptosis-associated speck-like protein containing a CARD
αSyn	Alpha-synuclein
ATP	Adenosine triphosphate
Aβ	Amyloid-β
BCA	Bicinchoninic acid
BSA	Bovine serum albumin
CARD	Caspase activation and recruitment domain
CCL	C-C motif ligand
CD68	Cluster of differentiation 68
CD8	Cluster of differentiation 8
CNS	Central nervous system
CO_2	Carbon dioxide
CXCL	C-X-C motif ligand
DAMP	Damage-associated molecular pattern
DC	Detergent compatible
DC	Dendritic cell
dH_2O	Distilled water

DMEM/F12	Dulbecco's modified Eagle's medium/Ham's F12
DMSO	Dimethylsulfoxide
DNA	Deoxyribonucleic acid
DPBS	Dulbecco's phosphate buffered saline
ELISA	Enzyme-linked immunosorbent assay
EM	Electron microscopy
F-actin	Filamentous actin
FAM	Carboxyfluorescein
FBS	Fetal bovine serum
FLICA	Fluorescent-labeled inhibitor of caspases
FMK	Fluoromethyl ketone
GFAP	Glial fibrillary acidic protein
GSDMD	Gasdermin D
h	Hour
H_2SO_4	Sulfuric acid
HFIP	1,1,1,3,3,3-Hexafluoro-2-propanol
hiPSC	Human induced pluripotent stem cell
His	Histidine
HRP	Horseradish peroxidase
IB	Immunoblotting
Iba-1	Ionized calcium-binding adapter molecule 1
ICC	Immunocytochemistry

IFN	Interferon
IL	Interleukin
IL-1R	IL-1 receptor
IP-10	IFNγ-induced protein 10
IPTG	Isopropyl β-D-1-thiogalactopyranoside
KC	C-X-C motif ligand 1
kDa	Kilodalton
LDH	Lactate dehydrogenase
LPS	Lipopolysaccharide
LRR	Leucine-rich repeat
MAP2	Microtubule-associated protein 2
MCP-1	Monocyte chemoattractant protein 1
min	Minutes
MIP-2	Macrophage inflammatory protein 2
mQH_2O	MilliQ water
MYD88	Myeloid differentiation primary response gene 88
N-GSDMD	N-terminal GSDMD
NAC	Non-amyloid-β-component
NACHT	NAIP, CIITA, HET-E and TP1
NAMP	Neurodegeneration-associated molecular pattern
NF-κB	Nuclear factor kappa-light-chain-enhancer of activated B cells
NK	Natural killer

NLR	NOD-like receptor
NLRP3	NLR family, pyrin domain containing 3
NOD	Nucleotide-binding oligomerization domain
NRC	National Research Council Canada
O/N	Overnight
P-S	Penicillin-streptomycin
p10	10 kDa subunit of Caspase-1
p20	20 kDa subunit of Caspase-1
PAMP	Pathogen-associated molecular pattern
PBS	Phosphate buffered saline
PD	Parkinson's disease
PDL	Poly-D-lysine
PE	Phycoerythrin
PFA	Paraformaldehyde
PFD	Pore-forming domain
PFF	Pre-formed fibril
PI	Protease/phosphatase inhibitor
PRR	Pattern recognition receptor
PVDF	Polyvinylidene difluoride
PYD	Pyrin domain
RA	Rheumatoid arthritis
RANTES	Regulated on activation, normal T cell expressed and secreted

RD	Repressor domain
RGB	Red, green and blue
RIPA	Radioimmunoprecipitation buffer
ROS	Reactive oxygen species
rpm	Revolutions per minute
RT	Room temperature
SDS	Sodium dodecyl sulfate
SDS-PAGE	SDS-polyacrylamide gel electrophoresis
SEC	Size-exclusion chromatography
SEM	Standard error of mean
SMOC	Supramolecular organizing centre
SNCA	Alpha synuclein gene
SN	Substantia nigra
SNpc	Substantia nigra pars compacta
TBS	Tris-buffered saline
TBS-T	Tris-buffered saline containing Tween
TDP-43	Transactive response DNA binding protein 43
TEM	Transmission electron microscope
Th	T helper
TLR	Toll-like receptor
TMB	3, 3', 5, 5'-tetramethylbenzidine
TNF-α	Tumour necrosis factor-alpha

TRIF	TIR-domain-containing adapter inducing interferon-β
UT ctrl	Untreated control

LIST OF FIGURES

LIST OF TABLES

1. INTRODUCTION

1.1 Parkinson's disease

Parkinson's disease (PD) is the world's second most prevalent neurodegenerative disease, affecting 2-3% of the population aged over 65 years (1). Neurological disorders are currently the leading source of disability around the world and PD is the fastest growing of these disorders in age-standardized rates of prevalence, disability, and deaths (2). Triggered by aging populations, increasing longevity, and the by-products of industrialization, PD prevalence and incidence are dramatically increasing and have been termed the "Parkinson pandemic" (3). PD is clinically characterized by several motor symptoms, such as bradykinesia, rigidity, tremors, and with progression, postural instability. However, non-motor signs, such as sleep disorders, hyposmia, neuropsychiatric symptoms, cognitive impairment, and pain are also present and may occur prior to the onset of motor features, contributing to its overall disability (4,5). While the cause of PD remains unknown, the risk of developing PD appears to result from a complex interplay of genetic and environmental factors that converge on immune function and inflammation, affecting several important cellular processes (6).

Two key neuropathological hallmarks of PD at autopsy include 1) the relatively selective loss of dopaminergic neurons in the Substantia nigra pars compacta (SNpc), although neurodegeneration is not limited to only the nigral dopaminergic neurons and encompasses cells located in other circuits, and 2) the presence of intracellular inclusions of aggregated and misfolded α-synuclein (αSyn) protein, termed Lewy bodies, in the surviving neurons (7). Excessive accumulation and spreading of 'toxic' αSyn aggregates are widely presumed to be major

molecular events underlying PD pathogenesis (8). Consequently, PD has been classified within a heterogenous group of diseases termed α-synucleinopathies, in which PD is the most prevalent. It is important to highlight that the existence of co-pathologies in PD, for instance, the development of amyloid-β (Aβ) plaques, tau-containing neurofibrillary tangles, and TAR DNA-binding protein 43 (TDP-43) protein inclusions, also occur within the nigrostriatal system and in other brain regions (9). Yet, current symptomatic treatments, such as levodopa supplementation, deep brain stimulation and physical therapy, cannot significantly slow or halt disease progression and impact the underlying disease pathology.

1.2 The structure and role of αSyn

αSyn is an intracellular, 14 kilodalton (kDa)-sized protein composed of 140 amino acids. In healthy neurons and other cell types, αSyn predominantly exists in the form of unfolded monomers (10–12). As monomeric αSyn lacks a native three-dimensional (3D) structure, it is considered an intrinsically disordered protein. Thus, it is characterized by structural flexibility and susceptibility to modifications, rendering αSyn prone to misfolding and aggregation (13). Attributable to its flexibility, monomeric αSyn can dynamically interconvert between various conformational states, which is influenced by environmental conditions and the molecular characteristics of different αSyn domains (14,15). Natively unfolded αSyn monomers may take the form of an α-helix, tetramer, or membrane-bound multimer. Several factors, such as intrinsic properties of the protein, biological and chemical stimuli, mutations of the αSyn gene (*SNCA*), and post-translational modifications, may initiate misfolding of αSyn and aggregation. αSyn proteins can assume structurally distinct amyloid-like conformations, referred to as strains, and

such structural variations can be observed in αSyn deposits, differing across PD patients and neurologically-related conditions (16,17). Conformations of αSyn range from monomeric, oligomeric, fibrillar, and combined forms, which impact the interaction of αSyn with microglia and their subsequent internalization (18). Thus far, the direct mechanism of αSyn aggregation is not well understood. It is considered that αSyn participates in a multifactorial process wherein an unfolded monomer undergoes primary nucleation, elongation, and secondary nucleation (19). During primary nucleation, monomers self-assemble to form soluble oligomeric intermediates (nuclei). Elongation includes the addition of monomers to existing aggregates, leading to the formation of highly organized structures, such as protofibrils and fibrils. Finally, during secondary nucleation, fibrils may further form nucleation centers and provide autocatalytic amyloid amplification and contribute to the rapid generation of new aggregates or further assemble into Lewy bodies (Figure 1B) (20). A study showed that 10 years after transplantation of dopamine cells in humans, surviving human fetal neurons adopt the histopathology of PD, suggesting that classical Lewy body formation takes a decade to achieve (21–24).

The primary amino acid sequence of αSyn includes three characteristic regions: N-terminal, non-amyloid-β-component (NAC), and C-terminal, all of which, possess different properties (Figure 1A) (25). The amphipathic N-terminal region (residues 1-60) frequently adopts an α-helical structure and functions as an anchor for lipid membrane binding (26). The tendency of membrane-bound, monomeric αSyn to exist as an α-helix is increased when features, for instance membrane curvature or lipid rafts within cell or vesicle membranes, are present (25). Moreover, under physiological conditions, αSyn monomers are N-terminally acetylated, which assists in preserving their structures and preventing spontaneous aggregation (27). The central,

hydrophobic NAC region (residues 61-95) is involved in the regulation of αSyn transport within axons and has a tendency for adopting a cross-β-sheet structure (28). Consequently, the cross-β-sheet structure promotes protein aggregation and fibrillization by recruiting further monomers, ultimately leading to the formation of amyloid fibrils (29). The acidic C-terminal region (residues 96-140) structurally displays a flexible random coil arrangement and is involved in calcium-mediated synaptic vesicle binding, thus promoting membrane fusion and neurotransmitter release (30–32). While engaging with the N-terminal via long-range electrostatic interactions, the C-terminal provides an electrostatic defence which prevents the NAC region from engaging in cross-β-sheet folding. Truncation of the C-terminal region may suggest an increased exposure of the NAC region, thus promoting a pro-aggregatory conformational state (33). Indeed, truncation of the C-terminal has been estimated to occur in 10-30% of total αSyn within Lewy Bodies (34).

In the healthy brain, αSyn is enriched in the presynaptic terminals of neurons as a lipid-associated, readily soluble protein that regulates presynaptic vesicle turnover (35). αSyn is well-conserved in mammals and expressed in non-neuronal and innate immune cells of the central nervous system (CNS), such as microglia (36,37). Despite extensive research, the complete understanding of the function of αSyn remains ambiguous. However, it has been suggested that αSyn has a potential role in regulating essential synaptic processes due to the preferential localization of αSyn and its strong affinity for synaptic proteins (19). Native αSyn mutually interacts with molecular chaperones, downregulates proapoptotic factors, and supports neurogenesis, acting as a potential neuroprotective agent (38–42). Several reports have revealed that αSyn modulates dopaminergic signalling, such as by negatively regulating its reuptake, as PD is characterized by the decline of dopaminergic neurotransmission (43,44).

Moreover, it has been reported that αSyn serves as a critical mediator of inflammatory and immune responses by the host, and αSyn is required for the development of a normal inflammatory response (45). αSyn also comprises an anti-viral role in which expression of αSyn restricts RNA viral infections in the brain (46). In PD patient brains, synaptic accumulation of aggregated and misfolded αSyn results in synaptic impairments, and aberrant neural network activity, ultimately leading to cell death (47,48). Importantly, loss-of-function of the native protein leads to synaptic disturbances, which has been proposed as one of the earliest molecular events driving PD (8,49).

Further, αSyn is a very stable protein with a long half-life that can circulate in the brain and serve as part of a platform for pathology spread (50). Besides its several intracellular functions, αSyn is considered to spread in a prion-like manner, as shown by the grafting of fetal mesencephalic dopaminergic neurons into the SN of PD patients, which later developed αSyn-positive inclusions (22). A small portion of its pool can be secreted by neurons and spread to neighbouring cells via several mechanisms, such as exocytosis and direct cell-to-cell transfer (51,52). Cell-to-cell propagation of αSyn may occur when αSyn is released into the extracellular milieu from a dying cell or released from a viable cell that is burdened with αSyn. Small quantities of αSyn are similarly released from neuronal cells by unconventional exocytosis, and extracellular αSyn contributes to various brain pathologies, such as neurodegeneration and inflammation (53). Extracellular αSyn levels have been demonstrated to be regulated by neuronal activity (54). In addition, aggregated forms of extracellular αSyn trigger trans-cellular spreading of αSyn pathology and extracellular αSyn oligomers activate inflammatory responses in microglia (55–59). In particular, secreted monomeric αSyn has been shown to display toxicity to cells, perturb

calcium homeostasis and induce fragmentation of lipid rafts (60–62). Overall, αSyn plays a versatile role in modulating synaptic homeostasis and loss-of-function of the native protein, originating from protein misfolding and/or aggregation, and extracellularly available αSyn may contribute to synaptic dysfunction and progression in PD.

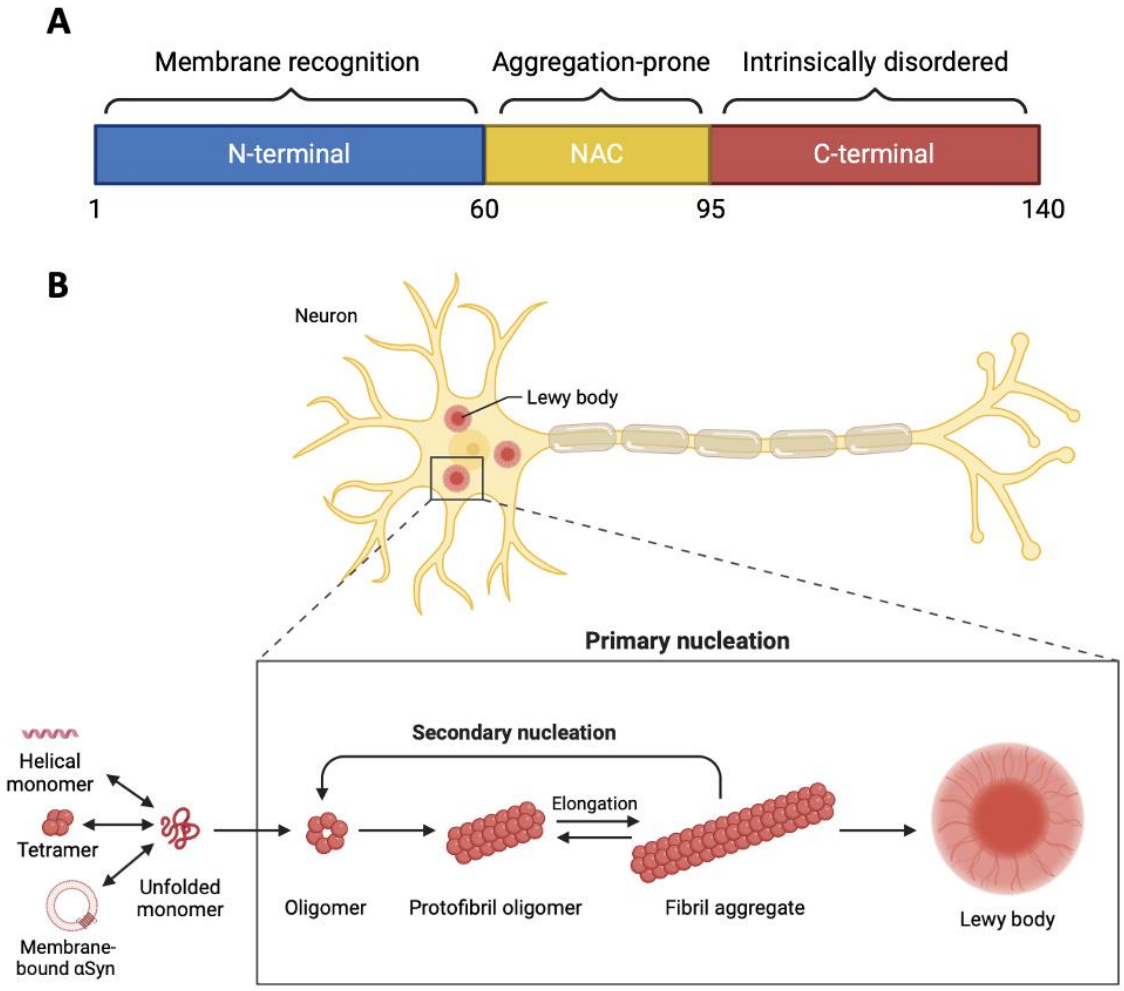

Figure 1. Mechanisms of αSyn aggregation.

(A) The primary sequence of αSyn with three regions, each displaying unique properties. (B) It is believed that αSyn participates in a multi-step process wherein an unfolded monomer undergoes primary nucleation and self-assemble to form soluble oligomeric intermediates. During elongation, addition of monomers to existing oligomers can lead to the formation of highly organized structures, such as protofibrils and fibrils. Fibrils may further form nucleation centers and provide autocatalytic amyloid amplification and contribute to the rapid generation of new aggregates or further assemble into Lewy bodies in a process known as secondary nucleation. Ultimately, synaptic accumulation of aggregated and misfolded αSyn results in synaptic impairments, and aberrant neural network activity, leading to cell death. Adapted from Saramowicz et al. (2024). Figure was created with BioRender.com.

1.3 Microglia in the CNS

Microglia are the resident immune cells of the CNS and represent the largest population of myeloid cells in the CNS (63). They constitute about 10-15% of cells found within the brain (64). As the essential macrophages of the brain parenchyma, microglia play a fundamental role in the innate immune response and are critical in the maintenance of CNS homeostasis, neurogenesis, synaptic plasticity maintenance, synaptic pruning, neural circuit shaping, injury repair and overall brain health (65). During CNS injury, microglia are responsible for phagocytosis and elimination of microbes, dead cells, and protein aggregates, in addition to other particulate and soluble antigens that may compromise the CNS. Furthermore, microglia secrete several soluble factors, such as cytokines, chemoattractants, and neurotropic factors, that contribute to various aspects of neuroprotective responses and tissue repair in the CNS (65). Microglia have demonstrated to jointly degrade fibrillar αSyn cargo by transferring it through tunneling nanotubes, attenuating the inflammatory microglia profile (66). More recently, αSyn and tau have been shown to engage as triggers tunneling nanotube formation between microglia and neurons, facilitating their relocation from aggregate-burdened neurons into healthy microglia and rescue neurons from aggregate-induced neuronal dysfunction and death (67).

Microglial cells encompass a high level of plasticity and manifest a phenotypical heterogeneity, undergoing a variety of morphological changes in response to perturbations (Figure 2) (68). Microglial morphological plasticity contributes to many developmental processes and physiological functions of the brain by adopting a specific phenotype. As such, microglia of diverse phenotypes have been classified based on their morphological features. In the healthy brain, microglia are in a “surveillant” or “resting” state and appear morphologically ramified with

small cell bodies and fine, long branched processes (69). Surveillant microglia are involved in the monitoring of potential danger molecules and continuously scan the brain microenvironment for extracellular triggers by extending and retracting their processes (70,71). Hence, it may be incorrect to refer to microglia as "resting" under physiological conditions, because ramified microglia are actively scanning the brain microenvironment and perform many functions during normal physiological conditions. The branches of microglia are extremely sensitive to minor changes in environmental conditions and microglia may be transformed at any occasion in response to injury or threat (72). In comparison, activated microglia mounting an immune response transform into an "amoeboid" phenotype, where such cells are spherical in shape, lack abundant and long processes, are capable of migration, and contain numerous phagocytic vacuoles (73). It is important to note that the bulk of our knowledge concerning microglial physiology has been attained using *in vitro* microglial cultures and due to their extreme sensitivity, cell isolation from the tissue inevitably triggers physical alteration-induced, microglial activation. Thus, the activation state of microglial cells should always be considered during *in vitro* experimentation. Most importantly, morphology does not reliably signify function or dysfunction, however only demonstrates that the cell is responding to altered homeostasis (74).

In addition to the neuroprotective functions exerted by microglia, they may perform neurotoxic roles due to excessive uptake of protein aggregates, leading to microglial phagocytic ability impairment, altered inflammation signaling, and thus, potentially contributing to neurodegeneration (75). In response to CNS injury and disease, microglia undergo activation. Histopathological evidence has demonstrated activated microglia surrounding αSyn deposition in the brain tissues from PD patients, such as in midbrain sections of the SNpc, where they display

a higher proportion of the amoeboid morphology, suggesting an activated state (76,77). Of note, the SN, a susceptible brain region in PD, contains the highest density of microglia among different brain regions (78–80). Furthermore, microglial activation begins early and persists during PD progression, as it has been observed in patients with a recent diagnosis and in individuals with long-term illnesses (81,82). Longitudinal characterization of PD models and extensive analysis of human PD brain tissue have revealed that microgliosis may occur prior to neuronal cell death or even in its absence, suggesting that the immune response occurs early in PD and changes dynamically with disease progression, contributing to neuronal degeneration and symptomatology in patients (83,84). These findings have also been validated by *in vivo* positron emission tomography imaging (82,85). In PD, reactive microgliosis can be observed in brain regions with substantial αSyn pathology (86). During CNS surveillance, internalization of αSyn can induce microglial activation and neuroinflammation (87,88). Different aggregation and conformational states of αSyn have revealed to differentially activate microglia in PD with varying strengths of activation, leading to increased secretion of pro-inflammatory cytokines and reactive oxygen species (ROS) (8,18,89). Likewise, when combined with chronic inflammatory cues, PD-derived αSyn assemblies have demonstrated to promote a neurotoxic microglial phenotype (90).

There are several ways by which uptake of αSyn by microglia mediates αSyn-induced inflammation. Microglia are able to phagocytose extracellular monomeric and fibrillar αSyn via toll-like receptors (TLRs), an important family of pattern recognition receptors (PRRs) that detect pathogens, such as TLR2 and TLR4 (91,92). Moreover, microglia have been shown to engulf exosomes containing αSyn via macropinocytosis, where microglial exosomes can facilitate αSyn

transmission (93,94). Finally, neurotoxic molecules released from αSyn-activated microglia, including pro-inflammatory cytokines, chemokines, glutamate and ROS, may initiate or exacerbate neurodegeneration and induce an imbalance in the homeostatic functions of microglia, leading to a feedback cycle of microglial activation and neurodegeneration (Figure 2).

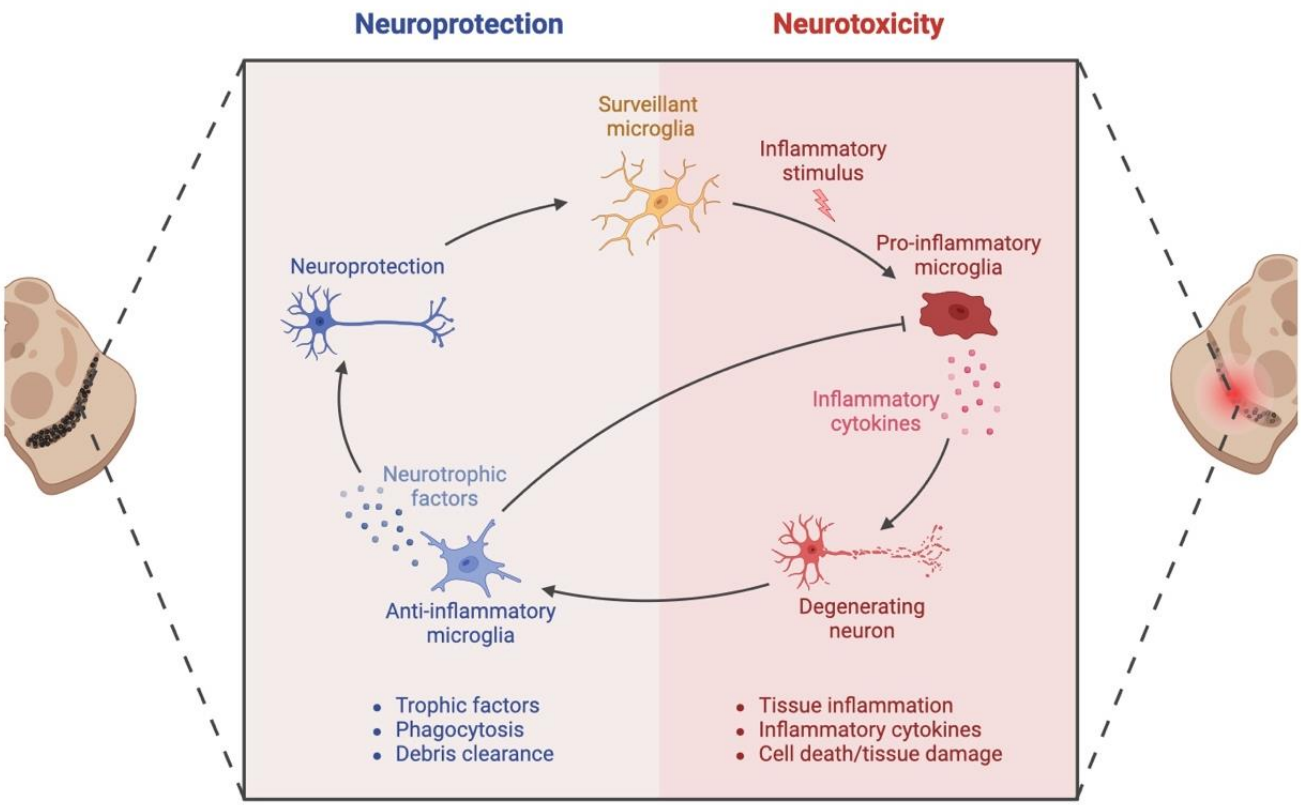

Figure 2. The morphological heterogeneity of microglia in different environments.

Microglia are composed of phenotypical plasticity, allowing them to change morphology depending on the surrounding environment. For instance, microglia in their homeostatic state are considered to be neuroprotective and anti-inflammatory by releasing neurotrophic factors, undergoing phagocytosis, and clearing cellular debris in response to acute CNS injury. In comparison, microglia can become neurotoxic and pro-inflammatory upon an inflammatory stimulus and chronic activation of microglia. As a result, microglia may release pro-inflammatory cytokines, produce tissue inflammation and cell death, negatively impacting neurons and surrounding cells. The changes observed in phenotype may or may not be reflective of the functional state. Figure was created with BioRender.com.

1.4 The NLRP3 inflammasome

The innate immune system acts as the first line of defense that protects the CNS against harmful stimuli, for instance invading pathogens, dead cells, or irritants (95). Inflammation is a protective immune response displayed by the evolutionarily conserved innate immune system that is tightly regulated by the host. Inadequate inflammation may lead to persistent infection of pathogens, while excessive inflammation may trigger chronic or systemic inflammatory diseases (96,97). In the past two decades, it has been increasingly recognized that the immune system and inflammatory processes are implicated in a wide-ranging list of mental and physical health difficulties that dominate present-day morbidity and mortality worldwide (98–101). In fact, chronic inflammatory diseases have been recognized as the most significant cause of death in the world today, with more than 50% of all deaths being attributable to inflammation-related diseases (102).

Inflammasomes are innate immune system receptors and sensors that regulate the activation of caspase-1 and produce inflammation in response to detrimental stimuli (103). They are cytosolic, multiprotein signalling complexes that respond to pathogen-associated molecular patterns (PAMPs) and damage-associated molecular patterns (DAMPs) in a PRR-dependent manner. PAMPs are only associated with foreign pathogens, whereas DAMPs are endogenous danger molecules that are released upon cellular stress, tissue damage and cell death (104). Nucleotide-binding oligomerization domain (NOD)-like receptors (NLRs) are a subset of cytoplasmic PRRs that can cooperate with TLRs and drive inflammasome formation (105). Both receptor families are expressed in resident CNS cells that participate in innate immunity; however, microglia, myeloid cells of the CNS, express all TLRs (106). In comparison, a more

restricted group is expressed in astrocytes (107,108). The NLR family pyrin domain containing-3 (NLRP3) inflammasome is the best characterized inflammasome, where it mediates sterile neuroinflammation in microglia (109–112). NLRP3 inflammasome activation has been noted in both microglia and astrocytes among other cell types, although only the former has been reported to express all NLRP3 inflammasome components and substrates (112–114). The NLRP3 inflammasome is composed of three major components (Figure 3A), namely NLRP3, which serves as an intracellular sensor for various PAMPs and DAMPs, the apoptosis-associated speck-like protein containing a caspase activation and recruitment domain or CARD domain (ASC) which serves as an adaptor protein, and the effector, caspase-1, which carries out the enzymatic cleavage of pro-inflammatory cytokines, such as interleukin (IL)-1β and IL-18, and causes pyroptosis, a type of lytic cell death (115). Activated caspase-1 results in the cleavage of gasdermin D (GSDMD), forming the N-terminal fragment of GSDMD (N-GSDMD), which self-assembles and creates transmembrane pores, resulting in pyroptosis and facilitation of bioactive IL-1β and IL-18 and ASC specks release into the extracellular space (116).

Assembly of the inflammasome is a key function mediated by the innate immune system and relies on homotypic interactions between the component proteins. NLRP3 is an NLR that contains a N-terminal pyrin effector domain (PYD), a central, conserved nucleotide-binding and oligomerization (NACHT), and a C-terminal leucine-rich repeats (LRR) domain which is involved in ligand binding or activator sensing (Figure 3A) (88). During inflammasome assembly, NLRP3 engages with the N-terminus of ASC via PYD–PYD interactions and the C-terminus of ASC recruits pro-caspase-1 via CARD-CARD interactions, resulting in proximity-induced autocatalytic cleavage leading to the production of active caspase-1 (95).

The activation of the NLRP3 inflammasome involves two steps (Figure 3B): priming (Signal 1) and activation (Signal 2). The priming step requires a stimulus to activate the transcription factor nuclear factor kappa-light-chain-enhancer of activated B cells (NF-κB), such as via the bacterial endotoxin lipopolysaccharide (LPS) binding to TLR4, which initiates translocation of NF-κB from the cytoplasm into the nucleus to induce gene transcription (117,118). Following recognition of LPS, engagement of TLR4 at the cell surface leads to the activation of downstream signaling cascades mediated by myeloid differentiation primary response gene 88 (MYD88) and TIR-domain-containing adapter inducing interferon-β (TRIF)-dependent pathways (119,120). Ultimately, TLR4 signalling and activation of NF-κB results in the transcription of NLRP3 and pro-IL-1β, yet the priming signal by itself is an inefficient secretion stimulus to produce cleaved substrates (121).

After priming, a second signal is required for the assembly and activation of the NLRP3 inflammasome, which involves numerous molecular and cellular events, including lysosomal damage/destabilization, mitochondrial dysfunction and ROS generation, and ion flux (K^+ efflux) (122). These signals are induced by a diverse collection of unrelated stimuli recognized as NLRP3 agonists, for instance pore-forming toxins, the presence of nucleic acids, and sensing of fungal, bacterial or viral pathogens (123,124). Of importance, the inflammasome may also be activated by neurodegeneration-associated molecular patterns (NAMPs), such as misfolded protein aggregates (125). One possible mechanism of activation comprises of various PAMPs and DAMPs being internalized into the cell via phagocytosis and trafficked to the lysosome, leading to lysosomal rupture and intracellular cathepsin B release, thus triggering NLRP3 inflammasome activation (126–128). In addition, mitochondrial ROS production was one of the first identified

triggers of NLRP3 inflammasome activation (129–131). For instance, fatty acids in a high-fat diet have shown to activate the NLRP3 inflammasome in an adenosine monophosphate-activated protein kinase–autophagy–ROS-dependent manner (132). Considering the quantity and diversity of NLRP3 inflammasome activators, several molecular or cellular events may converge on a common pathway that triggers initial or sustained activation.

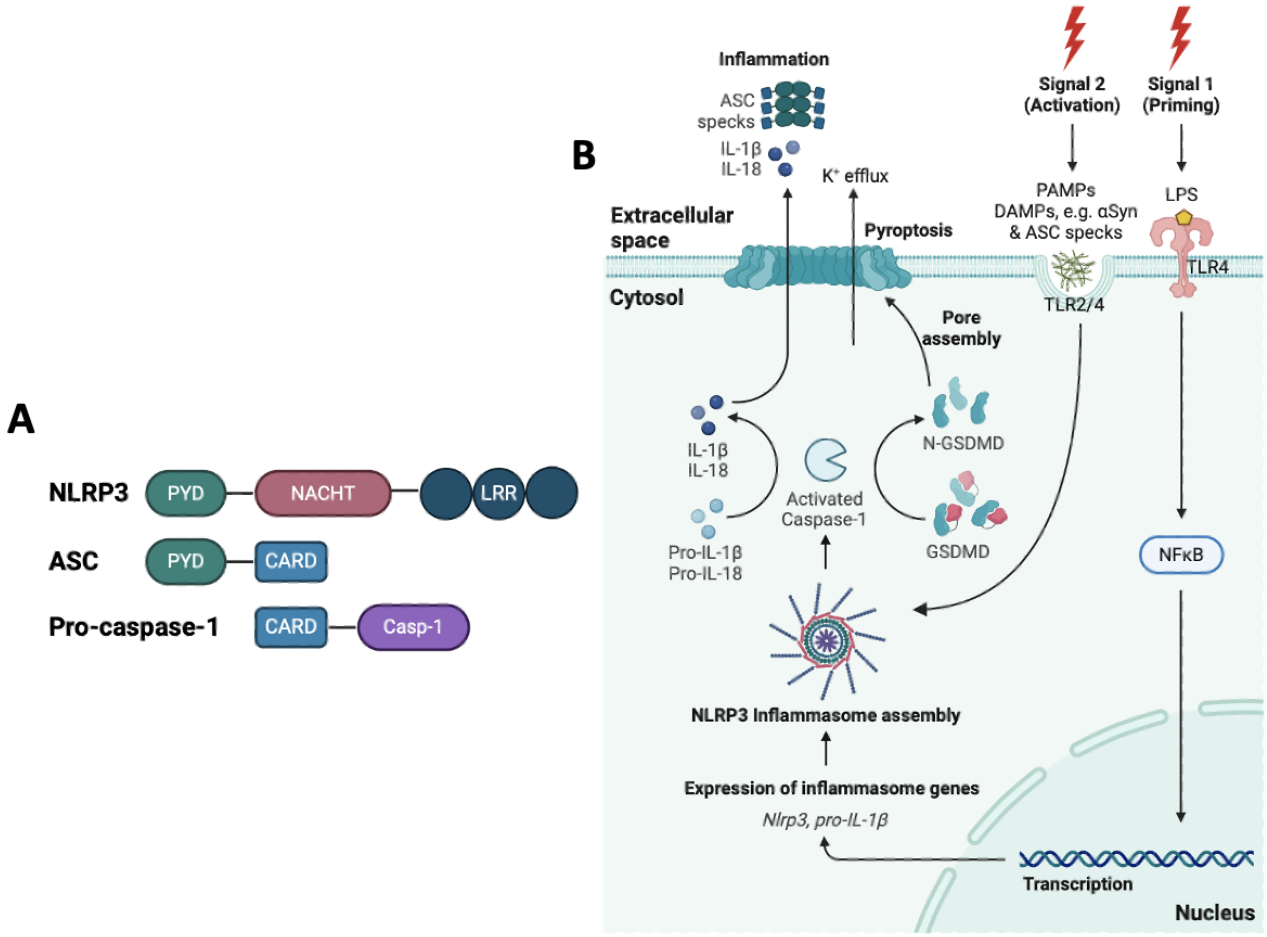

Figure 3. Overview of NLRP3 inflammasome priming and activation in microglia.

(A) The NLRP3 inflammasome is composed of three components: NLRP3, which serves as an intracellular sensor; ASC, which serves as an adaptor protein; and caspase-1, which serves as an effector protein. The NLRP3 inflammasome assembles via homotypic PYD-PYD and CARD-CARD interactions. (B) NLRP3 inflammasome activation requires two key signals: priming and activation. Priming via LPS induces NF-κB-dependent transcription of NLRP3 and pro-IL-1β. Inflammasome engagement results in caspase-1 recruitment and proteolytic self-cleavage to its mature form. Active caspase-1 may process pro-IL-1β and pro-IL-18 to its mature form, cleave GSDMD to induce pyroptotic cell death, and release ASC specks. Figure was created with BioRender.com.

1.5 The role of the ASC speck in inflammation

In the preceding decade, an inflammation-based hypothesis has emerged to elucidate the mechanism of neurodegenerative disease progression as many therapies targeting protein accumulation have been principally unsuccessful (133,134). In this hypothesis, inflammation serves as a triggering event early in the disease that contributes to protein misfolding and aggregation which supports neuroinflammation in a positive-feedback manner, ultimately leading to neuronal cell death. In addition to forming the basic inflammasome complex, NLRP3 inflammasome activation may also lead to the formation of a dense structure, known as the ASC speck, which is ~1 μm in diameter (109,111). The oligomerization of ASC into ASC specks creates a host of potential caspase-1 activation sites, thus serving as a signal amplification mechanism for inflammasome-mediated cytokine production (135). Post inflammasome activation and recruitment of ASC to the oligomerized NLRP3, ASC aggregation remains an ongoing process where large helical fibrils are formed via homotypic interactions between its PYD region. Next, many ASC fibrils are crosslinked via homotypic interactions on the ASC-CARD region to form a dense ASC speck. As a result, the ASC speck recruits pro-caspase-1 to its surface and functions via the same mechanism as the basic inflammasome complex, although at a larger scale (109).

An increasing number of neurodegenerative disorders and other diseases have been linked to protein misfolding and aggregation. The term ‘prion’ refers to the infectious protein primarily composed of major prion protein (PrP^{Sc}), the pathological aggregated form of the cellular prion protein PrP^{C}, that causes prion diseases (136). The term has broadened to describe protein aggregates irrespective of their infectivity and share principles governing aggregation and propagation, thus referred to as ‘prionoids’ (prion-like). The ASC speck possesses extracellular

and prion-like activity as it propagates from a pyroptotic macrophage to another recipient cell while preserving its activity. ASC speck formation upon activation of the NLRP3 inflammasome has shown to precede cell death (137). In support, NLRP3 inflammasome particles are secreted in the extracellular space where they can continue the maturation of caspase-1 in addition to within other macrophage cells upon phagocytosis of the particle, amplifying the inflammatory response (138). Macrophages can degrade subthreshold amounts of ASC specks during acute inflammation, however chronic inflammation could lead to the accumulation of ASC specks, further resulting in prolonged, harmful immune responses (139). Thus, the inflammatory effects of ASC speck uptake could be concentration-dependent and swayed by the balance between ASC speck accumulation vs clearance. Furthermore, ASC speck's prion-like structure is resistant to proteolytic degradation similar to the misfolded protein aggregates observed in PD and Alzheimer's disease (AD), contributing to failed degradation of the inflammasome and ASC speck (137). The ASC speck may also act as a scaffold for protein aggregation as ASC specks have been reported to have an intrinsic property to co-aggregate cytosolic proteins on their surface through non-specific hydrophobic interactions (140). As a result, ASC specks could provide an alternative mechanism of antigen cross-presentation and may shape adaptive immunity by skewing T-cell immunity via sustaining the production of IL-1 cytokines in the extracellular space (140–142).

1.6 Maturation of the effector protein caspase-1 and release of IL-1β and IL-18

Caspases are a family of intracellular cysteine proteases that cleave a limited number of substrates present following an aspartic acid residue. The role of caspases has been thoroughly studied in apoptosis, where they are crucial in executing programmed cell death (143).

Nonetheless, many caspases, including caspase-1, caspase-4 and caspase-5, are classified as inflammatory and are engaged in the processing and secretion of pro-inflammatory molecules (144,145). Caspase-1 was first identified in 1989 and is one of the most common and best studied inflammatory caspases that initiates pro-inflammatory responses through the cleavage of cytokines, such as IL-1β (144,146). Caspase-1 is present as a zymogen in the cytosol of phagocytic cells that can be cleaved into 20 kDa (p20) and 10 kDa (p10) subunits that become part of the active enzyme (147). Thus, pro-caspase-1 requires its activation to be functional, which can be accomplished through the assembly of an inflammasome complex. Upon NLRP3 inflammasome activation, dormant pro-caspase-1 is self-activated by proteolytic cleavage and mature caspase-1 proteolytically cleaves other proteins in a cascade of events, such as precursors of the inflammatory cytokines IL-1β and IL-18 together with the pyroptosis inducer GSDMD, into mature, biologically active forms.

IL-1β and IL-18 are cytokines of the IL-1 family of ligands and important mediators of inflammatory diseases (148,149). While there are several biological properties that overlap for these cytokines, differences exist. For instance, IL-1β is induced only in response to inflammatory stimuli whereas IL-18 is constitutively expressed under homeostasis (150). IL-1β expression is induced during stimulation with TLR ligands and other cytokines. Yet, LPS-mediated priming of NLRP3 is required for inflammasome activation and subsequent release of both IL-18 and IL-1β (151). Furthermore, IL-1β and IL-18 are differentially regulated. Despite being constitutively expressed, IL-18 expression was shown to be increased and sustained after stimulation of TLRs, whereas IL-1β was induced but not sustained after chronic treatment (152). Mature IL-1β has been linked to many immune system-linked responses, including the recruitment of

inflammatory cells to the site of infection, whereas IL-18 is involved in host defense against infections and regulates both the innate and acquired immune response (153). IL-18 can combine with IL-12 and is important for the production of interferon (IFN)-γ and enhancement of the cytolytic activity of natural killer (NK) cells and T lymphocytes (CD8+ T cells) (154). In addition, IL-18 promotes activation and differentiation of T cells (155).

IL-1β is the most well-characterised and studied of the 11 IL-1 family members. IL-1β is essential for the host-response and resistance to pathogens but also exacerbates damage during chronic disease processes and is linked to acute tissue injury (107). Following caspase-1-dependent processing of pro-IL-1β, it has been proposed that the secretion of IL-1β occurs on a continuum, dependent upon stimulus strength and the extracellular IL-1β requirement (156). Rather than the conventional endoplasmic reticulum-Golgi route of secretion, IL-1β may be secreted via three distinct mechanisms (156). For instance, the rescue and direct mechanism suggests that a fraction of cellular IL-1β that is targeted for degradation can be rescued and redirected to the extracellular environment and such a mechanism will likely be engaged when the extracellular requirement for IL-1β and commitment to cell death is low. It has been demonstrated that the majority of IL-1β in LPS-activated monocytes localizes to the cytosol, although a portion of IL-1β can be present in vesicles and is protected from tryptic digestion (157,158). Furthermore, IL-1β may be secreted via a protected release since IL-1β has a very short half-life in plasma and supports the notion that protected IL-1β is destined for sites distant to the inflammatory lesion (159). Protected release of IL-1β may be secreted via the shedding of microvesicles from the plasma membrane and in support, IL-1β-containing microvesicles have been isolated from LPS-treated microglia (160,161). Exosomes, which are membrane-bound

extracellular vesicles, have also shown to package and secrete IL-1β in a protected form (162). Lastly, the terminal release mechanism involves a commitment to cell death, such as pyroptosis, and may occur under conditions of extreme inflammatory stress. This mechanism appears to be well-equipped for the rapid release of large quantities of active IL-1β directly across a disintegrating plasma membrane. It has been demonstrated that a 30 minute (min) incubation with adenosine triphosphate (ATP), a NLRP3 inflammasome inducer, triggers LPS-primed murine peritoneal macrophages to swell, which is closely followed by the release of lactate dehydrogenase (LDH), a cytosolic enzyme released from lytic cells (163). However, cell lysis as such does not automatically induce release of active IL-1β, since LPS-treated murine peritoneal macrophages primarily release pro-IL-1β when subjected to oxidative injury (164).

Compared to the release of IL-1β, mechanisms supporting the release of IL-18 are less well understood. Despite distinct regulatory mechanisms that control the pro-inflammatory cytokines IL-1β and IL-18, both share a common secretory pathway that depends upon membrane permeability and can operate in the absence of complete cell lysis and cell death (165). In primary human monocyte-derived macrophage cultures primed with LPS and stimulated with nigericin, both IL-1β and IL-18 were released. In both instances, release was inhibited by a pre-incubation with the membrane-stabilizing agent punicalagin (165). In comparison, blocking cell lysis with a cytoprotectant, such as glycine, did not inhibit NLRP3-dependent release of IL-1β. Together, these findings suggest that IL-1β and IL-18 share a common secretory pathway that depends upon membrane permeability and further supports the well-accepted notion that release of IL-1β and IL-18 can be GSDMD-dependent.

1.7 Induction of pyroptosis

Active cell death is a fundamental biological process that is tightly regulated and serves to assist host defense (166). However, chronic activation of cell death pathways in response to PAMPs or DAMPs can lead directly to the development of neuroinflammation and pathology. Thus, distinct forms of regulated cell death have been classified as key drivers of CNS diseases, such as apoptosis, necrosis, and pyroptosis (167). Most notably, apoptosis, the primary form of programmed cell death, has been well defined and extensively researched (168). Apoptosis has been demonstrated to underlie mechanisms of physiological CNS development as well as common neurological disorders, for instance AD, PD and amyotrophic lateral sclerosis (169–171). More recently, an inflammatory cell death referred to as “pyroptosis” has been identified as a key mediator of inflammatory responses and instigator of different forms of neurological diseases (172–174).

In 2015, multiple studies discovered GSDMD as an executor of pyroptosis and that cleavage of GSDMD by inflammatory caspases determines pyroptotic cell death (116,175). GSDMD consists of two conserved domains, the N-terminal pore-forming domain (PFD; also referred to as N-GSDMD) and the C-terminal repressor domain (RD) (176,177). GSDMD, along with other proteins of the GSDM superfamily, maintain oligomerization through the interaction between PFD and RD and RD may inhibit the cytotoxic effects of PFD. Upon NLRP3 inflammasome activation and subsequent cleavage of caspase-1, GSDMD is cleaved, and the N-terminal PFD is dissociated from the C-terminal RD. Next, the N-terminal PFD oligomerizes and undergoes conformational changes and forms pores in the cell membrane, triggering the release of inflammatory molecules and pyroptotic cell death (Figure 3B) (178–180). Pore formation in the

plasma membrane, which is ~10-33 nm in diameter, allows processed IL-1β and IL-18, with diameters of 4.5 nm and 7.5 nm, respectively, as well as caspase-1 to pass through and be released into the extracellular milieu (178,179,181). Lastly, plasma membrane rupture, the final cataclysmic event in lytic cell death, is mediated by the cell-surface NINJ1 protein (182). NINJ1 mediates plasma membrane rupture downstream of various cell death processes, where plasma membrane rupture releases DAMPs that propagate the inflammatory response.

In addition to the canonical inflammasome-dependent pathway mediated by caspase-1, non-canonical inflammasome-dependent pathways may also induce pyroptosis. Caspase-4/5/11 can be directly activated by LPS in host immune cells, leading to GSDMD cleavage, though caspase-4/5/11 cannot process pro-IL-1β and pro-IL-18 (183). K^+ efflux via pore formation further promotes the activation of caspase-1 (184,185). Moreover, pyroptosis can be activated in an inflammasome-independent manner. Activation of caspase-3, an apoptotic caspase, has also proven to promote microglial pyroptosis in models of multiple sclerosis via cleavage of GSDME (186). Despite some similarities between pyroptosis and apoptosis, for instance DNA damage and chromatin condensation, several key differences exist (174). Morphologically, pyroptotic cells display cell swelling and many bubble-like protrusions on the surface of the cellular membrane before its rupture and are inflammatory in nature (187). As a result of the pore formation, water enters the cell, causing cell swelling and osmotic lysis, resulting in rupture of the plasma membrane and the release of IL-1β and IL-18 (188,189). Pyroptosis can also appear as flattening of the cytoplasm due to plasma membrane leakage (187). In contrast, apoptotic cells shrink and maintain membrane integrity in the absence of GSDMD cleavage and pore formation (190).

Overall, pyroptosis has been increasingly recognized as an important factor in mediating inflammatory responses against PAMPs and DAMPs.

1.8 Contribution of the NLRP3 inflammasome to neuroinflammation and neurodegeneration

The underlying molecular pathogenesis of PD is thought to involve multiple pathways and mechanisms, for example αSyn proteostasis, mitochondrial function, oxidative stress, calcium homeostasis, axonal transport and neuroinflammation (1). Neuroinflammation in the PD brain is mediated by activated microglia and invading immune cells (191). Increasing evidence indicates that activation of the microglial NLRP3 inflammasome by aggregated Aβ, tau and αSyn results in the release of IL-1β and IL-18, leading to chronic neuroinflammation and disease progression both in AD and PD (192–195). During neuroinflammation, activated microglia release the inflammasome adaptor protein ASC outside the cell as ASC specks which can act as a 'danger signal'. The extracellular ASC is biologically active and cross-seeds Alzheimer's-linked Aβ in neighbouring microglia (196). More recently, extracellular ASC has been shown to bind Aβ and internalization of ASC-Aβ complexes by microglia results in NLRP3 inflammasome activation and pyroptotic cell death. This further leads to the amplification and perpetuation of pro-inflammatory responses in a molecular feed-forward vicious cycle that can lead to neuronal damage (193). In addition, clustering around ASC fibrils also compromises clearance of Aβ by microglia.

Studies on human samples and preclinical animal models of PD have established a link between αSyn aggregation, microglial NLRP3 inflammasome activation and neuronal cell death

(197). PD patients have increased NLRP3, ASC, and caspase-1 localized exclusively within microglia in the SNpc or detectable as extracellular ASC and systemically circulating NLRP3, caspase-1, and IL-1β (197,198). Furthermore, caspase-1 can also be discovered at the core of Lewy bodies extracted from human PD patients' brains (199). Recently, it was revealed that ASC specks amplified NLRP3 inflammasome activation driven by αSyn pre-formed fibrils (PFFs) and reactive microgliosis, exacerbating αSyn pathology, dopaminergic neurodegeneration and motor deficits (200). However, the contribution of ASC specks and its interaction with αSyn in the propagation of inflammasome activation and amplification of inflammatory responses in PD has not been fully determined. Numerous therapeutics have only targeted protein accumulation in PD and other neurodegenerative diseases, failing to consider other etiologies. Hence, this therapeutic strategy has likely contributed to a significant failure rate in translating pre-clinical studies of clinical value. The recent failures in the development of antibody-based therapeutics against aggregated αSyn for PD treatment have prompted a re-evaluation of the existing therapeutic strategies and justify the need for alternative strategies targeting microglial immune responses (201,202). One of the greatest current challenges is to identify markers for prodromal disease stages, which would allow novel disease-modifying therapies to be started earlier. Therefore, it is critical to comprehend neuroinflammation in PD and develop therapeutic strategies to prevent further neuron loss and halt PD progression.

2. HYPOTHESIS AND OBJECTIVES

2.1 Hypothesis

I hypothesize that binding of αSyn to ASC in the extracellular space of the brain leads to the formation of 'ASC-αSyn complexes', which are recognized as novel danger signals by microglia leading to NLRP3 inflammasome activation and amplification of the pro-inflammatory response (Figure 4).

2.2 Objectives

The objective of this study was to gain insight into the underlying molecular mechanisms that perpetuate chronic inflammatory responses in PD models. The aims of this project were to 1) develop and characterize ASC-αSyn complexes; and 2) study the effects of ASC-αSyn complex formation on NLRP3 inflammasome activation in murine microglia using an *in vitro* model.

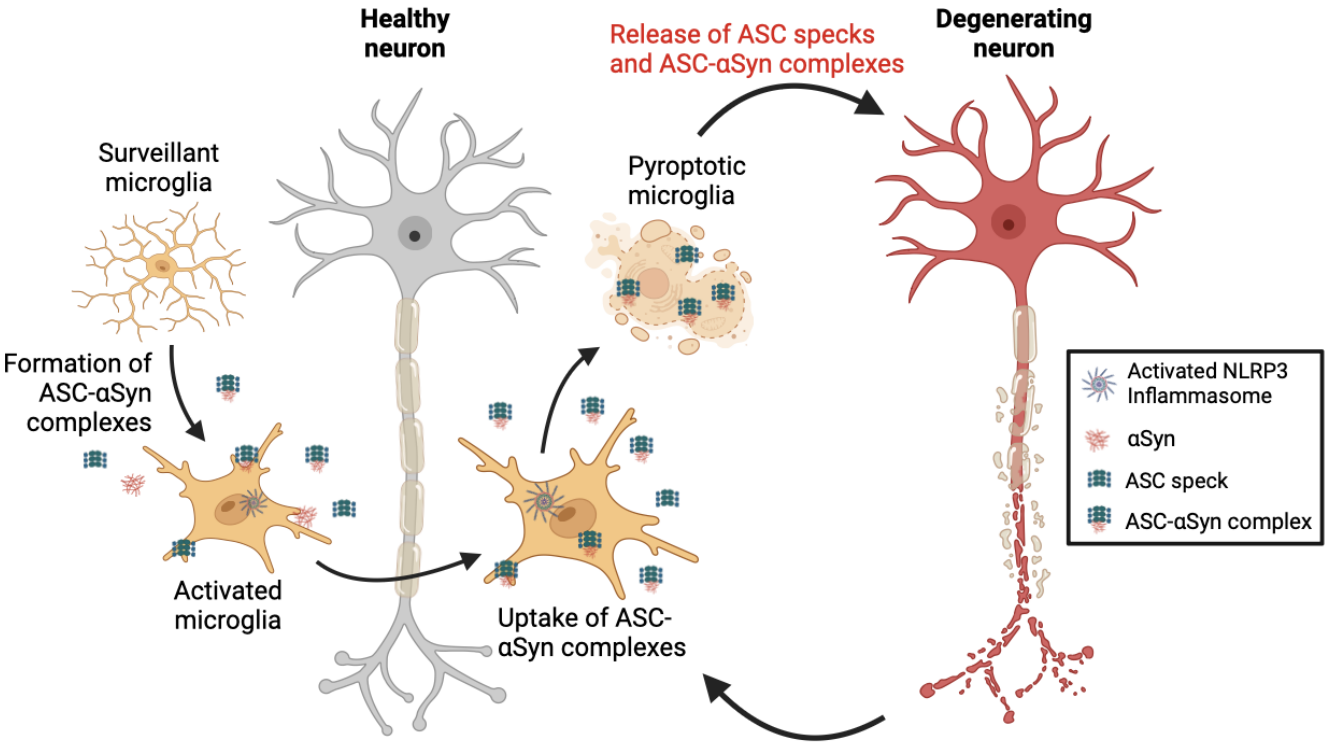

Figure 4. Schematic showing proposed mechanisms of microglial activation and chronic neuroinflammation.

Binding of ASC to αSyn in the extracellular milieu can result in the formation of ASC-αSyn complexes that are phagocytosed by surveillant microglia and can further amplify NLRP3 inflammasome activity. Sustained exposure of microglia to ASC-αSyn complexes may trigger pyroptosis, an inflammatory form of cell death and release more bioactive ASC which can be incorporated into the microglial inflammasome, leading to a vicious cycle of NLRP3 activation and neuroinflammation. Neuronal exposure to ASC-αSyn complexes may negatively impact neuronal health. Figure was created with BioRender.com.

3. MATERIALS AND METHODS

3.1 Cell culture

Mouse SIM-A9 microglia (ATCC; Cat# CRL-3265) were cultured in Dulbecco's modified Eagle's medium/Ham's F12 50/50 Mix (DMEM/F12) (Wisent; Cat# 319-075-CL) containing 10% heat-inactivated Qualified Fetal Bovine Serum (FBS) (Gibco; Cat# 12483-020) under standard conditions at 37°C and 5% CO_2. Cells were passaged every two to three days in T25 and T75 culture flasks. Cells between passage 16 to 30 were used for all experiments.

3.2 Preparation of recombinant ASC

Recombinant human ASC protein was produced by expression of ASC in *E. coli* BL21 cells. For expression, cultures were induced O/N at 28°C with 10 µM isopropyl β-D-1-thiogalactopyranoside (IPTG) and cells were lysed by sonication and centrifuged to fractionate the lysed preparation into pellet (insoluble protein) and supernatant (soluble protein). Proteins were expressed in high yields, almost exclusively in insoluble inclusion body forms. ASC protein from the insoluble inclusion body fraction was solubilized in 8 M urea and refolded by employing standard protocols (203). Refolded soluble ASC in 20 mM Tris/HCl 0.5 M L-arginine, 10 mM cystamine, and 1 mM cysteamine (pH 11) was purified by size-exclusion chromatography (SEC).

To induce fibrillation, the ASC-containing solution was first buffer exchanged to cold phosphate buffered saline (PBS) (Wisent; Cat# 311-010-CL) using an Amicon® Ultra 0.5mL Centrifugal Filter (10 kDa MWCO) (Millipore; Cat# UFC501024) for 10 min at 12,000 x g at 4°C (3x washes). Everything was kept cold and a filter volume of >100 µL was maintained. ASC was

transferred to LoBind Tubes (Eppendorf; Cat# 022431081) and ice-cold PBS was added until the desired concentration was reached. The final concentration of ASC was quantified by NanoDrop using the extinction coefficient ε = 30.94 and was incubated for 1 h at 37°C, as described previously (193). ASC fibrils were kept at 4°C for no longer than 2-3 days.

3.3 Preparation of αSyn, Aβ, and bovine serum albumin

Human Recombinant αSyn Protein Monomers (Type 1) was commercially purchased at a stock concentration of 5 mg/ml in PBS (pH 7.4) (StressMarq Biosciences Inc.; Cat# SPR-321) and stored at -80°C. As a working concentration, 2.5 and 5 μM was used for *in vitro* treatments. During preparation of working stocks, αSyn monomers were always on ice or at 4°C. Monomers may start to aggregate if left at RT or 37°C for prolonged amounts of time. αSyn monomers were used up to a maximum of two freeze/thaw cycles.

Aβ protein (1-42), specifically 1,1,1,3,3,3-Hexafluoro-2-propanol (HFIP)-treated (Bachem AG; Cat# 4090148), was dissolved in sterile Dulbecco's phosphate buffered saline (DPBS) (Gibco; Cat# 14040141) to create a stock concentration of 0.45 mg/ml and stored at -80°C. HFIP is a volatile solvent, which disrupts Aβ fibrils and generates monomers by breaking down β-sheet structures and disrupting hydrophobic forces in aggregated amyloid preparations (204). As a working concentration, 5 μM was used for *in vitro* treatments. During preparation of working stocks, Aβ monomers were always on ice or at 4°C and were used up to a maximum of two freeze/thaw cycles.

Bovine Serum Albumin Fraction V (BSA) (Sigma-Aldrich; Cat# 810533) was dissolved in PBS to create a stock concentration of 3 mg/ml and stored at -20°C. As a working concentration, 5 μM was used for *in vitro* treatments.

3.4 Generation of ASC-αSyn complexes

Fibrillar ASC (2.5 μM) and αSyn monomers (2.5 μM) were incubated in DMEM/F12 media with 1% FBS and 1% penicillin-streptomycin (P-S) (Wisent; Cat# 450-201-EL) in LoBind Tubes at 37°C, O/N (Figure 5B). The same procedure was applied to single protein treatments containing 1% FBS and 1% P-S. ASC-Aβ complexes (1.75 μM ASC and 5 μM Aβ) were used as a positive control, as previously described (193). ASC-BSA complexes (1.75 μM ASC and 5 μM BSA) were used as a negative, non-amyloidogenic control.

3.5 Electron microscopy (EM)

Fibrillary ASC (1.75 μM) and αSyn monomers (5 μM) were pre-incubated in Tris-buffered saline (TBS) (ThermoScientific; Cat# J60877.K2) O/N at 37°C, as described above in the "Generation of ASC-αSyn Complexes" section. Four to six Carbon Support films (300 mesh grids, Copper) (Ted Pella, Inc.; Cat# 01843-F) at a time were placed on a cover glass and glow discharged using the PELCO easiGlow^{TM} Glow Discharge System (Ted Pella, Inc.) on auto mode. It is important to note the Copper grids require delicate handling during specimen preparation. For negative staining EM, 5 μL of the protein sample was applied to a glow discharged copper grid and incubated for 2 min at room temperature (RT). Fluids were removed with the aid of a Whatman filter paper and samples were negatively stained by adding 5 μL of 2% uranyl acetate onto the

copper grid following a 30 second incubation step. Finally, residual fluids were removed using a filter paper and the EM grid was air-dried. Samples were imaged using a JEOL JEM-1400Plus TEM (120 kv) equipped with a 16MP digital camera (GATAN One View). Images were processed using ImageJ (National Institute of Health).

3.6 *In vitro* treatments

For *in vitro* experiments, mouse SIM-A9 microglia were seeded at a density of 5 x 10^4 cells/well in 500 µL DMEM/F12 containing 10% FBS in a 24-well plate and allowed to adhere overnight (O/N). For inflammasome priming, SIM-A9 microglia were first stimulated with 100 ng/mL lipopolysaccharide (LPS; from *Escherichia coli* [O55:B5]) (Sigma; Cat# L6529) for 3 h. Following washing the cells once with serum-free DMEM/F12, cells were then treated with either 2.5 µM ASC, 2.5 µM αSyn, ASC-αSyn complexes (containing 2.5 µM ASC and 2.5 µM αSyn) for 24 h. After 24 h of treatment, supernatants and cell lysates were collected for various assays. All treatments were performed in DMEM/F12 media with 1% FBS and 1% P-S in a final volume of 200 µL, unless specified otherwise, with a minimum of two technical replicates (Figure 5C).

3.7 Immunocytochemistry (ICC)

SIM-A9 microglia were seeded at a density of 5 x 10^4 cells/well in 500 µL DMEM/F12 media with 10% FBS in a 24-well plate containing 100 µg/mL poly-D-Lysine (PDL)-coated (Sigma-Aldrich; Cat# A-003-E) coverslips. To confirm the microglial origin of mouse SIM-A9 microglia, rabbit anti-Iba-1 (1:500; Fujifilm Wako; Cat# 019-19741), rabbit anti-CD68 (1:100; Abcam; Cat# ab303565), mouse anti-MAP2 (1:250; Sigma-Aldrich; Cat# M4403) and rabbit anti-GFAP (1:250;

Dako; Cat# Z0334) were used. The remaining immunocytochemical steps were performed as described below.

Treatments were performed as described above in the ‘‘Cell Culture and Treatments’’ section. After the treatments, cells were washed once with PBS and fixed in 4% paraformaldehyde (PFA) (Biotium; Cat# 22023) dissolved in PBS for 15 min. For permeabilization, cells were washed once with PBS and incubated with 0.25% Triton X-100 for 10 min. Thereafter, cells were blocked using Dako Protein Block, Serum-Free (Agilent Technologies, Inc.; Cat# X0909) for 20 min and without washing, primary antibodies were diluted in Dako Antibody Diluent (Agilent Technologies, Inc.; Cat# S0809) and added O/N at 4°C in a humidified chamber. To create a humidified chamber, a Whatman filter paper was placed inside a large petri dish and PBS was added on top until the filter paper absorbs the solution and the dish containing coverslips with the primary antibodies was wrapped with parafilm. To visualize activation of the NLRP3 sensor and ASC speck formation, the mouse anti-NLRP3/NALP3 (1:100; Cryo-2; AdipoGen; Cat# AG-20B-0014-C100) and rabbit anti-ASC (1:100; clone AL177; AdipoGen; Cat# AG-25B-0006-C100) was used, respectively. After three washing steps in PBS, the secondary antibodies goat anti-mouse Alexa Fluor™ 488 (1:500; Invitrogen; Cat# A-11029) or goat anti-rabbit Alexa Fluor™ 488 (1:500; Invitrogen; Cat# A-11008) were applied for 30 min followed by three more washing steps. Along with the goat anti-rabbit antibody, Phalloidin-iFluor 594 Reagent (Abcam; Cat# ab176757) was added at a 1:2,000 ratio to stain actin filaments. Coverslips were quickly rinsed once in dH_2O and dried perpendicularly on a kimwipe and placed onto a microscope slide. Dako Fluorescent Mounting Medium (Agilent Technologies, Inc.; Cat# S3023) spiked with 5 µg/mL Hoechst 33258 was used to mount the coverslips.

To visualize caspase-1 activity, the FAM-FLICA® Caspase-1 (YVAD) Assay Kit (ImmunoChemistry Technologies LLC; Cat# 98) was used according to the manufacturer's protocol. A vial of FLICA was reconstituted with 50 µL DMSO to form the 150X stock. Immediately prior to addition to the samples and controls, FLICA was diluted 1:5 by adding 200 µL PBS to each vial to form the 30X FLICA solution and the 30X FLICA was used within 30 min or stored at ≤-20°C. Following treatments, the 24-well plate was centrifuged at 1,500 revolutions per minute (rpm) for 5 min and supernatants were collected. 1X FLICA with 1 µg/mL Hoechst 33342 was immediately added to the samples and controls and incubated for ~1 h at 37°C, mixing gently every 10-20 min to disperse the reagent. The cells were centrifuged at 1,500 rpm for 5 min and the overlay media containing FAM-FLICA was carefully removed and replaced with 1X Apoptosis Wash Buffer. The cells were incubated for 5 min at 37°C to allow any unbound FAM-FLICA to diffuse out of cells. The plate was re-centrifuged, and cells were fixed using Fixative at a dilution of 1:5 for 20 min at RT in the dark. The fixative was removed, and cells were allowed to dry for 15 min. The coverslips were briefly submerged in dH_2O and dried perpendicularly on tissue paper to remove excess dH_2O. Cells were mounted with mounting media onto a microscope slide and dried for a few min. Cells were viewed immediately with a fluorescence microscope since the FAM-FLICA fluorescent signal is not stable O/N.

All images were captured using Z-stack imaging, with a z-step of 0.8 µm, and with a 20x or 63x objective. Every image was imaged from the farthest point to the closest point from the objective. All images were acquired using a Leica STELLARIS 5 Confocal Microscope (Leica Microsystems). Image processing was accomplished using LAS X Office (Leica Microsystems) and image analysis (150-1200 cells per replicate sample; 20x images only) was completed using

ImageJ (National Institute of Health). The total number of cells and NLRP3 mean fluorescence intensity was performed using automated counting, whereas the number of ASC specks and active caspase-1 cells were completed via manual counting and marking. The protocols for each analysis method are as follows (modified from the protocol available online from Christine Labno, University of Chicago, Integrated Light Microscopy Core):

Automated counting

1) Import or open the image to be counted with ImageJ. The colour image (red, green and blue; RGB) will have to be converted to greyscale before proceeding. Check that you have set Edit → Options → Conversions to "scale when converting." Then use Image → Type → 16-bit to convert to greyscale.
2) Once the image is in greyscale, adjust the threshold to highlight all the cells you want to count. Use Image → Adjust → Threshold. Check the option "Dark background" and change the colour to "Red". Use the slider to highlight the cells red and until all the foreground is red in a dark background. Click "Apply" and close the Threshold window.
3) To convert the image into a binary image, use Process → Binary → Make Binary.
4) To convert grouped or clustered cells into single cells, use Process → Binary → Watershed. The software will add a 1-pixel thick line where it feels the division between cells should be.
5) To count the number of cells, use Analyze → Analyze Particles. Change the size to "200 – 25000" and check the "Pixel units" box. Adjust the size range if too many small "noise" pixels are being counted as pixels, or if you wish to exclude particles based on size.

Circularity excludes particles based on how close to perfectly round they are. Change the circularity to "0.4 – 1.0". To include or exclude particles, adjust these numbers, considering that 0.00 is a straight line and 1.00 is a perfect circle. In the "Show" dropdown, select "Outlines" to count the number of all particles. Check the "Summarize" and "Exclude on edges" boxes and click OK.

6) To continue the analysis and measure the fluorescence intensity of the cells, select the particles to be analyzed by retrieving the watershed image and use Analyze → Measure. Re-use Analyze → Analyze Particles and check the "Add to Manager" box and click OK. The cells from the watershed image will now be converted into numbered cells. The area and intensity will be assigned to the specific cell number.
7) Next, use Analyze → Set Measurements. Check the "Area" and "Mean gray value" boxes and click OK.
8) Import the original, unthresholded image into the software and open the ROI Manager window. Check the "Show All" and "Labels" boxes.
9) To measure the area and intensity of all the cells, hold down the Shift key and select the first ROI. Without releasing the Shift key, scroll down to the last ROI and select the last ROI. All the ROIs will be selected and click Measure. The Results window will display the area and mean of each particle. Use Results → Summarize. The mean fluorescence intensity of all the cells in the image will be calculated, including the minimum and maximum intensity of a particle.

Manual cell counting and marking

1) To manually count/mark ASC specks and active caspase-1 cells, install the Cell Counter plugin, which is widely available on the internet upon a quick search.
2) Import or open the image to be counted with ImageJ. Compared to the "Automated counting" protocol above, the colour image (RGB) does not have to be converted to greyscale. Colour images are preferred to ensure an accurate analysis.
3) Use Plugins → Cell Counter and a cell counter window will open, where next to each type of count, a tally will be kept.
4) To start counting, click "Initialize" and a counter window will open. Select a type of counter and begin counting.
5) Use Results → Save to save your counts as Excel formatted files.

3.8 Protein quantification

To determine the protein concentration of cell lysates used for immunoblotting, a *DC* (detergent compatible) Protein assay was performed (Bio-Rad) according to the manufacturer's microplate assay protocol. The working reagent was prepared as needed, adding 20 µL of reagent S to each mL of reagent A, and five dilutions of a BSA protein standard containing from 0.2 mg/mL to 1 mg/mL protein. The absorbance was measured at 750 nm with a standard laboratory spectrophotometer.

To determine the protein concentration of cell lysates used for Simple Western immunoassays, a QuantiPro™ bicinchoninic acid (BCA) assay (Sigma; Cat# QPBCA) was performed according to the manufacturer's instructions using 96-well plate format (Becton

Dickinson; Cat# 351172). Two µL of lysate was added to 150 µL of MilliQ water (mQH_2O) in wells of a 96-well plate, then 150 µL of BCA reagent, prepared according to the manufacturer's instructions, was added with gentle mixing by pipetting. The plate was incubated at 60°C for 1 h in a Shel-Lab 1300U oven and cooled to RT. The absorbance was measured at 560 nm with a microplate reader and compared to BSA standards (0.5-20 µg/mL) prepared in mQH_2O from a 50 µg/mL stock.

3.9 Immunoblotting (IB)

To confirm the purity of human recombinant ASC and αSyn monomers and formation of ASC oligomers, they were subjected to sodium dodecyl sulfate–polyacrylamide gel electrophoresis (SDS-PAGE) and western blot analysis. To identify molecular masses of ASC and αSyn, primary antibodies against rabbit ASC (1:1,000; AdipoGen; Cat# AG-25B-0006-C100) and mouse αSyn (1:1,000; Abcam; Cat# ab27766), respectively, were used. The remaining steps were performed as described below.

Mouse SIM-A9 microglia were seeded at a density of 2.2 x 10^5 cells/well in 2 mL DMEM/F12 containing 10% FBS in a 6-well plate and allowed to adhere O/N. Following inflammasome priming with 100 ng/mL LPS for 3 h, cells were treated as described in the ''Cell Culture and Treatments'' section above. Treatments were performed in DMEM/F12 media with 1% FBS and 1% P-S in a final volume of 1 mL. Cell lysates were subjected to western blot analysis to determine the protein levels of NLRP3, ASC, full-length and cleaved caspase-1, and full-length and cleaved GSDMD, in cell lysates. For lysate collection, cells were scraped off the well plate in PBS, centrifuged at 3,000 rpm for 5 min at 4°C and pellets were lysed on ice using 1X

radioimmunoprecipitation buffer (RIPA) buffer (Sigma; Cat# R0278) supplemented with freshly added 1X Protease/Phosphatase Inhibitor Cocktail (PI) (ThermoScientific; Cat# 1861280). Cell lysates were denatured in 4x LaemmLi Sample Buffer (Bio-Rad; Cat# 1610747) for 5 min at 95°C. Proteins at 20, 30, and 40 µg were separated on a 4-20% Mini-PROTEAN TGX™ SDS–polyacrylamide Precast gel (Bio-Rad; Cat# 4561093) at 140V for ~1 h in 1x Tris/Glycine/SDS Buffer (Bio-Rad; Cat No.: 1610732) and transferred to 0.2 µm polyvinylidene difluoride (PVDF) membranes (Bio-Rad; Cat# 1620177) at 100V for 1 h in 1x Tris/Glycine Buffer (Bio-Rad; Cat No.: 1610734). After the transfer and before blocking, PVDF membranes were incubated with Ponceau S Staining Solution (ThermoScientific; Cat# A40000279) for 15 min at RT with gentle agitation to help quantify the protein transfer and allow for standardization of protein loading between lanes. The membrane was carefully washed in ultrapure water for 30–90 seconds or until the desired staining intensity was achieved. The blot was imaged using the Ponceau S imaging function and the membrane was de-stained by washing with TBS containing Tween (TBS-T; ThermoScientific; Cat# 28360) until all the "red" stain was removed. Membranes were then blocked with TBS-T in 5% non-fat dry milk (Bio-Rad; Cat# 1706404) for 1 h at RT. Post-blocking, membranes were processed and incubated O/N at 4°C with primary antibodies against mouse NLRP3 (AdipoGen; Cat# AG-20B-0014-C100), rabbit ASC (AdipoGen; Cat# AG-25B-0006-C100), mouse caspase-1 (Adipogen; Cat# AG-20B-0042), and rabbit GSDMD (Abcam; Cat# ab209845) at a 1:1,000 dilution in TBS-T in 5% non-fat dry milk. The membranes were washed 3 times for 10 min each in TBS-T on a horizontal shaker and later incubated with goat anti-rabbit (1:10,000; Sigma; Cat# A0545) and rabbit anti-mouse (1:7,500; Sigma; Cat# A9044) horseradish peroxidase (HRP)–conjugated secondary antibodies in TBS-T containing 5% non-fat dry milk. The membranes

were again washed 3 times for 10 min each in TBS-T. Immunoreactive proteins were visualized by the addition of SuperSignal™ West Pico PLUS Chemiluminescent Substrate (ThermoScientific; Cat# 34577) for 5 min and were imaged with the ChemiDoc™ Imaging System (Bio-Rad). Densitometric, semi-quantitative analysis of immunoblots was performed using ImageLab software (Bio-Rad). Band intensity measurements obtained from proteins of interest were normalized to the Ponceau S stain (total lane protein) and divided by the untreated control (UT ctrl) and graphically displayed as fold changes.

3.10 Simple Western immunoassay and Wes-based visualization of protein electrophoresis

Simple Western analysis was performed on a Wes instrument (ProteinSimple; Cat# 004–600) according to the manufacturer's instructions using a 12–230 kDa Separation Module (ProteinSimple; Cat# SM-W001) under reducing and denaturing conditions and the Anti-Rabbit Detection Module (ProteinSimple; Cat# DM-001) or the Anti-Mouse Detection Module (ProteinSimple; Cat# DM-002), depending on the primary antibody used.

Cell pellets were collected as mentioned in the ''Immunoblotting" section above. One hundred µL of 1X RIPA buffer with 1X PI was added to each cell pellet on ice and the lysate was incubated on ice for 30 min. Lysates were later centrifuged at 21,000 x g for 10 min at 4°C. Samples were diluted to a concentration of 0.5 µg/mL (which results in a loading amount of 0.5 µg of total protein per capillary) in 0.1X sample buffer (ProteinSimple; Cat# 042-195), then mixed with Master Mix (ProteinSimple; Cat# PS-ST03) at a 1:4 ratio (1 µL of Master Mix and 4 µL of sample) and heated at 95°C for 5 min. Samples were cooled to RT, vortexed to mix and

centrifuged in a Mandel mini microfuge. Five µL of biotinylated ladder (ProteinSimple; Cat# PS-ST01-8) was loaded in the first well of row A1. Three µL of samples were loaded in the remaining wells of row A. Ten µL of antibody diluent (ProteinSimple; Cat# 042-203) was added to row B and the first well of row C. Primary antibodies against mouse, rabbit ASC, mouse caspase-1, and rabbit GSDMD were diluted with antibody diluent at a 1:100 dilution and added to the remaining wells of row C. Ten µL of streptavidin-HRP (ProteinSimple; Cat# 042-414) was added to the first well of row D. Secondary antibodies were added to the other wells of row D. Luminol (ProteinSimple; Cat# 043-311) and peroxide (ProteinSimple; Cat# 043-379) were mixed (200 µL of each) and 15 µL was added to each well of row E. The plate (ProteinSimple; Cat# SM-W004-1) was covered with a lid and centrifuged at 1,200 x g for 10 min in an Eppendorf 5810R centrifuge. Five hundred µL of wash buffer (ProteinSimple; Cat# 042-202) was added to three rows of wells on the plate. The foil was removed from the separation reagents and the plate and capillaries (ProteinSimple; Cat# SM-W008-1) were placed in Wes. Wes was run according to the following protocol (Table 1): separation at 375 V for 28 min; blocking reagent for 5 min, primary and secondary antibody for 30 and 60 min, respectively; Luminol/peroxide chemiluminescence detection for ~15 min (exposures of 1-2-4-8-16-32-64-128-512 seconds). Anti-actin-HRP (Sigma; Cat# A3854) was used as a protein loading control (1:500 dilution in antibody diluent).

The resulting electropherograms were inspected to check whether automatic peak detection required any manual correction. Automatically detected peaks were quantified by calculation of the area under the curve. Band intensity measurements obtained from proteins of interest were normalized to actin from its respective lane and divided by the UT ctrl and

graphically displayed as fold changes. Quantitative data analysis and generation of figures were performed using the Compass for Simple Western Software (ProteinSimple).

Table 1. Workflow of the Simple Western procedure including time to complete a Wes run.

Separation Matrix	
Well Row	L1
Load Time (sec)	200.0
Stacking Matrix	
Well Row	M1
Load Time (sec)	20.0
Sample	
Well Row	A1
Load Time (sec)	12.0
Separation Time (min)	28.0
Separation Voltage (volts)	375
Standards Exposure (sec)	4.0
EE Immobilization Time (sec)	200.0
Antibody Diluent Time (min)	5.0
Well Row	B1
Primary Antibody Time (min)	30.0
Well Row	C1
Secondary Antibody Time (min)	60.0
Well Row	D1
Detection	
Well Row	E1
Detection Profile	HDR
Exposure 1 (sec)	1.0
Exposure 2 (sec)	2.0
Exposure 3 (sec)	4.0
Exposure 4 (sec)	8.0
Exposure 5 (sec)	16.0
Exposure 6 (sec)	32.0
Exposure 7 (sec)	64.0
Exposure 8 (sec)	128.0
Exposure 9 (sec)	512.0

3.11 Measurement of cytokine and chemokine concentrations

Following treatment of SIM-A9 microglia, cell supernatants were collected and IL-1β and IL-18 levels were measured using the mouse IL-1β (R&D Systems; Cat# DY401-05) and IL-18 (R&D Systems; Cat# DY7625-05) enzyme-linked immunosorbent assays (ELISAs), respectively. ELISAs were performed according to the manufacturer's protocols in Immulon 4 HBX Flat Bottom Plates (ThermoScientific; Cat# 3855). TMB (3, 3', 5, 5'-tetramethylbenzidine) ELISA Substrate (High Sensitivity) (Abcam; Cat# ab171523) was added for 7 min and the reaction was terminated by adding 2 N H_2SO_4. The absorbance was measured at 450 nm with a microplate reader. Readings at 540 nm were subtracted from the readings at 450 nm.

The MILLIPLEX® Mouse Cytokine/Chemokine Magnetic Bead Panel (Millipore; MCYTOMAG-70K) was used to measure the secretion of several cytokines and chemokines, including IL-1α, IL-1β, IL-4, IL-6, IL-10, IP-10, KC, MCP-1, MIP-2, RANTES, and TNF-α. The assay was performed according to the manufacturer's protocols. One hundred and fifty μL of Drive Fluid PLUS was added to all wells and the plate was run on a MAGPIX® instrument with xPONENT® software. The Median Fluorescent Intensity was analyzed using a 4-parameter logistic curve-fitting method to calculate the concentration of each analyte.

3.12 Cell death/Cytotoxicity assay

Quantification of cell death and cell lysis was based on the measurement of lactate dehydrogenase (LDH), released from the cytosol of cells with plasma membrane damage, using the Cytotoxicity Detection Kit^{PLUS} (LDH) (Roche; Cat# 04744926001). Treatments were performed as described above in the ''Cell Culture and Treatments'' section. Subsequently, LDH release was

measured by adding 100 µL of freshly prepared Reaction mixture to 100 µL supernatant in a 96-well plate for 8 min at RT (protected from light). The reaction was stopped with 50 µL of the provided stop solution and absorbance was measured at 490 and 620 nm using a microplate reader (CLARIOstar Plus; BMG LabTech). Readings at 620 nm were subtracted from the readings at 490 nm. To determine the percentage cytotoxicity, the average absorbance values of the samples and controls was calculated (background subtracted from each) and substituted the resulting values in the following equation:

$$\text{Cytotoxicity } (\%) = \frac{\text{exp. value} - \text{low control}}{\text{high control} - \text{low control}} \text{ x } 100$$

Experimental controls included the background, low, and high control. Background control consisted of the assay medium only (without cells). In comparison, the low control consisted of cells treated with the assay medium only and the high control was prepared by adding 5 µL Lysis solution to cells and the incubating the plate at RT for 15 min.

3.13 Statistical analyses

Data are presented as mean ± standard error of mean (SEM) in all displayed diagrams. Statistical significance was calculated using an ordinary one-way ANOVA (analysis of variance) test followed by Tukey's multiple comparisons test where the means of the test columns was compared individually to the mean of every other column. Normal distribution (Gaussian distribution) was assumed for all tests. ASC-Aβ and ASC-BSA complexes (containing 1.75 µM ASC)

were not statistically compared to ASC only or ASC-αSyn complexes (containing 2.5 μM ASC) since they comprised of varying amounts of oligomerized ASC. Statistical significance was shown as: *p < 0.05, **p < 0.01, ***p < 0.001, ****p < 0.0001. All statistical analyses were performed using GraphPad Prism 9.0 (GraphPad Software Inc., San Diego, CA, USA).

4. RESULTS

4.1 Monomeric αSyn clusters around ASC fibrils, forming ASC-αSyn complexes

The inflammasome adaptor protein, ASC, is observed to be elevated in the SNpc of PD patients and multiple preclinical PD models (197). Moreover, Aβ monomers have been demonstrated to associate and bind to extracellular, microglia-derived ASC specks (196). To reproduce previous findings from the literature in my experimental setup and establish a positive control, ASC-Aβ complexes were produced. First, we produced recombinant human ASC protein by large scale expression of ASC in *E. coli* BL21 cells. Upon protein purification by SEC (data not shown), ASC was observed only in its monomeric form with an approximate size of 25 kDa, as shown by immunoblot (Figure 5A). To induce oligomerization, purified ASC protein monomers were buffer exchanged to ice-cold PBS using an Amicon® Ultra 0.5mL Centrifugal Filter (10 kDa MWCO) and later transferred into LoBind tubes for 1 h at 37°C to enable ASC 'prionoid' activity, as previously described (193). ASC specks were subjected to SDS-PAGE and immunoblot analysis, confirming the generation of ASC monomers (~25 kDa), dimers (~50 kDa) and higher order oligomers (>50 kDa) (Figure 5A). Next, oligomerized ASC (1.75 µM) with a ~3-fold molar excess of monomeric Aβ (5 µM) was co-incubated for 16 h at 37°C to enable protein complex formation, as described.

To characterize the ASC-Aβ complexes to be used as a positive control, negative stain electron microscopy (EM) was performed (193). The protein samples were applied to a glow discharged Copper grid and negatively stained with 2% uranyl acetate. In EM, ASC was seen to arrange into long, slightly twisted helical filaments showing a uniform surface (Figure 6A). In comparison, Aβ alone largely retained its monomeric form (Figure 6D).

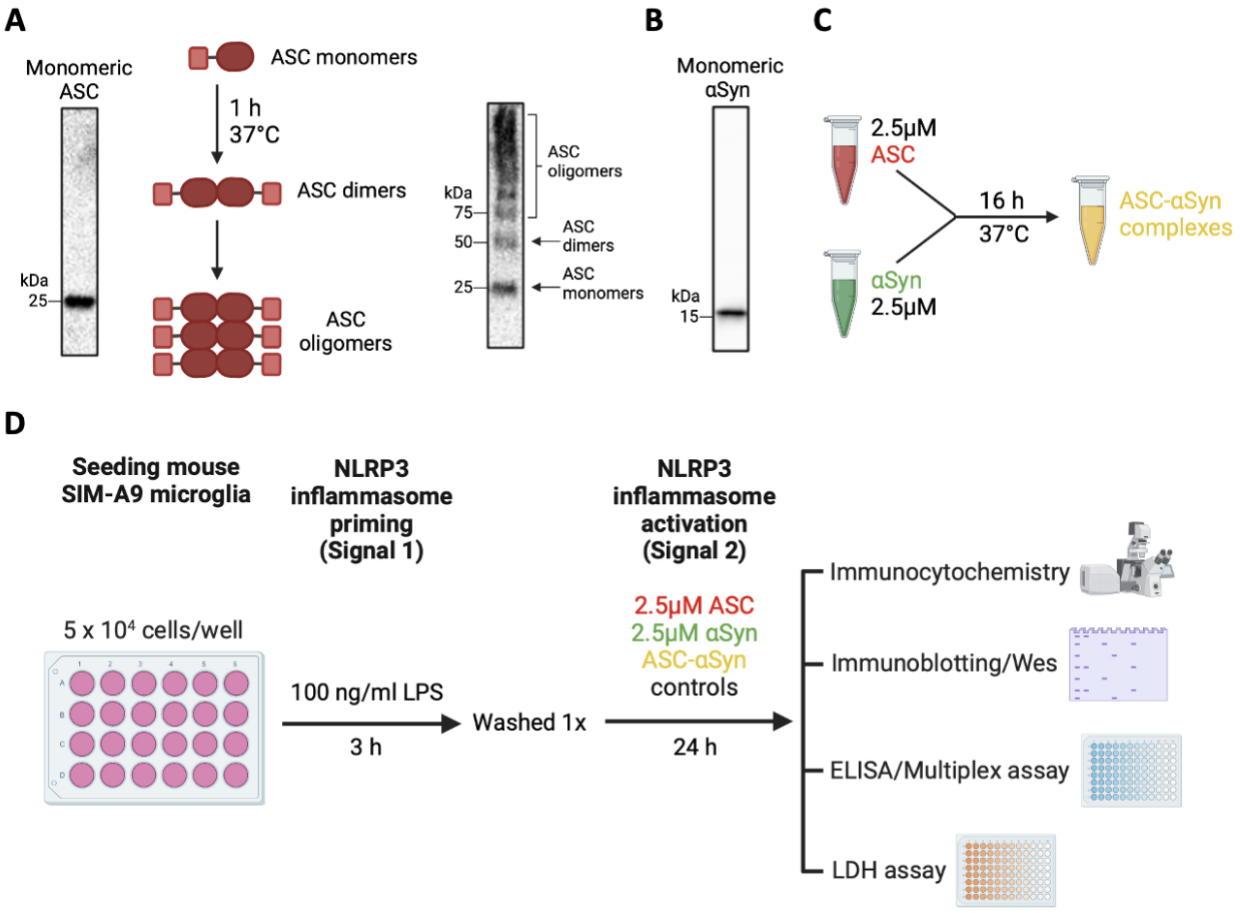

Figure 5. Experimental workflow used in this study.

(A) Schematic drawing of the formation of human oligomerized ASC. Purified A6 ASC protein (produced by Dr. David Cai) was transferred into LoBind tubes and oligomer formation was induced by incubation of ASC at 37°C for 1 h to enable ASC 'prionoid' activity, as described previously (193). Oligomerized ASC was produced and subjected to SDS-PAGE and Western blot analysis. Immunoblotting with an anti-ASC antibody identified bands for ASC at molecular masses corresponding to ASC monomers (~25 kDa), dimers (~50 kDa), and higher-order oligomers (>50 kDa). Data courtesy of Dr. David Cai. (B) Human monomeric αSyn (StressMarq; SPR-321) was subjected to SDS-PAGE and Western blot analysis, confirming its purity. (C) Schematic drawing of the ASC-αSyn complex-building protocol. Fibrillary ASC (2.5 μM) and αSyn monomers (2.5 μM) were incubated in DMEM/F12 containing 1% FBS and 1% P-S in LoBind Tubes at 37°C for 16 h. (D) Schematic drawing of the experimental setup used in this study. ASC-Aβ (1.75 μM ASC-5 μM Aβ) and ASC-BSA (1.75 μM ASC-5 μM BSA) were used as positive and negative controls, respectively (193). Figure was created with BioRender.com.

As expected, in samples that were co-incubated, Aβ monomers were found in close proximity to ASC fibrils, forming ASC-Aβ complexes (Figure 6E) (193).

After establishing the positive control, oligomerized ASC (2.5 μM; Figure 5A) was co-incubated with a 1:1 molar ratio of human, monomeric αSyn (2.5 μM; Figure 5B) for 16 h at 37°C to produce ASC-αSyn complexes (Figure 5B). αSyn alone maintained its monomeric structure under these conditions (Figure 6B), as observed in the literature, and clustered around ASC fibrils when co-incubated, confirming the binding of both proteins and the formation of ASC-αSyn complexes by EM (Figure 6C) (205). Both ASC-αSyn and ASC-Aβ complexes also revealed unbound αSyn and Aβ, respectively, suggesting not all monomers bind to the ASC fibrils.

4.2 ASC-Aβ complexes activate the NLRP3 inflammasome

Before assessing NLRP3 inflammasome activation in response to ASC-Aβ and ASC-αSyn complexes, mouse SIM-A9 microglia, a relatively novel cell line from spontaneously immortalized murine microglia, were characterized as a suitable *in vitro* model system (206). Microglia were chosen for experimentation since they are the resident immune effector cells of the CNS that express a wide array of PRRs, wherein the NLRP3 inflammasome is best characterized to mediate sterile inflammation in microglia (110,112). In addition, microglia have been reported to express all NLRP3 inflammasome components and substrates (113). SIM-A9 microglia expressed microglia/macrophage-specific proteins, ionized calcium-binding adapter molecule 1 (Iba-1) and cluster of differentiation 68 (CD68), suggesting the cells retained their microglial properties after their expansion (Figure 7). Conversely, SIM-A9 cells were not immunoreactive to either microtubule-associated protein 2 (MAP2) or glial fibrillary acidic protein (GFAP), signifying that

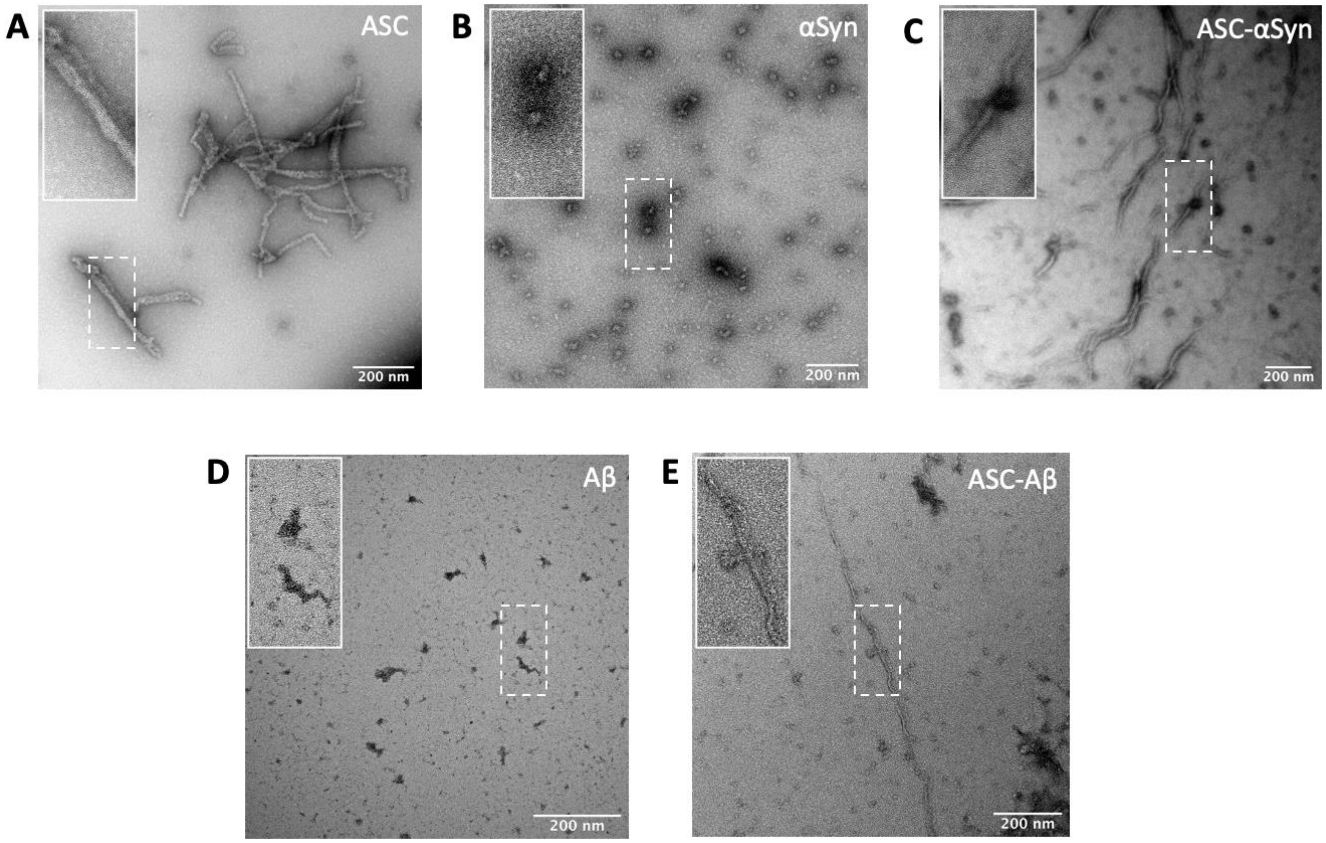

Figure 6. αSyn clusters around ASC fibrils, forming ASC-αSyn complexes.

(A–E) Transmission electron microscopy images of ASC fibrils (A), αSyn monomers (B), ASC-αSyn complex (C), Aβ monomers (D) and ASC-Aβ complex (E). ASC-Aβ complex was used as a positive control. Scale bars, 200 nm (A–E).

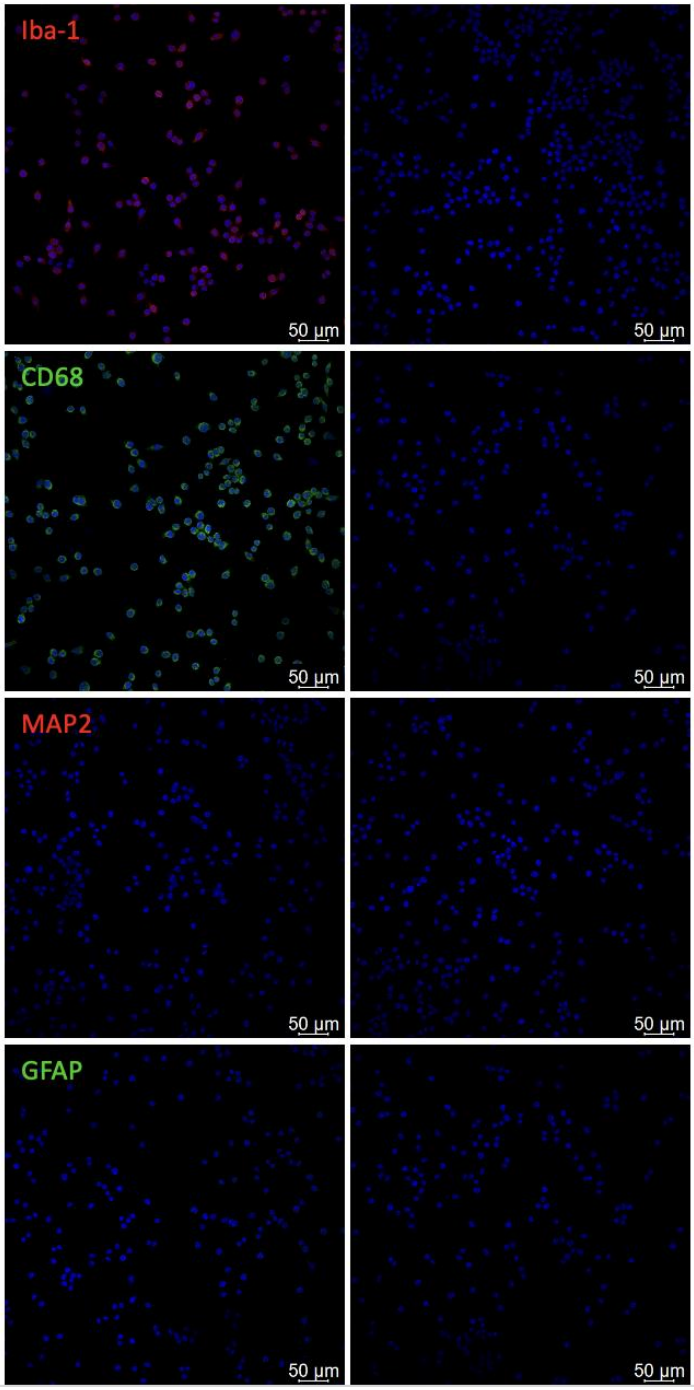

Figure 7. SIM-A9 cells express microglia/macrophage-specific proteins.

Immunocytochemical detection of Iba-1 and CD68, two microglia/macrophage-specific proteins, and MAP2 and GFAP, a marker for neurons and astrocytes, respectively, in untreated mouse SIM-A9 cells. Right panel shows secondary antibody controls against rabbit Iba-1 (rabbit Alexa 568), rabbit CD68 (rabbit Alexa 488), mouse MAP2 (mouse Alexa 568), and rabbit GFAP (rabbit Alexa 488). Hoechst 33258 highlights the cell nuclei. Images were taken at 20x magnification. Scale bars, 50 µm.

they do not express neuron- or astrocyte-specific proteins, respectively (Figure 7). Based on these findings, I concluded that SIM-A9 cells exhibit a microglia phenotype despite having been suggested to also display a neuronal-like morphology.

To analyze the effect of the ASC-Aβ complexes on NLRP3 inflammasome activation and subsequent IL-1β release in mouse SIM-A9 microglia, cells were primed with 100 ng/ml LPS for 3 h and stimulated with 1.75 μM ASC, 5 μM Aβ, or ASC-Aβ complexes for 12 h in DMEM/F12 media containing 1% FBS and 1% P-S. As expected, LPS stimulation of microglia induced priming of the inflammasome, as shown by an increased protein expression of the NLRP3 sensor in the cell lysate compared to untreated cells (Figure 8A and 8B). The addition of a second treatment post-LPS, including Aβ and ASC-Aβ complexes, led to further increases in the expression of NLRP3, signifying higher activation of the NLRP3 inflammasome. Interestingly, non-specific bands were observed near the molecular weight of ASC (~25 kDa) when probing for NLRP3 in the ASC-Aβ complex-treated group (Figure 8C), implying that NLRP3 particles may be a part of the ASC signal amplification platform (135). The levels of pro-caspase-1 remained relatively unaltered; however, cleaved caspase-1 peptide (p20) was undetectable in these samples (Figure 8A). Conversely, caspase-1-dependent IL-1β secretion was observed in response to treatment with ASC-Aβ complexes (Figure 8D), signifying occurrence of caspase-1 activation (and a technical limitation of detecting cleaved caspase-1 directly under these conditions). Compared to ASC and Aβ alone, the ASC-Aβ complexes produced a synergistic effect in the release of IL-1β.

To gain insight into the release of additional pro-inflammatory cytokines and chemokines, a multiplex bead array assay was performed. In principle, a mixture of colored beads coated with specific antibodies bind the analyte of interest, allowing for detection of numerous analytes

within the same sample in one experiment. The biotinylated detection antibodies, in turn, bind the analyte and an analyte-antibody sandwich is formed. Streptavidin conjugated with phycoerythrin (PE) binds the biotinylated detection antibodies and the signal strength of PE is proportional to the concentration of the specific analyte. LPS priming alone was sufficient to induce a multitude of pro-inflammatory cytokines and chemokines, including tumour necrosis factor-α (TNF-α), IL-6, C-X-C motif ligand 1 (KC, also referred to as CXCL1), IFNγ-induced protein 10 (IP-10, also referred to as CXCL10), monocyte chemoattractant protein-1 (MCP-1, also referred to as CCL2), macrophage inflammatory protein-2 (MIP-2), and regulated on activation, normal T cell expressed and secreted (RANTES; also referred to as CCL5) (Figure 9). IL-1α, a cytokine of the IL-1 family, was also released in response to LPS priming and further augmented when stimulated with ASC-Aβ complexes (Figure 9A). Very low concentrations of LPS have been shown to induce the production of various cytokines and chemokines, including IL-6 and TNF-α, and serve as a potent innate immune stimulus (207). However, when assessing inflammasome-specific cytokines, such as IL-1β, both a priming and activation signal are required and the effect of LPS alone on cytokine release is significantly diminished (Figure 8F). Together, upregulation in the NLRP3 inflammasome-dependent IL-1β and further inflammatory cytokines support that ASC-Aβ complexes can elicit a pro-inflammatory response and serve as a context-relevant positive control.

4.3 ASC-αSyn complexes activate the NLRP3 inflammasome

The effects of ASC-αSyn complexes (Figure 6C) were next tested on SIM-A9 microglia to determine whether they too activate the NLRP3 inflammasome. Comparable to the treatments

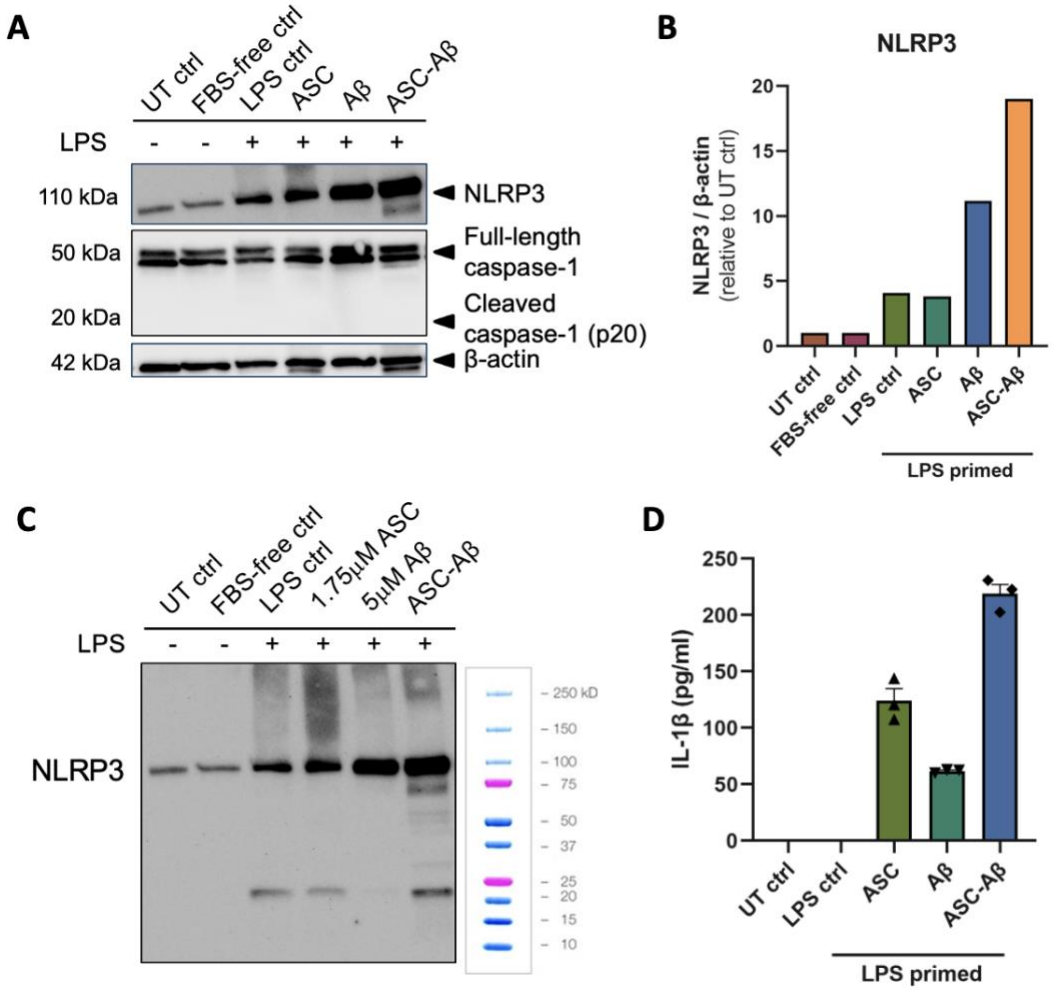

Figure 8. ASC-Aβ complexes activate the NLRP3 inflammasome and induce IL-1β release.

(A-C) Western blot analysis and quantification of cell lysates (20 µg) of SIM-A9 microglia primed for 3 h with 100 ng/mL LPS and exposed to 1.75 µM ASC, 5 µM Aβ, or 1.75 µM ASC-5 µM Aβ complexes for 12 h. Blot of cell lysates of SIM-A9 microglia (A) was immunostained for NLRP3, caspase-1 and β-actin (loading control). Data was collected from one independent experiment (n = 1) and normalized to β-actin. Using the normalized values, the fold change (ratio of the experimental sample to the UT control) for each sample was calculated. (C) Full blot probed with an anti-NLRP3 antibody. (D) IL-1β levels in conditioned medium of SIM-A9 microglia (n = 1 single experiment with triplicate treatments for all conditions). The graphs are presented as mean ± SEM. Recombinant human Aβ (Biomatik) was used in these experiments.

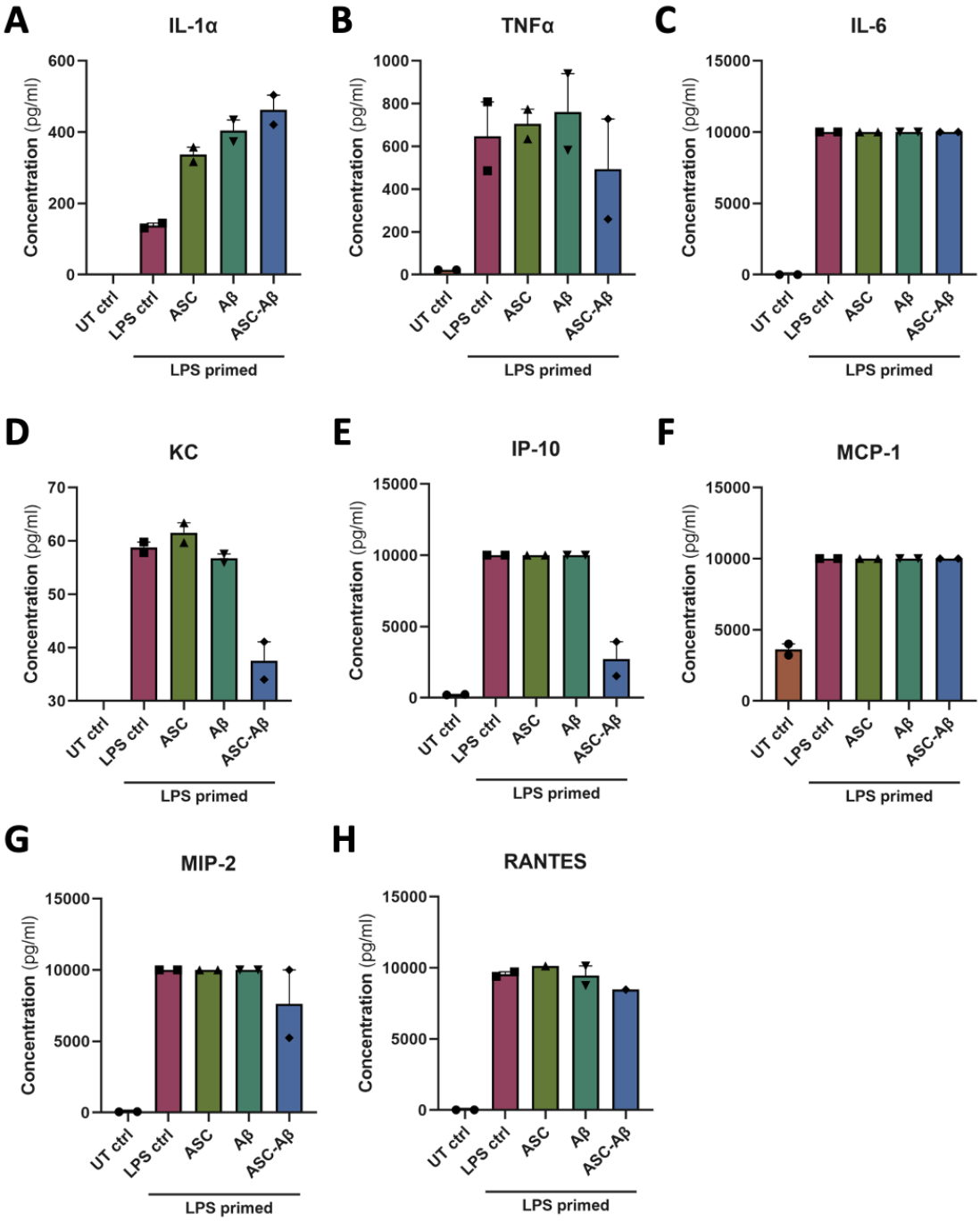

Figure 9. ASC-Aβ complexes induce pro-inflammatory cytokine and chemokine release.

(A–H) IL-1α (A), TNF-α (B), IL-6 (C), KC (D), IP-10 (E), MCP-1 (F), MIP-2 (G) and RANTES (H) levels in conditioned medium of SIM-A9 microglia after 3 h exposure of 100 ng/ml LPS followed by 12 h exposure of 1.75 µM ASC, 5 µM Aβ, or 1.75 µM ASC-5 µM Aβ complexes, as revealed by a MILLIPLEX® Mouse Cytokine/Chemokine Magnetic Bead Panel. Data was collected from one single experiment (n = 1) with two technical replicates per assay (N = 2). All graphs are presented as mean ± SEM. Recombinant human Aβ (Biomatik) was used in these experiments.

with ASC-Aβ complexes, SIM-A9 microglia were primed with 100 ng/ml LPS for 3 h followed by treatment with 2.5 µM ASC, 2.5 µM αSyn, ASC-αSyn complexes or controls for 24 h in DMEM/F12 media containing 1% FBS and 1% P-S (as shown in Figure 5C). ASC-Aβ complexes were utilised as a positive control, whereas ASC-BSA complexes were employed as a negative, non-amyloidogenic control to confirm specific interactions of ASC to αSyn and subsequent inflammatory responses. Compared to untreated cells, LPS treatment only induced priming of the NLRP3 inflammasome (~5.1-fold increase), as revealed via ICC with an anti-NLRP3 antibody (Figure 10A and 10B). Untreated microglia also expressed a baseline level of NLRP3, as microglia are constantly involved in immune surveillance and are not considered inactive in their 'resting' state, as historically described (113,208). Following LPS priming, treatment with αSyn, ASC and ASC-αSyn complexes displayed an increased fluorescence intensity similar to ASC-Aβ complexes, suggesting activation of the NLRP3 inflammasome (Figure 10A and 10B). After 27 h of treatments and NLRP3 inflammasome activation, microglia displayed unique morphologies, suggestive of an alteration in homeostasis (Figure 10A; bottom row).

Upon inflammasome activation, ASC assembles into an ASC speck, a large protein complex. ASC speck formation has been used as a readout for inflammasome activation (209). Cell-derived ASC specks can be observed as they reach a diameter between ~800 and 1000 nm and in most cells only one speck forms upon inflammasome activation (210). In contrast to the LPS control, treatment with ASC-αSyn complexes demonstrated a significant increase in ASC speck formation when probed with an anti-ASC antibody and a phalloidin conjugate to highlight filamentous actin (F-actin) (Figure 11A and 11B). Additionally, ASC-αSyn complex-treated cells displayed a ~1.7- and 2.5-fold increase in ASC specks than ASC and αSyn treatments alone,

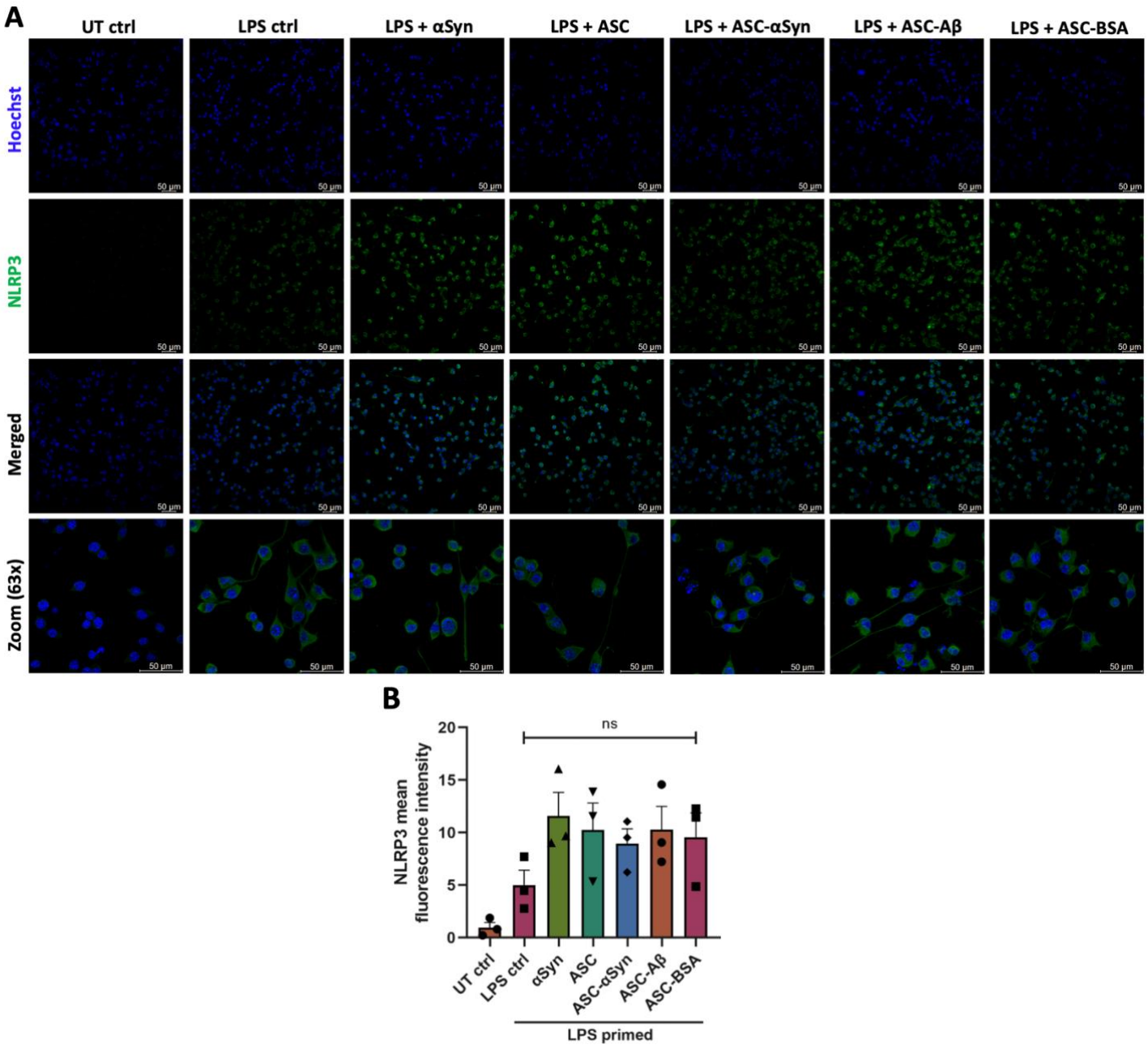

Figure 10. ASC-αSyn complexes activate the NLRP3 inflammasome via increased expression of NLRP3.

(A–B) Immunocytochemical detection and quantification of NLRP3 protein (B) in mouse SIM-A9 microglia after 3 h exposure of 100 ng/ml LPS followed by 24 h exposure of ASC, αSyn, or ASC-αSyn complexes. Anti-NLRP3 antibody was used for the detection of NLRP3. Images were taken at 20x and 63x magnification. Scale bars, 50 µm. Data was collected from three independent experiments (n = 3). The graph is presented as mean ± SEM and was analyzed by one-way ANOVA followed by Tukey's post-hoc multiple comparisons test, where "ns" indicates not significant.

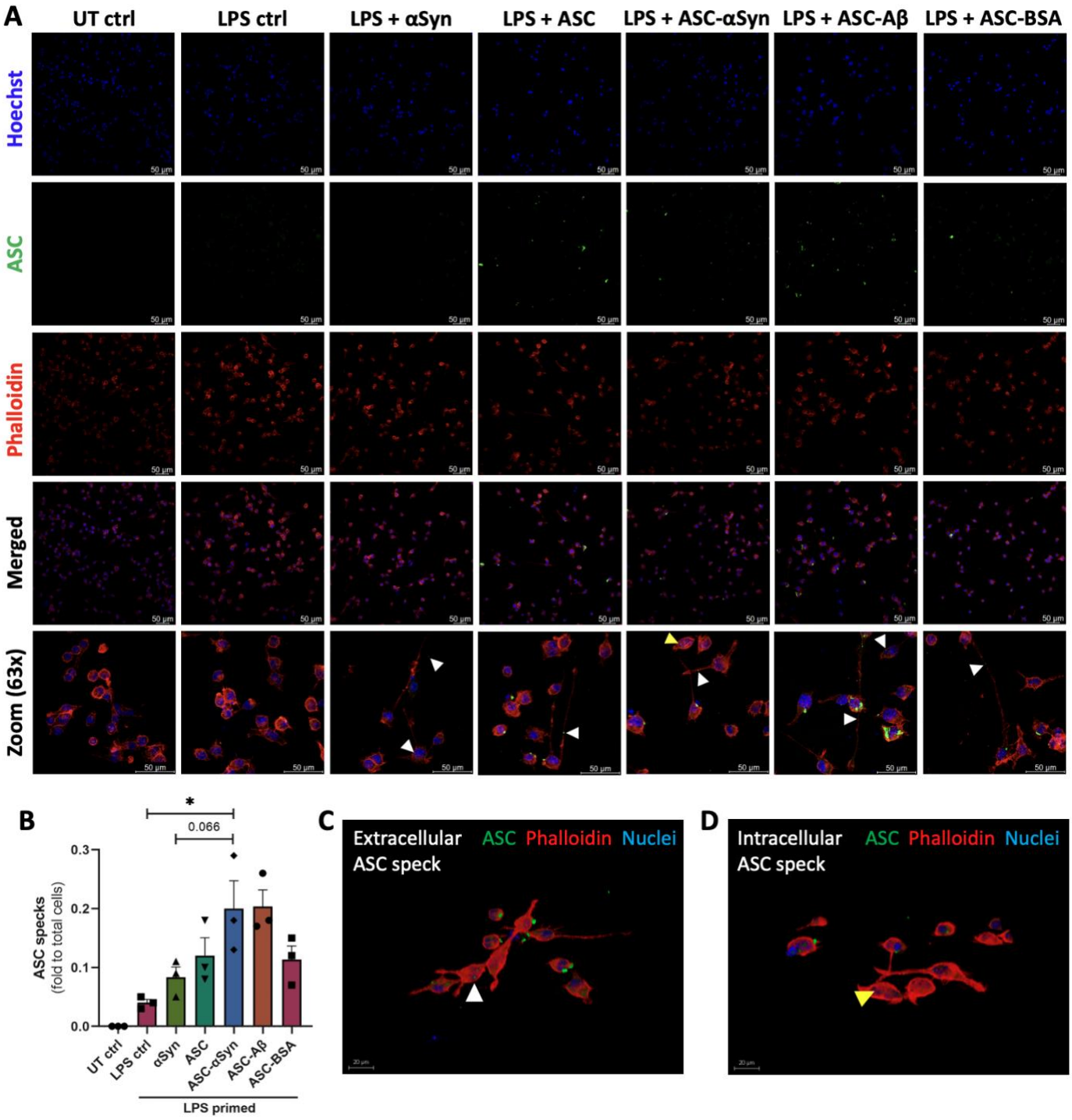

Figure 11. ASC-αSyn complexes activate the NLRP3 inflammasome via increased ASC speck formation.

(A–B) Immunocytochemical detection and quantification of ASC specks (B) in mouse SIM-A9 microglia after 3 h exposure of 100 ng/ml LPS followed by 24 h exposure of ASC, αSyn, or ASC-αSyn complexes. Anti-ASC antibody was used for the detection of ASC. (C and D) 3D projection

of extracellular (C) and intracellular (D) ASC specks from ASC-αSyn complex-treated cells. Yellow arrowheads point to the same ASC speck, highlighting its intracellular localization (A and D). *Arrowheads show ASC specks, which are ~1 µm in size. Images were taken at 20x and 63x magnification. Scale bars, 20 (C and D) and 50 µm (A). Data were collected from three independent experiments (n = 3). The graph is presented as mean ± SEM and was analyzed by one-way ANOVA followed by Tukey's post-hoc multiple comparisons test. Levels of significance are indicated as follows: *$p < 0.05$. Asterisks indicate significance between groups.

respectively, signifying an amplified level of NLRP3 inflammasome activation (Figure 11B). Interestingly, ASC specks are released by inflammasome-activated cells into the extracellular space, where they outlive cells and continue to recruit and activate pro-caspase-1 and catalyze the maturation of IL-1β (137,138). 3D projections of microglia treated with ASC-αSyn complexes confirmed both the extracellular (Figure 11C) and intracellular (Figure 11D) localization of ASC specks with respect to F-actin. Localization of ASC specks is better illustrated when observing 3D projection movies (Figure S1). Due to the addition of recombinant ASC to induce inflammasome activation, incubation with an anti-ASC antibody also highlighted numerous, recombinant ASC structures of large sizes amongst cell-derived ASC specks. Thus, endogenous ASC specks were counted for analysis based on known size and localization; this analysis requires further optimization for more accurate quantification.

Next, to monitor caspase-1 cleavage post-ASC speck formation, I examined caspase-1 activity using the FAM-FLICA® Caspase-1 assay after 24 h of ASC-αSyn complex treatment. Fluorescent-labeled inhibitor of caspases (FLICA) is a cell-permeant, non-cytotoxic probe that covalently binds to active caspase enzymes by recognizing a specific amino acid sequence (YVAD) that is sandwiched between a green, fluorescent label, carboxyfluorescein (FAM), and a fluoromethyl ketone (FMK) (211,212). Compared to ASC and αSyn alone, immunofluorescence microscopy analysis revealed increased caspase-1 activity in response to ASC-αSyn treatment (2- and 6-fold increase in the number of active caspase-1 cells, respectively; Figure 12A and 12B). In the ASC-αSyn complex-treated sample, a higher number of cells appeared brighter in the green channel, indicating an increased level of caspase-1 activity (Figure 12A). Remarkably, activated caspase-1-positive cells resembled cells undergoing pyroptosis, displaying nuclear condensation,

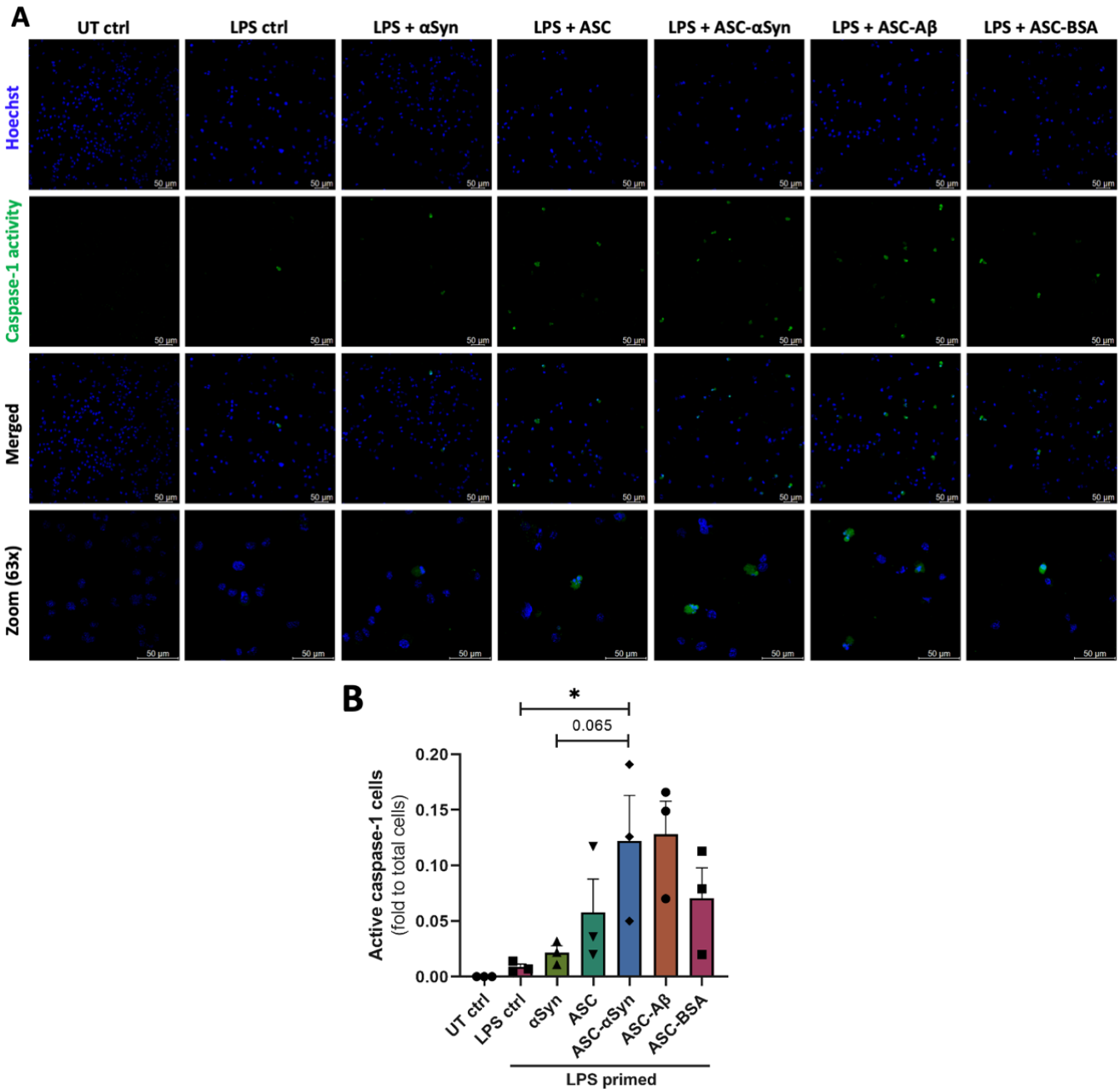

Figure 12. ASC-αSyn complexes increase caspase-1 activity using FAM-YVAD-FMK.

(A–B) Immunocytochemical detection and quantification of caspase-1 activity in mouse SIM-A9 microglia after 3 h exposure of 100 ng/ml LPS followed by 24 h exposure of ASC, αSyn, or ASC-αSyn complexes. The FAM-FLICA® Caspase-1 (YVAD) Assay Kit was used for the detection of caspase-1 activity. Images were taken at 20x and 63x magnification. Scale bars, 50 μm. Data was collected from three independent experiments (n = 3). The graph is presented as mean ± SEM and was analyzed by one-way ANOVA followed by Tukey's post-hoc multiple comparisons test. Levels of significance are indicated as follows: *p < 0.05. Asterisks indicate significance between groups.

membrane ballooning and rupture (Figure 12A; bottom row) (174). Previously while establishing the positive control, cleaved caspase-1 was undetectable in response to ASC-Aβ treatment by immunoblotting yet displayed caspase-1-dependent release of cytokines, such as of IL-1β (Figure 8A and 8F). Here, caspase-1 activation was visualized, thus supporting the findings of ASC-Aβ complex formation as a positive control (193). In contrast, ASC-BSA complexes generated a similar activity for caspase-1 to that of ASC exposure only, confirming its non-cytotoxic effects, in contrast to the effects of binding of αSyn or Aβ to ASC. Overall, ASC-αSyn complexes amplified the pro-inflammatory response mediated by the NLRP3 inflammasome and the resulting activation of caspase-1.

To further assess the effects of ASC-αSyn complexes on NLRP3 inflammasome activation and support the findings from above, Western blot analysis of cell lysates was performed using antibodies against NLRP3, caspase-1 and GSDMD (Figure 13). Comparable to the immunofluorescence microscopy analysis, priming with LPS and stimulation with the various inducers increased NLRP3 protein levels in comparison to untreated cells, indicating activation of the NLRP3 inflammasome (Figure 13B). Again, cleaved caspase-1 (p20) peptide was not detectable under these experimental conditions; however, a reduction in the full-length caspase-1 protein was observed, indirectly implying conversion to the cleaved caspase-1 subunits (Figure 13C). ASC-αSyn complex-treated cells displayed a significant, 1.3-fold decrease in full-length caspase-1 compared to LPS alone whereas ASC-treated cells revealed a trend towards a decrease (p-value = 0.09; Figure 13C). On the contrary, insignificant differences were observed in the full-length protein levels of GSDMD (Figure 13D). GSDMD, a substrate of caspase-1, is required for pyroptosis and for the secretion of IL-1β (116). Yet compared to LPS- and αSyn-treated cells,

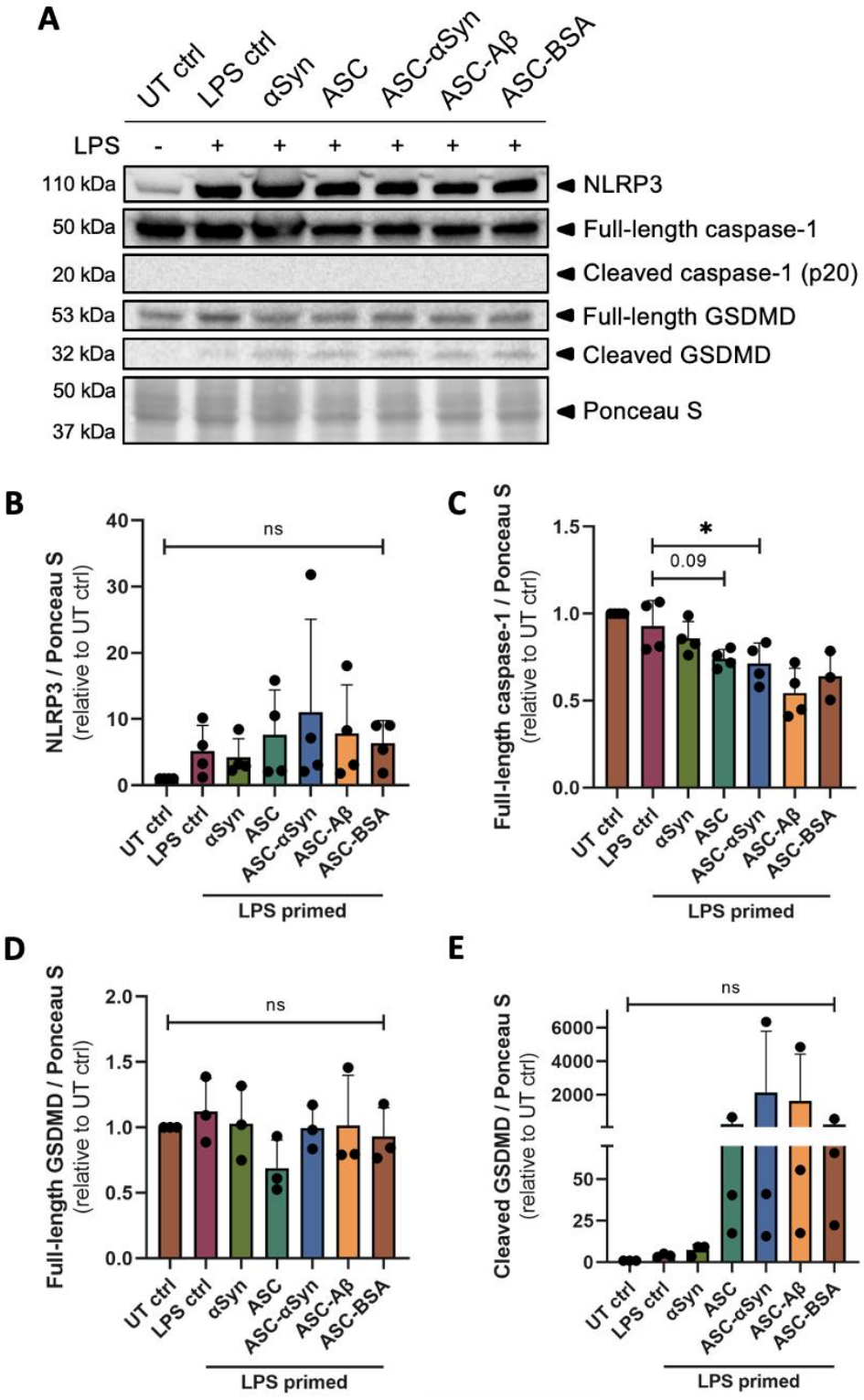

Figure 13. Detection of the NLRP3 inflammasome pathway via immunoblotting.

(A–E) Western blot analysis and quantification of cell lysates from SIM-A9 microglia that were primed for 3 h with 100 ng/mL LPS and exposed to ASC, αSyn, or ASC-αSyn complexes for 24 h.

Blots of cell lysates of SIM-A9 microglia (B–E) were stained for NLRP3 (B), caspase-1 (C), and full-length and cleaved GSDMD (D and E). Data were collected from three (D and E) or four (B and C) independent experiments (n = 3 or 4) and normalized to the total protein stain (Ponceau S). Using the normalized values, the fold change (ratio of the experimental sample to the UT control) for each sample was calculated. All graphs are presented as mean ± SEM and were analyzed by one-way ANOVA followed by Tukey's post-hoc multiple comparisons test. Levels of significance are indicated as follows: *$p < 0.05$. Asterisks indicate significance between groups and "ns" indicates not significant.

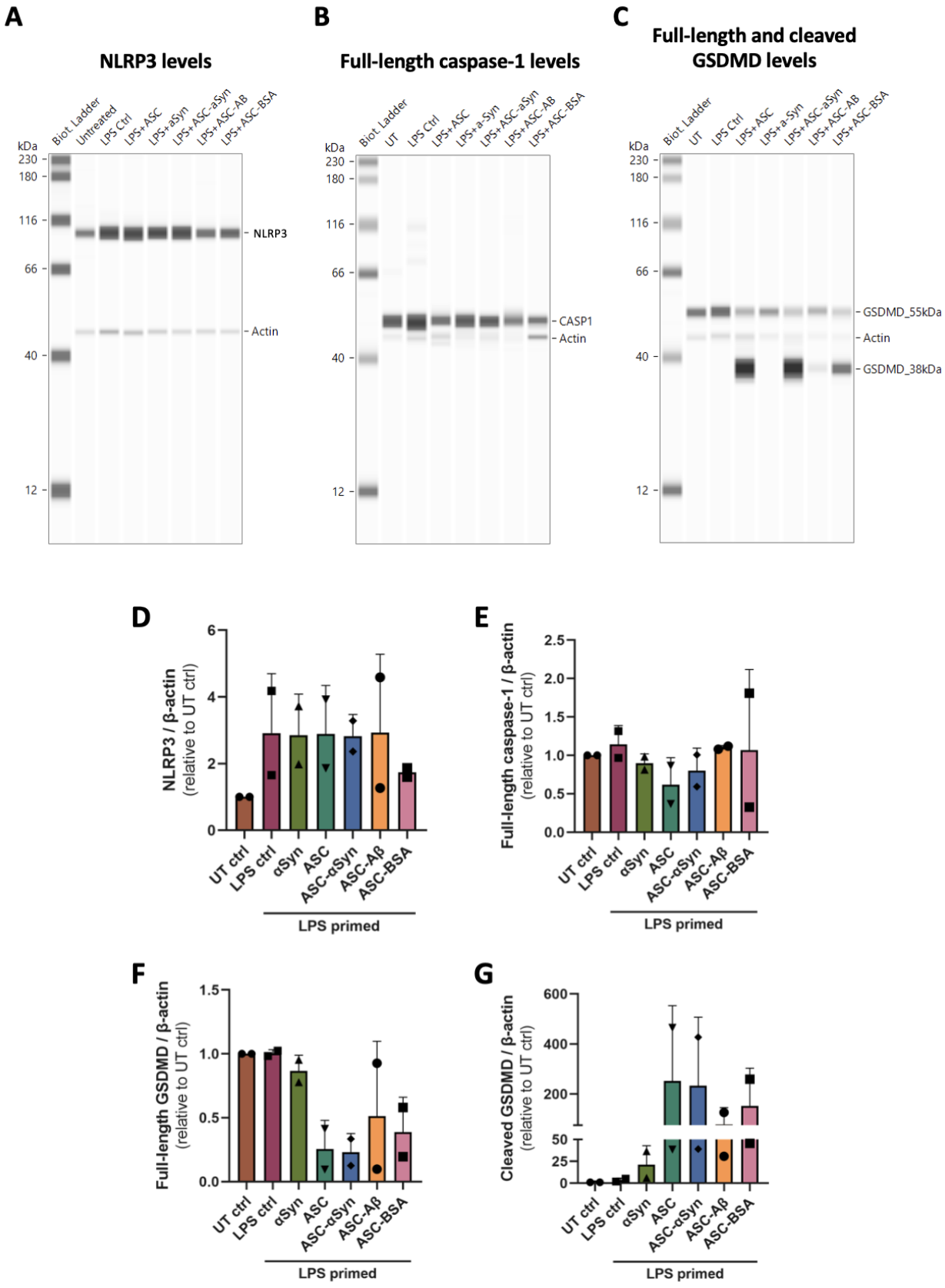
A
NLRP3 levels
Biot. Ladder
Untreated
LPS Ctrl
LPS+ASC
LPS+aSyn
LPS+ASC-aSyn
LPS+ASC-Aß
LPS+ASC-BSA
kDa
230
180
116
66
40
12
NLRP3
Actin
B
Full-length caspase-1 levels
Biot. Ladder
UT
LPS Ctrl
LPS+ASC
LPS+a-Syn
LPS+ASC-aSyn
LPS+ASC-AB
LPS+ASC-BSA
CASP1
Actin
C
Full-length and cleaved GSDMD levels
GSDMD_55kDa
Actin
GSDMD_38kDa
D
NLRP3 / β-actin (relative to UT ctrl)
E
Full-length caspase-1 / β-actin (relative to UT ctrl)
F
Full-length GSDMD / β-actin (relative to UT ctrl)
G
Cleaved GSDMD / β-actin (relative to UT ctrl)
UT ctrl
LPS ctrl
αSyn
ASC
ASC-αSyn
ASC-Aβ
ASC-BSA
LPS primed

Figure 14. Detection of the NLRP3 inflammasome pathway via Simple Western.

(A–G) Simple Western analysis of cell lysates from SIM-A9 microglia that were primed for 3 h with 100 ng/mL LPS and exposed to ASC, αSyn, or ASC-αSyn complexes for 24 h. Virtual blot-like images (A-C) display chemiluminescent signal generated from peak areas after incubation with primary antibodies against NLRP3 (A and D), full-length caspase-1 (B and E), and full-length (C and F) and cleaved GSDMD (C and G). β-actin was used as a protein loading control. Data were collected from two independent experiments (n = 2). All graphs are presented as mean ± SEM. Data courtesy of Ewa Baumann (A-C).

augmented levels of cleaved GSDMD were detected in all the experimental conditions containing oligomerized ASC, suggesting the induction of pore formation and pyroptosis (Figure 13E). Similar results were demonstrated using Simple Western-based readouts of the cell lysates to detect the protein levels of NLRP3, full-length and cleaved caspase-1 and GSDMD (Figure 14). In general, Simple Western-based detection systems provide more precise and sensitive quantification of protein expression levels, wherein proteins are size-separated in capillaries, compared to conventional immunoblotting (213,214). Likewise, LPS priming upregulated NLRP3 at the protein level (Figure 14D). Treatment with inflammasome activators, including oligomerized ASC and ASC-αSyn complexes, following LPS priming also reduced the levels of full-length caspase-1, suggesting cleavage of caspase-1 into its subunits (Figure 14E). Importantly, Simple Western analysis further revealed a major reduction in full-length GSDMD, specifically in response to oligomerized ASC and ASC-αSyn complexes (Figure 14F). Correspondingly, a significant increase in cleaved GSDMD levels was observed, signifying NLRP3 inflammasome activation and pyroptosis induction (Figure 14G).

4.4 ASC-αSyn complexes trigger NLRP3- and caspase-1-dependent IL-1β/IL-18 processing

Activation of caspase-1 leads to the maturation of both IL-1β and IL-18 (115). To measure the subsequent release of IL-1β and IL-18 into the extracellular space following NLRP3 inflammasome activation with ASC-αSyn complexes, IL-1β and IL-18 ELISAs were performed. Stimulation of microglia with ASC-αSyn complexes led to a significant increase in IL-1β release compared with αSyn (p-value < 0.0001) and ASC alone (p-value = 0.0025; Figure 15A). Equally, a

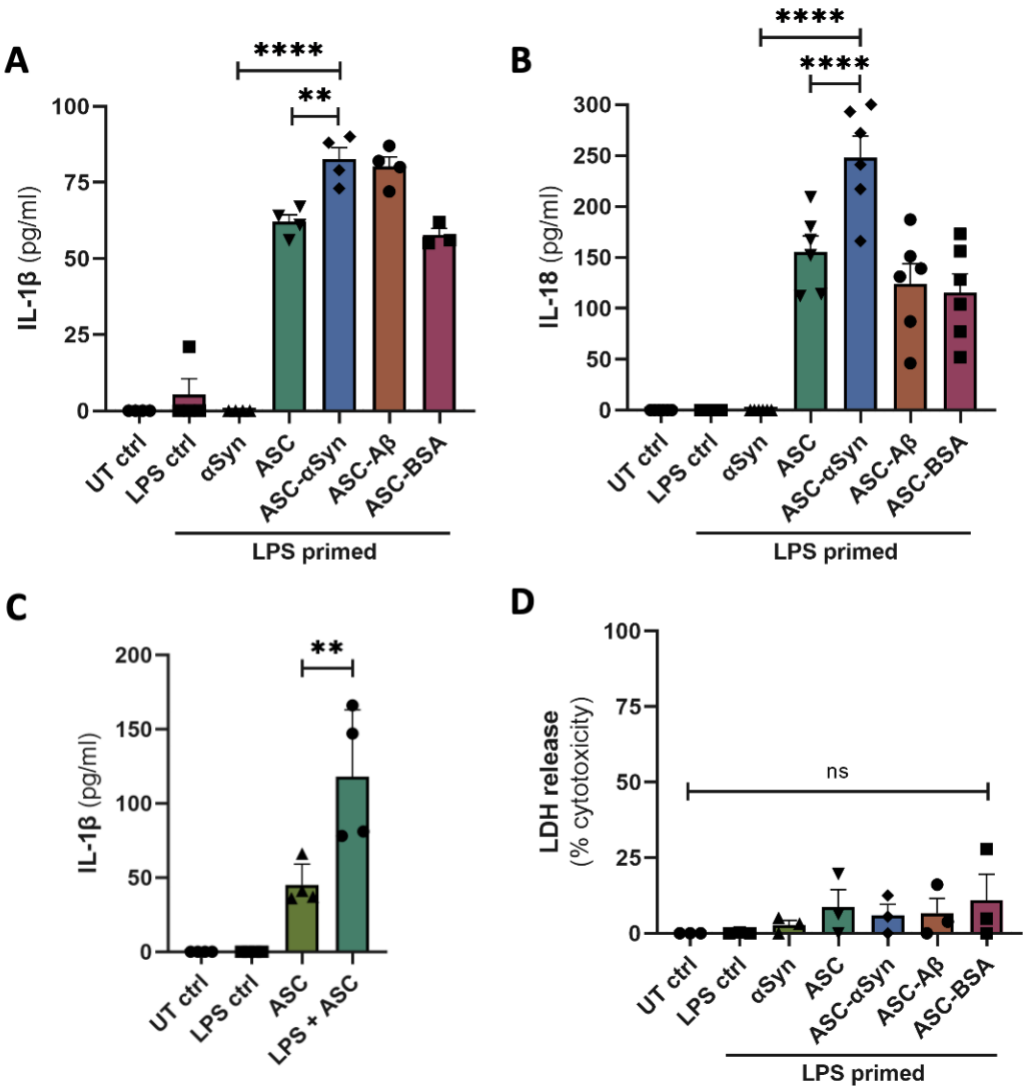

Figure 15. ASC-αSyn complexes induce IL-1β and IL-18 release without significant cell death.

(A and B) IL-1β (A) and IL-18 (B) levels in conditioned medium of SIM-A9 microglia after priming with LPS for 3 h followed by treatment with ASC, αSyn, or ASC-αSyn complexes for 24 h. (C) IL-1β levels in conditioned medium of SIM-A9 microglia after exposure to ASC for 12 h with or without LPS priming for 3 h. (D) LDH release measurements after treatment with different inducers. Data were collected from three (D), four (A and C), or six (B) independent experiments (n = 3, 4 or 6). All graphs are presented as mean ± SEM and were analyzed by one-way ANOVA followed by Tukey's post-hoc multiple comparisons test. Levels of significance are indicated as follows: **p < 0.01, ****p < 0.0001. Asterisks indicate significance between groups and "ns" indicates not significant.

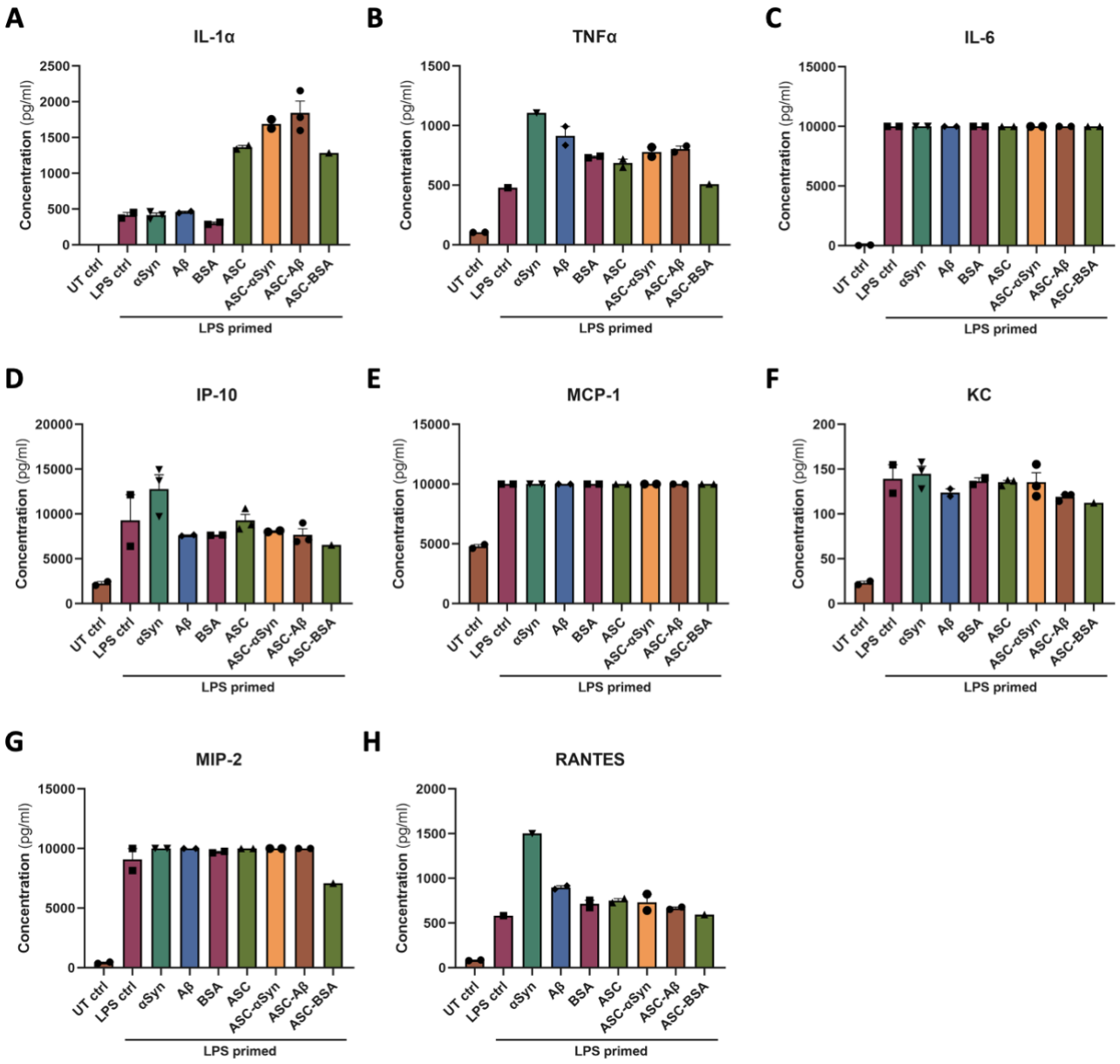

Figure 16. ASC-αSyn complexes induce pro-inflammatory cytokine and chemokine release.

Pro-inflammatory cytokine (A–C) and chemokine (D–H) levels in conditioned medium of SIM-A9 microglia after 3 h exposure of 100 ng/ml LPS followed by 12 h exposure of 1.75 µM ASC, 5 µM αSyn, or 1.75 µM ASC-5 µM αSyn complexes. (A-I) IL-1α (A), TNFα (B), IL-6 (C), IP-10 (D), MCP-1 (E), KC (F), MIP-2 (G) and RANTES (H) levels were assessed by a MILLIPLEX® Mouse Cytokine/Chemokine Magnetic Bead Panel. Data were collected from a single independent experiment (n = 1) with three technical replicates per assay (N = 3). All graphs are presented as mean ± SEM.

significant increase in IL-18 release was observed in response to ASC-αSyn complexes compared to ASC alone (p-value < 0.0001; Figure 15B). Treatment with LPS and αSyn alone resulted in undetectable amounts of IL-1β and IL-18, suggesting they do not activate the NLRP3 inflammasome. Rather, the observed effects are beyond synergism and the pro-inflammatory response is driven by the presence of ASC specks. Intriguingly, the addition of oligomerized ASC only without LPS priming displayed a diminished IL-1β release, suggesting priming of the NLRP3 inflammasome (Signal 1) is required for a canonical, pro-inflammatory NLRP3 inflammasome response (Figure 15C). To analyze the effect of the ASC-αSyn complexes on microglia survival, release of LDH in response to ASC-αSyn treatment was used as an indicator of cell death. Irrespective of LPS priming or ASC-αSyn stimulation, microglia displayed minimal release of LDH, suggesting low levels of cell death and high cell survival during prolonged treatments of 27 h altogether (Figure 15D). To gain a better understanding of the inflammatory response, a multiplex bead array assay (described above) was performed. LPS priming and ASC-αSyn complexes were sufficient to induce a multitude of pro-inflammatory cytokines and chemokines, including IL-1α, TNF-α, IL-6, IP-10, MCP-1, KC, MIP-2, and RANTES (Figure 16). Together, these findings suggest that ASC-αSyn complexes activate the NLRP3 inflammasome and amplify the pro-inflammatory response in intact microglial cells to a greater extent than when compared to ASC and αSyn exposure only.

Finally, phenotypical differences of microglia have been classified based on their morphological features in different contexts, such as neurodegenerative diseases (215). SIM-A9 microglia were subjected to treatments and examined using phase-contrast microscopy (Figure S2). After 3 h of LPS exposure followed by 24 h of various treatments, SIM-A9 microglia exhibited

morphological changes (Figure S2). Untreated microglia revealed relatively small cell bodies with few cells revealing branched processes. Nonetheless, the addition of LPS transformed them to appear morphologically ramified with longer, branched processes, potentially for scanning of the microenvironment for extracellular dangers (70,71). Following NLRP3 inflammasome priming with LPS, the addition of an activation signal (i.e., via ASC-αSyn complexes) activated microglia into an amoeboid phenotype, where such cells are spherical in shape, have larger cell bodies and lack abundant processes. To conclude, microglial SIM-A9 cells demonstrated morphological differences when eliciting a pro-inflammatory response via the NLRP3 inflammasome, potentially suggesting an imbalance in their homeostatic functions.

5. DISCUSSION

Inflammation produced by the innate immune system is a protective immune response that is tightly regulated by the host to prevail against invading pathogens. However, excessive inflammation can lead to the production of high concentrations of cytotoxic molecules and may trigger chronic or systemic inflammatory diseases (96,97). Inflammasomes are significant contributors to innate immunity, and one of the most extensively studied inflammasome complexes is NLRP3 (110). The NLRP3 inflammasome elicits a pro-inflammatory response mediated by caspase-1, members of the IL-1 family of cytokines and pyroptotic cell death. A growing body of literature has recognized αSyn aggregation, microglial NLRP3 inflammasome activation and presence of ASC specks in PD, the latter of which may interact with αSyn and contribute to hyperactivation of the inflammatory response in ways that are yet not well understood (137,197). In this thesis, I have demonstrated that in an *in vitro* model of mammalian microglia the presence of oligomerized ASC when combined with exogenous, human αSyn monomers contributes to an amplified inflammatory response driven that is mediated by the endogenous NLRP3 inflammasome.

5.1 Oligomerized ASC binds monomeric amyloid proteins

Upon NLRP3 inflammasome activation by PAMPs and DAMPs, NLRP3 recruits the adaptor protein ASC and pro-caspase-1 via homotypic interactions. Caspase-1 activation leads to the processing of IL-1β, IL-18, and GSDMD, which contribute to the inflammatory response. Importantly, a perinuclear punctate structure composed of insoluble and aggregated ASC, referred to as an 'ASC speck' is also formed during NLRP3 activation and is considered a hallmark

of inflammasome activation (209,216,217). Under physiological conditions, ASC is a monomer diffusely distributed throughout the cytosol; nonetheless, this protein has started to emerge as a critical player in the pathogenesis of numerous diseases involving inflammatory processes. Recent studies have suggested that ASC specks display prion-like polymerization and supramolecular organizing center (SMOC)-like threshold properties (218,219). Franklin et al. (2014) revealed that after pyroptosis, ASC specks accumulate rapidly in the extracellular space, where they promote further maturation of IL-1β (137). In addition, phagocytosis of ASC specks by macrophages induced lysosomal damage and nucleation of soluble ASC, as well as activation of IL-1β in recipient cells (137). More recently, microglia-derived ASC specks cross-seed Aβ and exposure of primary microglia to exogenous ASC and ASC-Aβ complexes resulted in a vicious cycle involving amplified NLRP3 inflammasome activity and reduced Aβ clearance in the presence of ASC (193,196). These findings suggested a potential mechanism for disease progression in AD, wherein Aβ clearance by microglia is prevented. In this study, I first re-demonstrated the binding of Aβ monomers to ASC specks (Figure 6E) and stimulation of microglial cells to ASC-Aβ complexes that induced the release of IL-1β (Figure 8F) as well as of numerous pro-inflammatory cytokines and chemokines (Figure 9); this observation, served as a positive control in my approach.

Post-mortem brain tissues from PD patients and preclinical PD models have demonstrated up-regulated ASC levels and the formation of ASC specks in the SN of PD patients and striatum of mice (197). Further, in pilot biomarker studies, when compared to control individuals, gene expression levels of ASC have been found to be elevated in peripheral blood mononuclear cells of PD patients (220). αSyn, a pathologically relevant protein of PD, can be

released into the extracellular space upon neuronal damage and be scavenged by neighbouring microglia to induce its activation (54,60,221,222). Considering similar studies reporting sustained microglial NLRP3 inflammasome activity upon αSyn exposure and the ability of ASC to cross-seed amyloid formation-prone proteins, I hypothesized that monomeric αSyn, which also represents an amyloidogenic protein, may bind to ASC specks in the extracellular space (Figure 4). Indeed, via EM, I observed the presence of monomeric, recombinant human αSyn in close association with ASC fibrils when co-incubated *in vitro*, thereby producing ASC-αSyn complexes (Figure 6C). Numerous studies have revealed that microglial interaction with αSyn depends on its structure, with fibrillar αSyn inducing the greatest inflammatory response via NLRP3 activation and IL-1β release, reflecting microglial activation (18,89,197,223). In comparison, monomeric αSyn by itself was found to provoke only a minimal pro-inflammatory state, or none at all (Figures 11-15) (18,89). In my hypothesis, pro-inflammatory responses could be initiated by ASC specks in the presence of a non-pathogenic form of αSyn, generating an augmented response compared to ASC alone. Hence, the reason to employ αSyn monomers. Despite ASC and αSyn being in close proximity of each other, it remains unclear how αSyn may bind to ASC fibrils structurally.

Mutagenesis studies have shown that the clustering of ASC-PYD domain filaments and their condensation into ASC specks is mediated by the ASC-CARD domain exposed to the surface of the filament initiated by the ASC-PYD domain (183). Importantly, ASC filament formation serves as a signal amplification mechanism for inflammasome-mediated cytokine production (106). However, filament formation of the CARD domain only is almost completely disturbed due to mutations within the CARD domain, suggesting the ASC-CARD domain is required for speck formation and downstream signaling (184). Furthermore, full-length human ASC carrying

mutations within the PYD-PYD interface and CARD domain, rendering it incapable of filament formation, does not cross-seed Aβ aggregation and decreases the release of IL-1β, suggesting that the filamentous structure of ASC is required for NLRP3 inflammasome activation in response to ASC-Aβ complexes (196). On the other hand, αSyn truncation of the C-terminal domain can increase exposure of the NAC region, thus promoting a pro-aggregatory conformational state (33). As such, caspase-1 performs truncation of αSyn at the C-terminal (at Asp121) in neurons to induce αSyn aggregation and neuroinflammation, which aggravates cytotoxicity and creates a positive-feedback loop (18,162,183). Conversely, caspase-1 inhibition rescued neuronal cells from αSyn-induced toxicity. In addition, Lewy bodies isolated from postmortem PD brains were positively stained for both caspase-1 and αSyn, substantiating their co-existence in Lewy bodies and supporting the belief that caspase-1 may be involved in generating the truncated αSyn found in Lewy bodies (199). Based on the size of the Lewy body core and what is known about the ASC speck's ability to cross-seed protein aggregation, it has been speculated that ASC specks can likely be found in the core of αSyn Lewy bodies comparably to Aβ plaques (126,196). Truncation of the C-terminal has been estimated to occur in 10-30% of total αSyn within Lewy bodies (34). Studies have similarly shown that caspase-cleaved tau (at Asp421) can also become prionoid, seed tau aggregation and activate microglia (224–226). Finally, ASC specks have an intrinsic property to co-aggregate cytosolic proteins on their surface through non-specific hydrophobic interactions, indicating a role for ASC specks as supramolecular platforms and allowing extracellular amyloid proteins to cross-seed (140).

5.2 LPS acts as a PAMP to prime the NLRP3 inflammasome

I next hypothesized that microglial exposure to ASC-αSyn complexes activates the NLRP3 inflammasome and amplifies the pro-inflammatory response. To test my hypothesis, I first primed mouse SIM-A9 microglia with LPS for 3 h (Figure 5C), replicating signal 1 of canonical NLRP3 inflammasome activation (Figure 3B). LPS, a component of gram-negative bacteria, is the most common pro-inflammatory priming stimulus for microglia to influence the transcription of inflammasome components via TLR4 engagement, both *in vitro* and *in vivo* (227,228). TLR4 stimulation by LPS initiates translocation of NF-κB from the cytoplasm into the nucleus to induce gene transcription of *Nlrp3* and *pro-IL-1*β (117,118). As expected, LPS priming alone induced an increase in NLRP3 protein levels (Figures 10B, 13B, and 14D). Though, a very minor rise was observed in the formation of cell-derived ASC specks and caspase-1 activity compared to other treatments, suggesting that LPS primes the NLRP3 inflammasome as a PAMP but does not prompt its assembly/activation (Figures 11B and 12B). In addition, LPS induced negligible or undetectable levels of IL-1β and IL-18 release in cell-free supernatants (Figure 15A and 15B), supporting the notion that LPS acts as a priming signal for the NLRP3 inflammasome. Nonetheless, LPS alone triggered the release of non-inflammasome-specific cytokines and chemokines (Figure 16). Activation of NF-κB, via LPS stimulation, increases the production of inflammatory cytokines, chemokines and adhesion molecules, yet also regulates cell proliferation, apoptosis, morphogenesis and differentiation (229). Thus, NF-κB serves as a central inflammatory mediator in many signaling pathways. Lower concentrations of LPS have shown to induce the production of various cytokines and chemokines, including IL-6 and TNF-α, and serve as a potent innate immune stimulus in other contexts (207).

Non-inflammasome-related cytokines, such as TNF-α or type I IFN, may also enhance the priming process of inflammasome activation, yet the mechanisms by which they contribute to inflammasome priming remain to be fully characterized (152,230,231). Certainly, as neuroinflammation has been strongly linked in the pathogenesis of PD, recent studies have used LPS to model the pro-inflammatory events seen in clinical PD (232). Some PD patients have raised serum LPS levels, which may reflect increased intestinal permeability and gut dysfunction evident in the early stages of PD, highlighting a specific disease subtype where inflammation may precede neurodegeneration (233,234). Peripheral stimulation of the innate immune system with LPS has shown to cause an exaggerated neuroinflammatory response and promote microglial hyperactivity in aged mice that is associated with the exaggerated induction of IL-1β (235). Interestingly, acute administration of LPS in different regions of the brain does not lead to permanent neuronal damage, except for in the substantia nigra (79,236–238). Sterile, chronic, and low-grade inflammation involving immunosenescence, commonly termed as 'inflammageing' (understood to be not simply a consequence of increased chronological age), may also contribute to the increased priming and activation of the NLRP3 inflammasome and thus development of neurodegeneration (239–241). The role of LPS in the context of PD and LPS models of PD has been reviewed in these articles in more depth (232,234).

5.3 ASC-αSyn complexes upregulate upstream NLRP3 inflammasome components

Following LPS priming and a wash step to ensure canonical NLRP3 activation, microglia were exposed to ASC-αSyn complexes and controls for 24 h, mimicking signal 2 of canonical NLRP3 inflammasome activation (Figure 5C). Compared to LPS alone, stimulation with DAMPs,

including αSyn, oligomerized ASC, and ASC-αSyn complexes, all led to enhanced levels of the NLRP3 sensor, implying additional activation of the NLRP3 inflammasome (Figure 10B). Yet, Western blot and Simple Western analysis revealed similar levels of NLRP3 to LPS priming (Figures 13B and 14D). In PD, inflammasome activation is one of the most well-delineated inflammatory pathogenic factors (242–244). Importantly, NLRP3 inflammasome activation has been recognized in post-mortem brains of human PD patients (197,245).

Next, I further monitored NLRP3 activation and assessed endogenous ASC speck formation as it is used as a simple upstream readout for inflammasome activation (209). ASC-dependent inflammasome activation is complemented by rapid rearrangement of the NLR and ASC into a singular, perinuclear, punctate 'speck' structure of ~1 μm (209,246). The ASC speck is believed to act as a SMOC, which are higher-order structures that locally concentrate weakly interacting proteins required for signal transduction (218,219,247). SMOC assembly is tightly regulated, and ASC speck formation follows the SMOC assembly mechanism, signifying that specks enable inflammasome proteins to adopt a conformation that efficiently senses the activation signal (218,247,248). Notably, signal-induced polymerization of ASC into SMOCs allows for an all-or-none response, which is only triggered once a threshold is exceeded. Here, exposure of microglia to ASC-αSyn complexes generated the highest number of ASC specks, indicating heightened NLRP3 inflammasome activation when compared to αSyn and ASC only (Figure 11B). Speck formation *in vitro* is rapid, as NLRP3 and ASC oligomerize under three min to form a speck and produce a concomitant drop in the cytosolic ASC concentration by nearly 200-fold (217,249–251). However, the kinetics of speck formation differ *in vivo*. For instance, the speck size in Zebrafish stabilizes after a continuous growth period of 15 min (252). Typically, inflammasome

activation is characterized by the presence of a single speck per cell. Yet, multiple studies have described the induction of multiple ASC specks per cell, suggestive of differing experimental conditions and mechanisms that may stimulate ASC speck formation . Lastly, the prion-like structure of ASC specks is resistant to proteolytic degradation, serving as amplification mechanisms for inflammasome signaling and leads to a toxic, chronic progressive inflammatory state (discussed more in-depth below) (106,108,208,209).

Visualization of ASC specks was enabled with the use of an anti-ASC, polyclonal antibody and subsequent confocal microscopy. However, one crucial limitation is the co-appearance of recombinant human ASC protein used to stimulate microglia *in vitro*. Both cell-derived and recombinant human ASC were identified upon detection of ASC (Figure 11A). To perform accurate quantification of endogenous ASC specks formed in response to *in vitro* treatments, specks were manually quantified based on known localization, size, and appearance. Endogenous ASC specks are commonly localized to the perinucleus, although some ASC specks are found in the extracellular space (Figure 11A) (256). ASC specks may also be found in microglial processes in a potential attempt to offload their cellular cargo and/or perpetuate the inflammatory response, although this has been shown with αSyn (66). Moreover, ASC specks exhibit a diameter of ~1 μm and are circular in appearance. In contrast, ASC specks formed using recombinant ASC are of various sizes, mostly larger than 1 μm and sporadic in appearance (176). Larger, irregular-shaped ASC specks were also observed near the cellular membrane or within microglia, suggesting internalization of the recombinant ASC as endogenous ASC specks are smaller, more uniform and frequently observed near the perinucleus (Figure 11A).

Due to the tendency of ASC to self-aggregate, it is unclear whether the endogenous structure resembles the complexes observed *in vitro* or upon ASC overexpression. Since the recombinant ASC expressed a polyhistidine (His)-tag, an approach that I attempted to overcome this limitation was co-incubating cells with an anti-His-tag antibody to detect recombinant ASC among the cell-derived ASC. Despite this, non-specific staining of Histidine was observed in all the cells (data not shown), restricting direct recognition of the exogenous ASC. On the other hand, biotinylation of ASC, which involves the process of covalently attaching biotin to ASC, can be performed. Thus, biotinylated ASC may be used for *in vitro* treatments and cells can be incubated with a streptavidin antibody to detect the recombinant ASC specks, since biotin binds to streptavidin with an extremely high affinity and high specificity. In addition, to further discriminate between cell-derived and recombinant human ASC used for cell treatment, a mouse-specific anti-ASC antibody can be applied to visualize ASC aggregation and speck release into the extracellular environment.

5.4 ASC-αSyn complexes act as a DAMP, amplifying downstream NLRP3 inflammasome components

Caspase-1, an inflammatory caspase, is present as a zymogen that requires activation to mediate its effects. This can be accomplished through the assembly of an inflammasome complex (147). Upon NLRP3 inflammasome activation, pro-caspase-1 is self-activated by proteolytic cleavage and mature caspase-1 proteolytically cleaves downstream proteins, including pro-IL-1β and pro-IL-18 and GSDMD, into mature, biologically active forms. PD patients display increased caspase-1, localized exclusively within microglia in the SNpc or systemically circulating caspase-1

and IL-1β (197,198). Additionally, caspase-1 is also present at the core of Lewy bodies extracted from the brains of PD patients (199). To investigate caspase-1 cleavage, Western blot analysis of cell lysates was performed. Surprisingly, cleaved caspase-1 (p20) was undetected in all samples (Figure 13A). Yet, a reduction in the full-length caspase-1 protein was observed, indirectly indicating conversion to the cleaved caspase-1 subunits (Figure 13C). To provide more sensitive detection and precise quantification of protein expression levels compared to immunoblotting, Simple Western immunoassays were performed using the Wes instrument (176,177). In Wes, proteins are size-separated in capillaries, where they are incubated with primary and HRP-conjugated secondary antibodies and Luminol/peroxide in a fully automated Western blotting workflow. The produced chemiluminescence is detected at several exposure times and automatically quantified where the chemiluminescent signal can be displayed as an electropherogram or as a virtual blot-like image, as shown in Figure 14A-C. Detection of cleaved caspase-1 (and thus, GSDMD) via immunoblotting can be difficult due to lack of relative abundance of the cleaved proteins compared to the total protein, hence the Simple Western may be a better alternative. Likewise, only decreases in the full-length caspase-1 protein were observed (Figure 14E), suggesting the overall abundance of cleaved caspase-1 in these samples is too low for detection.

To overcome the challenge of cleaved caspase-1 detection, the FAM-FLICA® Caspase-1 assay was employed. FLICA is a non-cytotoxic probe that covalently binds to active caspase enzymes by recognizing a specific 4 amino acid sequence (YVAD) that includes an aspartic acid (D) residue in the P1 position that is sandwiched between a green, fluorescent label (FAM) and a FMK (211,212). Binding of the YVAD amino acid sequence will retain the green, fluorescent signal

within the cell. FLICA is also cell-permeant and efficiently diffuses in and out of all cells, wherein unbound FLICA can be diffused out of the cell during wash steps. Ultimately, apoptotic and pyroptotic cells retain a higher concentration of FLICA and fluoresce brighter than healthy cells. Compared to ASC and αSyn alone, imaging analysis revealed increased caspase-1 activity in response to ASC-αSyn treatment (Figure 12B), a trend analogous to that of the increase in ASC speck formation. Microglia exposure to ASC-BSA complexes revealed comparable caspase-1 activity to ASC alone (Figure 12B), suggesting ASC specks preferentially bind to monomeric forms of αSyn and Aβ, but not BSA, to provoke an inflammatory response. Moreover, 12% of ASC-αSyn complex-treated cells displayed caspase-1 activity, indicating an overall, low inflammatory response, which may contribute to lack of caspase-1 detection in cell lysates via immunoblotting or Simple Western. It is important to note that processed caspase-1 has a short half-life of approximately nine min in cell extracts, while other caspases are active for hours (257). Consequently, while maturation dramatically increases catalytic activity, it also limits activity to a very short time and thus, an appropriate detection technique is required (258).

Post-caspase-1 activation, two potent cytokines of the IL-1 family of ligands involved in host defense, IL-1β and IL-18, are processed to mediate an inflammatory response (148,149). Both cytokines IL-1β and IL-18 are recognized by type 1 IL-1 receptor (IL-1R1) and IL-18R, respectively, and IL-1R1 signalling links with TLR signalling to competently manage invading pathogens (222). IL-1β is the most well-characterised and studied of the 11 IL-1 family members, where its release has been observed in numerous inflammatory contexts, such as autoinflammatory and autoimmune diseases, respiratory diseases, cardiovascular disorders, and neurodegenerative conditions among many others (259). While IL-18 is constitutively expressed,

IL-1β is absent in cells from healthy individuals and thus requires a series of intracellular events, including inflammasome assembly, before it can trigger inflammation. IL-1β is a product of a limited number of cells, such as tissue macrophages and blood monocytes, and transcription is the rate-limiting step in the production of IL-1β (260). Here, exposure of LPS-primed microglia to ASC-αSyn complexes generated a statistically significant release of both IL-1β (Figure 15A) and IL-18 (Figure 15B) compared to ASC only, suggesting ASC-αSyn complexes elicit the production of an amplified inflammatory cytokine cascade. Unlike IL-1β, ASC-Aβ complex formation did not induce the release of IL-18 to the same extent as ASC-αSyn complexes (Figure 15B), likely reflecting the difference in the addition of oligomerized ASC (1.75 μM ASC used for ASC-Aβ complex vs. 2.5 μM ASC used for ASC-αSyn complex) and the constitutive expression of IL-18. In contrast, exposure of SIM-A9 microglia to LPS and αSyn alone failed to produce any measurable IL-1β and IL-18 cytokine release, proposing that the inflammatory response is driven by the presence of recombinant ASC specks and influences αSyn monomers in ways that are yet unknown.

IL-1β and IL-18 are known to mediate numerous innate and adaptive immune responses that contribute to chronic inflammation (261). IL-1β exerts its effects by binding to IL-1R1, where its activation leads to the release and nuclear translocation of NF-κB (262). Next, NF-κB enhances transcription of genes for cytokines, including IL-1α, IL-1β, IL-6 and TNF-α, and supplementary chemokines (229). IL-1β can engage with TLR4 to initiate an inflammatory cytokine cascade to propagate inflammation since IL-1β can induce further expression of TNF-α and IL-6, while IL-18 stimulates the production of IL-17 (128,263,264). Additionally, administration of IL-1β along with other cytokines into a healthy animal has shown to display significantly greater tissue damage,

suggesting a functional reinforcement in the action of these inflammatory features (216). IL-1β and additional inflammatory cytokines may also alter blood-brain barrier permeability and influence the transport of substances from systemic circulation into the brain, which may allow infiltrating immune cells to enter the parenchyma and promote neurotoxicity (265). Upon CNS injury and NLRP3 inflammasome activation, it has been demonstrated that IL-1β and IL-18 cytokines promote the local recruitment of leukocytes to the CNS (266,267). IL-1β and IL-18 also play a known role in the polarization of IL-17-producing T-helper 17 (Th17) cells and IFN-γ-producing Th1 cells, respectively (268–271). It is worth noting that Th17 cells are injurious to dopaminergic neurons in models of PD and other neurological disorders (272,273). Moreover, IL-1β, along with IL-23, promotes granulocyte-macrophage colony-stimulating factor expression by T cells (226), implicating microglial-T cell interactions. In addition to inducing pro-inflammatory cytokines, IL-18 has been described to upregulate adhesion molecules, stimulate NK cell activity, and recruit monocytes and T lymphocytes (153,274). Synergistically with IL-12, IL-18 induces IFN-γ production and inhibition of angiogenesis (274,275). In addition, IL-18, in collaboration with IL-3, induces basophils and mast cells to produce IL-4 and IL-13 (276,277). Notably, in experimental mice models of AD, microglia activated with Aβ produced IL-1β that further promoted synthesis and aggregation of neurotoxic Aβ peptides (278). Likewise, released cytokines may influence endogenously expressed αSyn to misfold and aggregate. Thus, aggregated αSyn may prompt a subsequent inflammatory response that continues to release cytokines and justify the sustained presence of inflammation and progressive αSyn pathology (279). Increased levels of inflammatory cytokines, including IL-1β, IL-18, IL-6, and TNF-α, have been detected in the cerebrospinal fluid of PD patients when compared with controls (280–282). Post-mortem analysis

of patients with neurodegenerative diseases present with both neuroinflammation as well as tissue damage, making it challenging to confirm whether elevated IL-1β levels contribute to pathological changes as a primary event (as during the induction of pyroptosis) or secondary event (as in the process of debris clearance following cell death). Multiple studies using experimental brain injury models have implied that IL-1β-induced leukocyte recruitment and additional inflammatory processes leads to neuronal damage and cell death (283,284). However, persistent expression of the IL-1 receptor antagonist has been shown to cause a delay in pro-inflammatory cytokine induction and improvement in healing and neurological recovery following traumatic brain injury (285). Importantly, blocking IL-1 in a broad spectrum of diseases to treat inflammation has been proposed as a therapeutic strategy (260,286). This has been shown to result in a rapid and sustained reduction in disease severity (260,286). Overall, both IL-1β and IL-18 perform central roles in mediating various innate and adaptive immune responses that may reinforce neuroinflammation in a positive-feedback manner.

To gain insight into the general inflammatory response, a multiplex assay probing several inflammatory markers was performed as IL-1β and IL-18 influence several immune responses and cell types that may propagate the overall inflammatory response. As briefly discussed above, LPS priming and subsequent treatment with different DAMPs resulted in the release of numerous cytokines and chemokines (Figure 16). The pro-inflammatory cytokines, IL-1α, IL-6, and TNF-α, are essential for coordinating cell-mediated immune responses and modulating the immune system. They generally regulate growth, cell activation, differentiation, and orient immune cells to the sites of infection with the purpose to control and eliminate the intracellular pathogens (170). Moreover, IL-1α is considered an alarmin, an indicator of cell damage (287). IL-1β and IL-

1α bind to the same receptor and have mostly overlapping inflammatory activities, hence displaying a similar trend in cytokine release (Figure 16A) (288). On the other hand, chemokines, for instance IP-10, KC, MCP-1, MIP-2 and RANTES, are cytokines with chemotactic activities. They also perform a critical role in regulating the movement and localization of lymphocytes and a subset of dendritic cells (DCs) (171). While chemokines are not specific to the inflammasomes, they can mediate inflammation, thus displaying a more robust and distinctive trend compared to the release of IL-1β (Figures 7E-I and 14E-I). Of note, the release of IL-4 and IL-10, two notable anti-inflammatory cytokines that serve to suppress inflammation and immunity, were also assessed. Upon treatment with ASC-αSyn complexes, no detectable amounts of both IL-4 and IL-10 were observed (data not shown), highlighting the balance of the immune system being skewed towards pro-inflammatory signaling (289).

Along with processing of the pro-inflammatory cytokines IL-1β and IL-18, caspase-1 also induces pyroptosis, a necrotic form of regulated cell death characterized by plasma membrane permeabilization and rupture. Pyroptotic cell death is mediated by proteolytically activating the pore-forming GSDMD, which allows the release of cytokines into the extracellular space. Following the discovery of GSDMD's role in executing pyroptosis, many studies have noted differences in GSDMD expression and cleavage within the nigrostriatal pathway of PD mouse models (290–293). Both *in vivo* and *in vitro* experiments have demonstrated that GSDMD contributes to glial activation and death of dopaminergic neurons across different PD models. In addition, ablation of *Gsdmd* in mice attenuated PD-like pathology by reducing dopaminergic neuronal death, microglial activation, and the detrimental transformation of both microglia and astrocytes (294). In this study, insignificant differences were observed in the full-length protein

levels of GSDMD in response to stimulation with ASC-αSyn complexes via immunoblotting (Figures 13D). Yet compared to LPS- and αSyn-treated cells, increased levels of cleaved GSDMD were detected, suggesting the moderate induction of pore formation and pyroptosis (Figure 13E and 14G). Moreover, Simple Western analysis revealed a greater disparity in full-length GSDMD levels in microglia treated with LPS and αSyn alone, compared to ASC only and ASC-αSyn complexes (Figure 14F). Treatment of SIM-A9 microglia with all inflammasome inducers also led to minimal detection of LDH, denoting a lack of cell death in this model (Figure 15D). Pyroptosis results in the release of large amounts of immature pro-caspase-1 and pro-IL-1β which constitute the dominant bands in immunoblots of cell-free supernatants from inflammasome-activated cells, although this was not shown in this study (295). GSDMD cleavage and pyroptosis may be occurring at a minor level, making it challenging to detect significant differences.

Most, not all, inflammasome activators induce both cytokine maturation and pyroptosis. Formation of N-GSDMD, which forms transmembrane pores, is required for efficient cytokine release (175,178,179,181). In this study, relatively low levels of GSDMD correspond with reduced caspase-1 activity and lower release of IL-1β and IL-18. Similar treatments with ASC-Aβ complexes led to more robust responses in mouse primary microglia, proposing the treatments in SIM-A9 microglia in this study do not generate an inflammatory response to the same extent (193). Furthermore, the mere existence of GSDMD, a caspase-1 substrate, does not define the pyroptotic outcome of inflammasome activation. It has been previously discussed that caspase-1 activation does not necessarily cause pyroptosis in all scenarios and thus, secretion of cytokines and release of ASC specks does not always rely on pyroptosis (139). Different types of cell death are likely to be present simultaneously, for example apoptosis and necroptosis. Thus, this has led

to the recent establishment and development of the concept of 'PANoptosis'. PANoptosis is an intricate form of inflammatory cell death that integrates components from other programmed cell death pathways, including pyroptosis, apoptosis, and necroptosis (296,297). In addition, cell death is not essential for caspase-1-mediated IL-1β activation and secretion (298). After the genetic identification of GSDMD as a regulator of pyroptosis, following work demonstrated that GSDMD pore formation does not necessarily lead to death (299,300). Cell death after GSDMD pore formation is regulated and can be delayed or avoided altogether (301). In this experimental setup, the lack of significant cell death and pyroptosis suggests that much of the ASC speck release may occur through more complex, yet unexplored mechanisms. High GSDMD expression is necessary for pyroptosis, whereas low expression can influence the response towards apoptosis. For instance, in the absence of GSDMD, caspase-1 has been shown to induce apoptosis, but not pyroptosis (302,303). Mast cells, which express low levels of GSDMD, undergo caspase-1-dependent apoptosis accompanied by the activation of caspase-3 (303). Once activated within a GSDMD-low cell, caspase-3 may bias caspase-1-induced cell death towards apoptosis through the inactivation of GSDMD (302,304). This suggests that a threshold expression level of GSDMD is required to trigger pyroptosis as caspase-1-induced apoptosis and pyroptosis suppress each other (173). Regarding the release of cytokines, IL-1β has shown to be released via GSDMD-formed pores when blocking cell membrane rupture (300). Further studies have reported IL-1β release from living cells via GSDMD pores, referred to as hyperactivation (299,305). Hyperactivation has also been observed in macrophages and DCs (306,307). Overall, the expression level of GSDMD and the number of GSDMD pores determine the induction of pyroptosis and the maturation and release of cytokines.

5.5 ASC specks serve as a signal amplification platform

Traditionally, many therapeutics for PD and AD have focused solely on targeting amyloid protein accumulation, overlooking other co-pathologies. As a result, there are very few effective therapies to treat or slow the progression of these debilitating, neurodegenerative diseases, and diagnostic tools for early detection and monitoring disease progression are limited. Many treatments only targeting amyloid protein accumulation have shown to be of clinical insignificance, encouraging a re-evaluation of the existing therapeutic strategies (201,202,308,309).

In recent years, an inflammation-based hypothesis has gained traction to explain the mechanism of neurodegenerative disease progression. This hypothesis suggests that inflammation may act as an early inciting event in the disease, contributing to protein misfolding and aggregation, which in turn reinforces neuroinflammation in a positive-feedback manner, ultimately leading to neurodegeneration (241). Sterile inflammation, which occurs as a result of trauma, ischemia-reperfusion injury or chemically induced injury that typically occurs in the absence of any microorganisms, is one factor amongst others that contributes to the progression of CNS pathologies (310,311). In particular, inhibition of the NLRP3 inflammasome, a key mediator of sterile inflammation, has emerged as a therapeutic target where many inhibitors have been validated through *in vitro* studies and *in vivo* experiments in animal models of NLRP3-associated disorders (312,313). While many inhibitors directly or indirectly target the NLRP3 protein, some studies have targeted the adaptor protein ASC and inhibition of ASC oligomerization for the treatment of inflammatory diseases (314,315). Inhibition of ASC oligomerization has shown to prevent activation of pro-caspase-1 and inhibit the activation of

different ASC-dependent inflammasomes. On the other hand, serum ASC (also referred to as PYCARD) has been proposed as a new diagnostic marker for patients with rheumatoid arthritis (RA), where it plays a key role in the progression of RA (316). Given ongoing research into the role of ASC specks in neurodegenerative diseases, ASC may emerge as a potential biomarker. It is important to note that the hypothesis and mechanistic insights from these findings may be particularly relevant to an inflammatory subtype of PD, potentially stemming from sterile inflammation, as it is a heterogenous disease and may differ from patient to patient.

As mentioned above, prion-like ASC specks can serve as a platform for the propagation of inflammation and protein aggregation that drives PD. I hypothesized that binding of αSyn to ASC in the extracellular space of the brain leads to the formation of ASC-αSyn complexes, which are recognized as novel danger signals by microglia leading to NLRP3 inflammasome activation and amplification of the pro-inflammatory response. Here, I demonstrated that treatment of murine SIM-A9 microglia with ASC-αSyn complexes generated a pro-inflammatory response characterized by an increase in cell-derived ASC specks, caspase-1 activity, IL-1β and IL-18 release, and GSDMD cleavage. All the responses were consistently higher compared to treatment with ASC or αSyn alone and displayed similar trends, where results of the downstream components in the inflammasome pathway were more profound. Notably, αSyn alone minimally activated the NLRP3 inflammasome, suggesting ASC specks largely contribute to the amplified pro-inflammatory response.

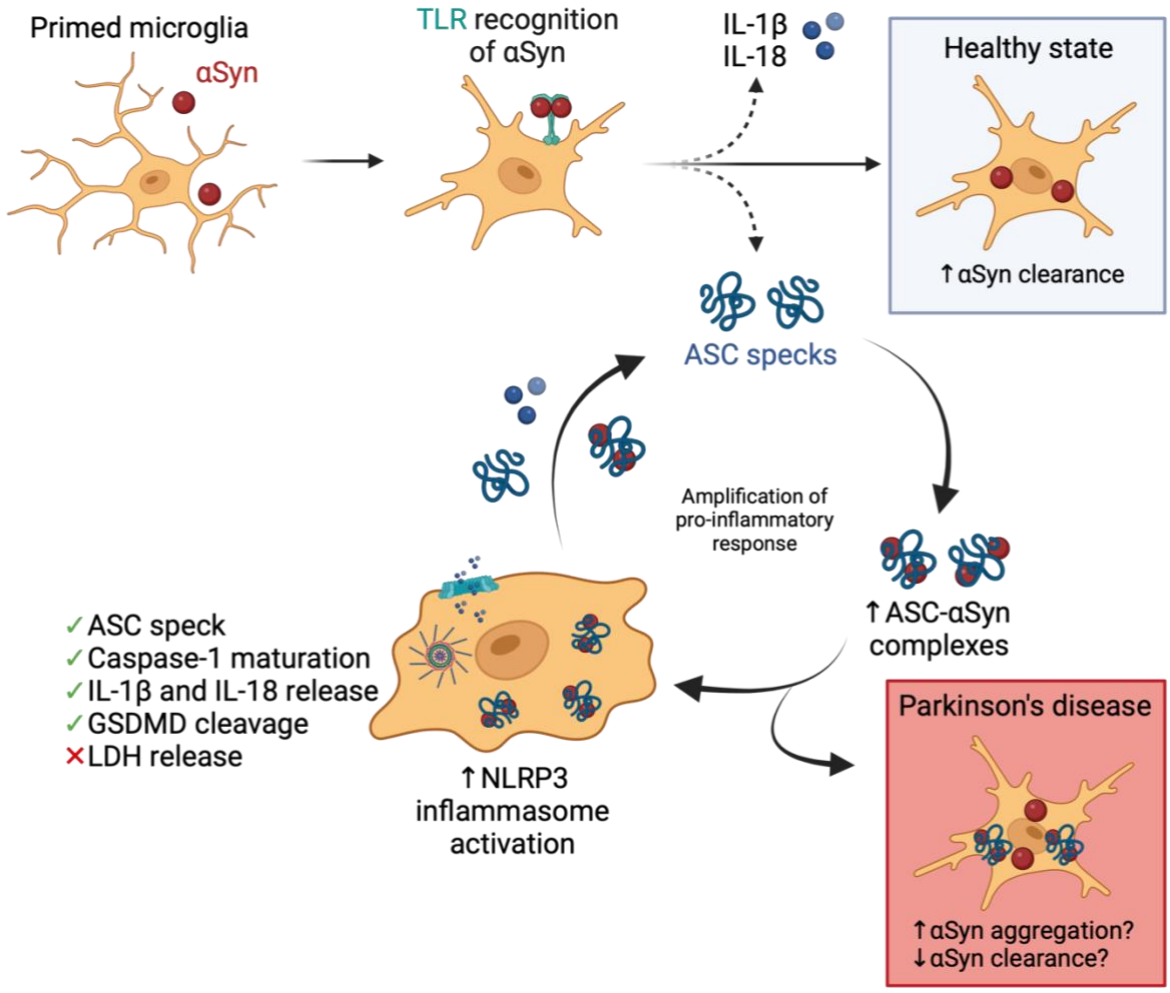

Figure 17. Binding of ASC and αSyn induces a feed-forward inflammatory cycle in microglia.

Different conformations of αSyn induce microglia priming and activation via cell surface receptors, such as TLRs. Under a healthy state, activated microglia internalize and reduce αSyn deposition. During microglia activation, components of the NLRP3 inflammasome, including the inflammasome adaptor protein ASC and cleaved pro-inflammatory cytokines IL-1β and IL-18, are released into the extracellular space to mediate an apt inflammatory response. In the extracellular space, oligomerized ASC, referred to as ASC specks, may bind extracellular αSyn and form ASC-αSyn complexes. ASC-αSyn complexes trigger chronic activation of the NLRP3 inflammasome and may influence αSyn aggregation and promote phagocytic exhaustion, reducing αSyn clearance by microglia. Highly activated and pyroptotic microglia release ASC specks, pro-inflammatory cytokines, and engulfed ASC-αSyn complexes, triggering an excessively toxic environment and a feed-forward cycle. ASC specks may nucleate soluble ASC and αSyn, amplifying the inflammatory response. Adapted from Friker et al. (2020). Figure was created with BioRender.com

Overall, it appears that the ASC specks and formation of ASC-αSyn complexes induce a positive-feedback cycle in microglia (Figure 17) (126). Firstly, neuronally-derived αSyn and/or misfolded αSyn aggregates bind to TLRs which activates the expression of NLRP3 and pro-IL-1β to prime the cell for inflammasome assembly in a NF-kB signaling dependent manner (Signal 1) (91,92). Extracellular, misfolded αSyn aggregates may also be internalized by the phagolysosomal pathway yet can escape lysosomal degradation and prompt assembly of the NLRP3 inflammasome (Signal 2) (317–319). Secondly, the NLRP3 inflammasome via caspase-1 in microglia catalyzes the processing of IL-1β and IL-18, which can be transferred extracellularly or released into the extracellular environment during pyroptosis for inflammatory signaling (174). In parallel, assembly of the NLRP3 inflammasome may progress to the formation of the ASC speck, a supramolecular complex with enhanced inflammatory signaling capacity, which may then be released into the extracellular environment following pyroptosis or some other non-pyroptotic mechanism (109,135). There may be scenarios in which pyroptotic cell death is beneficial. For instance, in response to infection with intracellular pathogens (139). Considering the levels of caspase-1 activity and release of cytokines in this study, pyroptosis and cell death appeared to be of less importance than expected. The cellular response may also be dependent on the dose and length of treatments. Additionally, pyroptotic cell death is not advantageous when intrinsic danger, such as cell damage occurs. Prolonged cell survival may be more advantageous to allow optimal cytokine secretion to attract more immune cells (320). Thirdly, once in the extracellular space, the ASC speck remains functionally active as a molecular scaffold for cross-seeding of neuronally derived misfolded protein aggregation, inflammatory cytokine processing, and potentially pro-aggregatory modifications of other proteins

(137,138,193,196,199,225). The presence of an increase in ASC specks allows for nucleation of soluble ASC, serving as additional binding sites for extracellular αSyn and stimulating caspase-1 independent of the inflammasome (135,321). Ultimately, this assists in initiating a cytokine storm and producing a feed-forward cycle. Histologic analysis of tissues from PD patients have identified an increase in ASC specks in the SN and observed ASC specks within and outside of microglial cells (322). Furthermore, PD-derived αSyn aggregates combined with chronic inflammatory cues have demonstrated to promote a neurotoxic microglial phenotype (90). Next, the ASC speck can also propagate inflammation from one microglial cell to another by inducing a pro-inflammatory phenotype in cells that phagocytose the ASC speck but fail to degrade it (137,138). ASC activates the inflammasome after transition from a soluble to an insoluble state, possibly rendering them extremely stable and resistant to proteolytic degradation (323). Failed degradation of the ASC speck by microglial autophagy pathways results in the persistence of the active ASC speck contributing to an unregulated inflammatory response (193). Consequently, extracellular ASC specks can directly activate caspase-1 in the extracellular milieu together within the cell after being internalized by phagocytes (137). Altogether, the reviewed activities of the ASC speck involve its role in the propagation of inflammation and spreading of protein aggregation in a vicious cycle that contributes to the chronic progressive nature of PD and other neurodegenerative conditions in an ASC-dependent manner.

5.6 Limitations of this study and other considerations

In this thesis, there are some key limitations to note. The first limitation is the lack of a dose-response experiment to determine the optimal inflammatory response to ASC-αSyn

complexes. Inflammatory effects of oligomerized ASC uptake could be concentration-dependent and influenced by the balance between oligomerized ASC accumulation vs clearance (139). One way to test this hypothesis is to test different concentration ratios of complexes (e.g., 1:1 vs. 1:2 molar ratio of ASC-αSyn) after various incubation times (e.g., 8, 12, 24, and 36 h of treatment) and monitor the subsequent release of either IL-1β or IL-18 as a downstream NLRP3 inflammasome readout. It may also be noteworthy to repeat the experiment to investigate cell death by measuring LDH release, as increased caspase-1 and pyroptosis contribute to an enhanced inflammatory response. These experiments were partially attempted in my project (data not shown), yet they were not fully characterized and completed. Moreover, it is important to consider the oligomeric state of the recombinant ASC used. ASC oligomers of different sizes are generated by various factors and thus, the size of the ASC oligomers can impact the inflammatory response. Yu et al. (2023) revealed oligomerization degrees of ASC specks regulate the caspase-1 activation in the extracellular space, wherein ASC specks with a low oligomerization degree were shown to enhance the activation of caspase-1 (321). In theory, ASC specks with a low degree of oligomerization have more ASC-CARD available for the homotypic interactions between ASC-CARD and caspase-1-CARD, increasing the activation of caspase-1 during inflammatory responses. Uncertainty of the oligomerization state during each independent experiment may also contribute to the variability in cellular responses. Another important limitation is the confirmation of the binding between αSyn and ASC. αSyn was observed to be in close association with ASC specks, yet whether the two proteins interact remains unknown. Performing a co-immunoprecipitation experiment, a popular technique to identify physiologically relevant protein-protein interactions, can help validate ASC-αSyn binding.

The mouse SIM-A9 microglial cell line used in this study as an *in vitro* culture model warrants consideration. SIM-A9 is a spontaneously immortalized microglial cell line derived from cerebral cortex of mouse pups (206). While mouse strains are commonly used to study human diseases, there are notable differences between the human and murine immune systems in both innate and adaptive responses (324). The organization of the immune system varies significantly between the species. In humans, resistance mechanisms are more prominent due to their longer lifespan, whereas tolerance mechanisms dominate in mice (325,326). Additionally, species-specific differences exist in the activation and function of effector molecules released by immune cells to control pathogens. While many TLR-induced signaling pathways are highly conserved, mice show limited responses to TLR agonists (327). Microglia isolated from neonatal mice display a greater number of differentially expressed genes in response to DAMP treatment compared to microglia isolated from adult mice (328). Furthermore, microglia isolated from mice at different developmental stages have unique transcriptional signatures. *Ex vivo* human adult microglia exhibit a more pro-inflammatory profile than microglia from younger developmental stages, showing higher immune responsiveness by secreting increased levels of pro-inflammatory cytokines in response to LPS treatment compared to prenatal microglia (329).

These interspecies differences highlight the need for human-based models to study neuroinflammation and immune responses more accurately. Human induced pluripotent stem cell (hiPSC)-derived microglia provide a promising alternative. Recent work from many laboratories has shown that hiPSCs can be differentiated into microglia-like cells that closely resemble primary human microglia in their ability to phagocytose, secrete cytokines, and respond to inflammatory stimuli (330–332). Human iPSC-derived microglia can be co-cultured with

neurons, astrocytes, microvascular endothelial cells, and other brain cell types in microfluidic 3D brain-chip models, better recapitulating the human brain's cellular interactions and microenvironment (333). This approach allows for a more accurate investigation of neuroinflammatory processes, overcoming the limitations of murine models and offering deeper insights into human neuroinflammation.

After the potential interaction of ASC and αSyn in the extracellular environment and sustained exposure of microglia to ASC-αSyn complex formation, I hypothesized that chronic NLRP3 inflammasome activation and neuronal exposure to ASC-αSyn complexes may negatively impact neuronal health (Figure 4). Studies carried out in preclinical models and human PD patients has documented that synaptic dysfunction and/or loss occurs early in the disease process (48). To determine the impact of ASC-αSyn complexes and microglia-driven responses on neuronal health, a co-culture system of microglia and neurons can be established. Microglia can be stimulated with the exogenous addition of ASC-αSyn complexes and neuronal health can be subsequently monitored. Otherwise, conditioned media from ASC-αSyn-treated microglia can be incubated with neurons to reveal neuronal and synaptic viability.

6. CONCLUSIONS AND FUTURE PERSPECTIVES

Neurodegenerative diseases represent a significant and growing societal challenge, with PD being the fastest growing neurological disease. In Canada alone, 30 new cases of PD are diagnosed every day (334). The heterogenous clinical manifestations in addition to the multifactorial background of PD suggests that the pathogenesis of PD may vary from patient to patient, highlighting the need for personalized therapies and development of specific diagnostic tests and biomarkers (335). This study highlights the complex molecular mechanisms underlying PD, particularly focusing on neuroinflammation. The research demonstrates that the activation of the microglial NLRP3 inflammasome results in the release of the inflammasome adaptor protein ASC as ASC specks outside the cell, which remain biologically active and are capable of cross-seeding amyloid proteins. The binding of ASC specks and amyloidogenic proteins results in their internalization, leading to reduced protein clearance and the amplification and perpetuation of pro-inflammatory responses in a molecular feed-forward cycle that can trigger neuronal damage. Overall, in this thesis, I have demonstrated that monomeric αSyn – when added to ASC – was found in close association with oligomerized ASC upon their co-incubation, producing ASC-αSyn complexes. I revealed mechanistic insights into how ASC-αSyn complexes elicit a pro-inflammatory response in microglia, amplify NLRP3 inflammasome activity in the presence of ASC, and contribute to a vicious cycle of inflammation.

This project links the inflammasome adaptor protein ASC and αSyn to mechanisms that lead to neuroinflammation, which have relevance to PD and related α-synucleinopathies. Together, results from this study aid in pointing at a potential role of ASC specks in the pathophysiology of PD and highlight the importance of ASC-αSyn complex formation, such as an

early trigger, in the initiation of propagation and thus, the potential exacerbation, of αSyn pathology. A detailed understanding of ASC-αSyn binding and internalization and neuronal exposure to ASC-αSyn complexes warrants thorough investigation and may provide novel opportunities to characterize the early pathological events that would ultimately result in the degeneration of dopaminergic neurons. Lastly, ASC-αSyn complexes can be targeted with available antibodies and inhibitors to demonstrate the direct role of ASC-αSyn complexes in amplifying NLRP3 inflammasome responses.

7. REFERENCES

1. Poewe W, Seppi K, Tanner CM, Halliday GM, Brundin P, Volkmann J, et al. Parkinson disease. Nat Rev Dis Primer. 2017 Mar 23;3:17013.

2. Global, regional, and national burden of neurological disorders during 1990–2015: a systematic analysis for the Global Burden of Disease Study 2015. Lancet Neurol. 2017 Nov;16(11):877–97.

3. Dorsey ER, Sherer T, Okun MS, Bloem BR. The Emerging Evidence of the Parkinson Pandemic. J Park Dis. 8(Suppl 1):S3–8.

4. Moustafa AA, Chakravarthy S, Phillips JR, Gupta A, Keri S, Polner B, et al. Motor symptoms in Parkinson's disease: A unified framework. Neurosci Biobehav Rev. 2016 Sep 1;68:727–40.

5. Santos García D, de Deus Fonticoba T, Suárez Castro E, Borrué C, Mata M, Solano Vila B, et al. Non-motor symptoms burden, mood, and gait problems are the most significant factors contributing to a poor quality of life in non-demented Parkinson's disease patients: Results from the COPPADIS Study Cohort. Parkinsonism Relat Disord. 2019 Sep;66:151–7.

6. Kline EM, Houser MC, Herrick MK, Seibler P, Klein C, West A, et al. Genetic and environmental factors in Parkinson's converge on immune function and inflammation. Mov Disord Off J Mov Disord Soc. 2021 Jan;36(1):25–36.

7. Oliveira LMA, Gasser T, Edwards R, Zweckstetter M, Melki R, Stefanis L, et al. Alpha-synuclein research: defining strategic moves in the battle against Parkinson's disease. Npj Park Dis. 2021 Jul 26;7(1):1–23.

8. Calabresi P, Mechelli A, Natale G, Volpicelli-Daley L, Di Lazzaro G, Ghiglieri V. Alpha-synuclein in Parkinson's disease and other synucleinopathies: from overt neurodegeneration back to early synaptic dysfunction. Cell Death Dis. 2023 Mar 1;14(3):176.

9. Chu Y, Hirst WD, Kordower JH. Chapter 4 - Mixed pathology as a rule, not exception: Time to reconsider disease nosology. In: Espay AJ, editor. Handbook of Clinical Neurology [Internet]. Elsevier; 2023 [cited 2024 Jul 29]. p. 57–71. (Precision Medicine in Neurodegenerative Disorders, Part I; vol. 192). Available from: https://www.sciencedirect.com/science/article/pii/B9780323855389000122

10. Gould N, Mor DE, Lightfoot R, Malkus K, Giasson B, Ischiropoulos H. Evidence of Native α-Synuclein Conformers in the Human Brain *. J Biol Chem. 2014 Mar 14;289(11):7929–34.

11. Burré J, Vivona S, Diao J, Sharma M, Brunger AT, Südhof TC. Properties of native brain α-synuclein. Nature. 2013 Jun;498(7453):E4–6.

12. Fauvet B, Mbefo MK, Fares MB, Desobry C, Michael S, Ardah MT, et al. α-Synuclein in Central Nervous System and from Erythrocytes, Mammalian Cells, and Escherichia coli Exists Predominantly as Disordered Monomer *. J Biol Chem. 2012 May 1;287(19):15345–64.

13. Lucas HR, Fernández RD. Navigating the dynamic landscape of alpha-synuclein morphology: a review of the physiologically relevant tetrameric conformation. Neural Regen Res. 2020 Mar;15(3):407.

14. Sandal M, Valle F, Tessari I, Mammi S, Bergantino E, Musiani F, et al. Conformational equilibria in monomeric alpha-synuclein at the single-molecule level. PLoS Biol. 2008 Jan;6(1):e6.

15. Menon S, Mondal J. Conformational Plasticity in α-Synuclein and How Crowded Environment Modulates It. J Phys Chem B. 2023 May 11;127(18):4032–49.

16. Malfertheiner K, Stefanova N, Heras-Garvin A. The Concept of α-Synuclein Strains and How Different Conformations May Explain Distinct Neurodegenerative Disorders. Front Neurol [Internet]. 2021 Oct 5 [cited 2024 Mar 14];12. Available from: https://www.frontiersin.org/journals/neurology/articles/10.3389/fneur.2021.737195/full

17. Li A, Rastegar C, Mao X. α-Synuclein Conformational Plasticity: Physiologic States, Pathologic Strains, and Biotechnological Applications. Biomolecules. 2022 Jul;12(7):994.

18. Hoffmann A, Ettle B, Bruno A, Kulinich A, Hoffmann AC, von Wittgenstein J, et al. Alpha-synuclein activates BV2 microglia dependent on its aggregation state. Biochem Biophys Res Commun. 2016 Oct 28;479(4):881–6.

19. Saramowicz K, Siwecka N, Galita G, Kucharska-Lusina A, Rozpędek-Kamińska W, Majsterek I. Alpha-Synuclein Contribution to Neuronal and Glial Damage in Parkinson's Disease. Int J Mol Sci. 2024 Jan;25(1):360.

20. Gaspar R, Meisl G, Buell AK, Young L, Kaminski CF, Knowles TPJ, et al. Secondary nucleation of monomers on fibril surface dominates α-synuclein aggregation and provides autocatalytic amyloid amplification. Q Rev Biophys. 2017 Jan;50:e6.

21. Kordower JH, Chu Y, Hauser RA, Freeman TB, Olanow CW. Lewy body–like pathology in long-term embryonic nigral transplants in Parkinson's disease. Nat Med. 2008 May;14(5):504–6.

22. Li JY, Englund E, Holton JL, Soulet D, Hagell P, Lees AJ, et al. Lewy bodies in grafted neurons in subjects with Parkinson's disease suggest host-to-graft disease propagation. Nat Med. 2008 May;14(5):501–3.

23. Mendez I, Viñuela A, Astradsson A, Mukhida K, Hallett P, Robertson H, et al. Dopamine neurons implanted into people with Parkinson's disease survive without pathology for 14 years. Nat Med. 2008 May;14(5):507–9.

24. Halliday G, Hely M, Reid W, Morris J. The progression of pathology in longitudinally followed patients with Parkinson's disease. Acta Neuropathol (Berl). 2008 Apr;115(4):409–15.

25. Fusco G, De Simone A, Gopinath T, Vostrikov V, Vendruscolo M, Dobson CM, et al. Direct observation of the three regions in α-synuclein that determine its membrane-bound behaviour. Nat Commun. 2014 May 29;5:3827.

26. Bartels T, Ahlstrom LS, Leftin A, Kamp F, Haass C, Brown MF, et al. The N-terminus of the intrinsically disordered protein α-synuclein triggers membrane binding and helix folding. Biophys J. 2010 Oct 6;99(7):2116–24.

27. Theillet FX, Binolfi A, Bekei B, Martorana A, Rose HM, Stuiver M, et al. Structural disorder of monomeric α-synuclein persists in mammalian cells. Nature. 2016 Feb;530(7588):45–50.

28. Anderson EN, Hirpa D, Zheng KH, Banerjee R, Gunawardena S. The Non-amyloidal Component Region of α-Synuclein Is Important for α-Synuclein Transport Within Axons. Front Cell Neurosci. 2019;13:540.

29. Hijaz BA, Volpicelli-Daley LA. Initiation and propagation of α-synuclein aggregation in the nervous system. Mol Neurodegener. 2020 Mar 6;15(1):19.

30. Kim TD, Paik SR, Yang CH. Structural and functional implications of C-terminal regions of alpha-synuclein. Biochemistry. 2002 Nov 19;41(46):13782–90.

31. Lautenschläger J, Stephens AD, Fusco G, Ströhl F, Curry N, Zacharopoulou M, et al. C-terminal calcium binding of α-synuclein modulates synaptic vesicle interaction. Nat Commun. 2018 Feb 19;9(1):712.

32. Zhang Z, Jiang X, Xu D, Zheng W, Liu M, Li C. Calcium accelerates SNARE-mediated lipid mixing through modulating α-synuclein membrane interaction. Biochim Biophys Acta Biomembr. 2018 Sep;1860(9):1848–53.

33. Farzadfard A, Pedersen JN, Meisl G, Somavarapu AK, Alam P, Goksøyr L, et al. The C-terminal tail of α-synuclein protects against aggregate replication but is critical for oligomerization. Commun Biol. 2022 Feb 10;5(1):1–10.

34. Ma L, Yang C, Zhang X, Li Y, Wang S, Zheng L, et al. C-terminal truncation exacerbates the aggregation and cytotoxicity of α-Synuclein: A vicious cycle in Parkinson's disease. Biochim Biophys Acta Mol Basis Dis. 2018 Dec;1864(12):3714–25.

35. Emanuele M, Chieregatti E. Mechanisms of Alpha-Synuclein Action on Neurotransmission: Cell-Autonomous and Non-Cell Autonomous Role. Biomolecules. 2015 May 13;5(2):865–92.

36. Shin EC, Cho SE, Lee DK, Hur MW, Paik SR, Park JH, et al. Expression patterns of alpha-synuclein in human hematopoietic cells and in Drosophila at different developmental stages. Mol Cells. 2000 Feb 29;10(1):65–70.

37. Grozdanov V, Danzer KM. Intracellular Alpha-Synuclein and Immune Cell Function. Front Cell Dev Biol [Internet]. 2020 Oct 15 [cited 2024 Mar 8];8. Available from: https://www.frontiersin.org/articles/10.3389/fcell.2020.562692

38. Ostrerova N, Petrucelli L, Farrer M, Mehta N, Choi P, Hardy J, et al. α-Synuclein Shares Physical and Functional Homology with 14-3-3 Proteins. J Neurosci. 1999 Jul 15;19(14):5782–91.

39. Chandra S, Gallardo G, Fernández-Chacón R, Schlüter OM, Südhof TC. α-Synuclein Cooperates with CSPα in Preventing Neurodegeneration. Cell. 2005 Nov 4;123(3):383–96.

40. Jin H, Kanthasamy A, Ghosh A, Yang Y, Anantharam V, Kanthasamy AG. α-Synuclein Negatively Regulates Protein Kinase Cδ Expression to Suppress Apoptosis in Dopaminergic Neurons by Reducing p300 Histone Acetyltransferase Activity. J Neurosci. 2011 Feb 9;31(6):2035–51.

41. Plotegher N, Kumar D, Tessari I, Brucale M, Munari F, Tosatto L, et al. The chaperone-like protein 14-3-3η interacts with human α-synuclein aggregation intermediates rerouting the amyloidogenic pathway and reducing α-synuclein cellular toxicity. Hum Mol Genet. 2014 Nov 1;23(21):5615–29.

42. Micheli L, Creanza TM, Ceccarelli M, D'Andrea G, Giacovazzo G, Ancona N, et al. Transcriptome Analysis in a Mouse Model of Premature Aging of Dentate Gyrus: Rescue of Alpha-Synuclein Deficit by Virus-Driven Expression or by Running Restores the Defective Neurogenesis. Front Cell Dev Biol. 2021;9:696684.

43. Abeliovich A, Schmitz Y, Fariñas I, Choi-Lundberg D, Ho WH, Castillo PE, et al. Mice lacking alpha-synuclein display functional deficits in the nigrostriatal dopamine system. Neuron. 2000 Jan;25(1):239–52.

44. Benskey MJ, Sellnow RC, Sandoval IM, Sortwell CE, Lipton JW, Manfredsson FP. Silencing Alpha Synuclein in Mature Nigral Neurons Results in Rapid Neuroinflammation and Subsequent Toxicity. Front Mol Neurosci [Internet]. 2018 Feb 13 [cited 2024 Mar 7];11. Available from: https://www.frontiersin.org/articles/10.3389/fnmol.2018.00036

45. Alam MM, De Y, Li XQ, Liu J, Back TC, Trivett A, et al. Alpha synuclein, the culprit in Parkinson disease, is required for normal immune function. Cell Rep. 2022 Jan 11;38(2):110090.

46. Beatman EL, Massey A, Shives KD, Burrack KS, Chamanian M, Morrison TE, et al. Alpha-Synuclein Expression Restricts RNA Viral Infections in the Brain. J Virol. 2015 Dec 30;90(6):2767–82.

47. Lashuel HA, Overk CR, Oueslati A, Masliah E. The many faces of α-synuclein: from structure and toxicity to therapeutic target. Nat Rev Neurosci. 2013 Jan;14(1):38–48.

48. Kulkarni AS, Burns MR, Brundin P, Wesson DW. Linking α-synuclein-induced synaptopathy and neural network dysfunction in early Parkinson's disease. Brain Commun. 2022 Aug 1;4(4):fcac165.

49. Espay AJ, Lees AJ. Loss of monomeric alpha-synuclein (synucleinopenia) and the origin of Parkinson's disease. Parkinsonism Relat Disord [Internet]. 2024 Mar 3 [cited 2024 Mar 8];0(0). Available from: https://www.prd-journal.com/article/S1353-8020(24)00089-0/fulltext

50. Li W, Lesuisse C, Xu Y, Troncoso JC, Price DL, Lee MK. Stabilization of alpha-synuclein protein with aging and familial parkinson's disease-linked A53T mutation. J Neurosci Off J Soc Neurosci. 2004 Aug 18;24(33):7400–9.

51. Steiner JA, Angot E, Brundin P. A deadly spread: cellular mechanisms of α-synuclein transfer. Cell Death Differ. 2011 Sep;18(9):1425–33.

52. Jan A, Gonçalves NP, Vaegter CB, Jensen PH, Ferreira N. The Prion-Like Spreading of Alpha-Synuclein in Parkinson's Disease: Update on Models and Hypotheses. Int J Mol Sci. 2021 Aug 3;22(15):8338.

53. Lee HJ, Bae EJ, Lee SJ. Extracellular α--synuclein-a novel and crucial factor in Lewy body diseases. Nat Rev Neurol. 2014 Feb;10(2):92–8.

54. Yamada K, Iwatsubo T. Extracellular α-synuclein levels are regulated by neuronal activity. Mol Neurodegener. 2018 Feb 22;13(1):9.

55. Volpicelli-Daley LA, Luk KC, Lee VMY. Addition of exogenous α-synuclein preformed fibrils to primary neuronal cultures to seed recruitment of endogenous α-synuclein to Lewy body and Lewy neurite-like aggregates. Nat Protoc. 2014 Sep;9(9):2135–46.

56. Danzer KM, Kranich LR, Ruf WP, Cagsal-Getkin O, Winslow AR, Zhu L, et al. Exosomal cell-to-cell transmission of alpha synuclein oligomers. Mol Neurodegener. 2012 Aug 24;7:42.

57. Danzer KM, Ruf WP, Putcha P, Joyner D, Hashimoto T, Glabe C, et al. Heat-shock protein 70 modulates toxic extracellular α-synuclein oligomers and rescues trans-synaptic toxicity. FASEB J. 2011 Jan;25(1):326–36.

58. Luk KC, Kehm V, Carroll J, Zhang B, O'Brien P, Trojanowski JQ, et al. Pathological α-Synuclein Transmission Initiates Parkinson-like Neurodegeneration in Non-transgenic Mice. Science. 2012 Nov 16;338(6109):949–53.

59. Kim C, Ho DH, Suk JE, You S, Michael S, Kang J, et al. Neuron-released oligomeric α-synuclein is an endogenous agonist of TLR2 for paracrine activation of microglia. Nat Commun. 2013;4:1562.

60. Emmanouilidou E, Elenis D, Papasilekas T, Stranjalis G, Gerozissis K, Ioannou PC, et al. Assessment of α-Synuclein Secretion in Mouse and Human Brain Parenchyma. PLOS ONE. 2011 Jul 14;6(7):e22225.

61. Melachroinou K, Xilouri M, Emmanouilidou E, Masgrau R, Papazafiri P, Stefanis L, et al. Deregulation of calcium homeostasis mediates secreted α-synuclein-induced neurotoxicity. Neurobiol Aging. 2013 Dec;34(12):2853–65.

62. Emanuele M, Esposito A, Camerini S, Antonucci F, Ferrara S, Seghezza S, et al. Exogenous Alpha-Synuclein Alters Pre- and Post-Synaptic Activity by Fragmenting Lipid Rafts. EBioMedicine. 2016 Apr 5;7:191–204.

63. Prinz M, Erny D, Hagemeyer N. Ontogeny and homeostasis of CNS myeloid cells. Nat Immunol. 2017 Apr;18(4):385–92.

64. Dos Santos SE, Medeiros M, Porfirio J, Tavares W, Pessôa L, Grinberg L, et al. Similar Microglial Cell Densities across Brain Structures and Mammalian Species: Implications for Brain Tissue Function. J Neurosci. 2020 Jun 10;40(24):4622–43.

65. Colonna M, Butovsky O. Microglia Function in the Central Nervous System During Health and Neurodegeneration. Annu Rev Immunol. 2017 Apr 26;35:441–68.

66. Scheiblich H, Dansokho C, Mercan D, Schmidt SV, Bousset L, Wischhof L, et al. Microglia jointly degrade fibrillar alpha-synuclein cargo by distribution through tunneling nanotubes. Cell. 2021 Sep 30;184(20):5089-5106.e21.

67. Scheiblich H, Eikens F, Wischhof L, Opitz S, Jüngling K, Cserép C, et al. Microglia rescue neurons from aggregate-induced neuronal dysfunction and death through tunneling nanotubes. Neuron [Internet]. 2024 Jul 25 [cited 2024 Jul 29];0(0). Available from: https://www.cell.com/neuron/abstract/S0896-6273(24)00491-4

68. Augusto-Oliveira M, Arrifano GP, Delage CI, Tremblay MÈ, Crespo-Lopez ME, Verkhratsky A. Plasticity of microglia. Biol Rev Camb Philos Soc. 2022 Feb;97(1):217–50.

69. Tremblay MÈ, Stevens B, Sierra A, Wake H, Bessis A, Nimmerjahn A. The role of microglia in the healthy brain. J Neurosci Off J Soc Neurosci. 2011 Nov 9;31(45):16064–9.

70. Davalos D, Grutzendler J, Yang G, Kim JV, Zuo Y, Jung S, et al. ATP mediates rapid microglial response to local brain injury in vivo. Nat Neurosci. 2005 Jun;8(6):752–8.

71. Nimmerjahn A, Kirchhoff F, Helmchen F. Resting microglial cells are highly dynamic surveillants of brain parenchyma in vivo. Science. 2005 May 27;308(5726):1314–8.

72. Microglia. In: Glial Physiology and Pathophysiology [Internet]. 2013 [cited 2024 Mar 9]. p. 343–80. Available from: https://doi.org/10.1002/9781118402061.ch7

73. Boche D, Perry VH, Nicoll J a. R. Review: Activation patterns of microglia and their identification in the human brain. Neuropathol Appl Neurobiol. 2013;39(1):3–18.

74. Perry VH. Contribution of systemic inflammation to chronic neurodegeneration. Acta Neuropathol (Berl). 2010 Sep;120(3):277–86.

75. Gao C, Jiang J, Tan Y, Chen S. Microglia in neurodegenerative diseases: mechanism and potential therapeutic targets. Signal Transduct Target Ther. 2023 Sep 22;8(1):1–37.

76. Dugger BN, Dickson DW. Pathology of Neurodegenerative Diseases. Cold Spring Harb Perspect Biol. 2017 Jul;9(7):a028035.

77. Smajić S, Prada-Medina CA, Landoulsi Z, Ghelfi J, Delcambre S, Dietrich C, et al. Single-cell sequencing of human midbrain reveals glial activation and a Parkinson-specific neuronal state. Brain J Neurol. 2022 Apr 29;145(3):964–78.

78. Lawson LJ, Perry VH, Dri P, Gordon S. Heterogeneity in the distribution and morphology of microglia in the normal adult mouse brain. Neuroscience. 1990;39(1):151–70.

79. Kim WG, Mohney RP, Wilson B, Jeohn GH, Liu B, Hong JS. Regional difference in susceptibility to lipopolysaccharide-induced neurotoxicity in the rat brain: role of microglia. J Neurosci Off J Soc Neurosci. 2000 Aug 15;20(16):6309–16.

80. Mittelbronn M, Dietz K, Schluesener HJ, Meyermann R. Local distribution of microglia in the normal adult human central nervous system differs by up to one order of magnitude. Acta Neuropathol (Berl). 2001 Mar;101(3):249–55.

81. Janda E, Boi L, Carta AR. Microglial Phagocytosis and Its Regulation: A Therapeutic Target in Parkinson's Disease? Front Mol Neurosci. 2018;11:144.

82. Gerhard A, Pavese N, Hotton G, Turkheimer F, Es M, Hammers A, et al. In vivo imaging of microglial activation with [11C](R)-PK11195 PET in idiopathic Parkinson's disease. Neurobiol Dis. 2006 Feb;21(2):404–12.

83. Sanchez-Guajardo V, Barnum CJ, Tansey MG, Romero-Ramos M. Neuroimmunological processes in Parkinson's disease and their relation to α-synuclein: microglia as the referee

between neuronal processes and peripheral immunity. ASN NEURO. 2013 Apr 30;5(2):e00112.

84. Imamura K, Hishikawa N, Sawada M, Nagatsu T, Yoshida M, Hashizume Y. Distribution of major histocompatibility complex class II-positive microglia and cytokine profile of Parkinson's disease brains. Acta Neuropathol (Berl). 2003 Dec;106(6):518–26.

85. Ouchi Y, Yoshikawa E, Sekine Y, Futatsubashi M, Kanno T, Ogusu T, et al. Microglial activation and dopamine terminal loss in early Parkinson's disease. Ann Neurol. 2005 Feb;57(2):168–75.

86. Sanchez-Guajardo V, Tentillier N, Romero-Ramos M. The relation between α-synuclein and microglia in Parkinson's disease: Recent developments. Neuroscience. 2015 Aug 27;302:47–58.

87. Grozdanov V, Danzer KM. Release and uptake of pathologic alpha-synuclein. Cell Tissue Res. 2018 Jul;373(1):175–82.

88. Choi I, Zhang Y, Seegobin SP, Pruvost M, Wang Q, Purtell K, et al. Microglia clear neuron-released α-synuclein via selective autophagy and prevent neurodegeneration. Nat Commun. 2020 Mar 13;11(1):1386.

89. Feng Y, Zheng C, Zhang Y, Xing C, Cai W, Li R, et al. Triptolide Inhibits Preformed Fibril-Induced Microglial Activation by Targeting the MicroRNA155-5p/SHIP1 Pathway. Oxid Med Cell Longev. 2019 Apr 28;2019:e6527638.

90. Yildirim-Balatan C, Fenyi A, Besnault P, Gomez L, Sepulveda-Diaz JE, Michel PP, et al. Parkinson's disease-derived α-synuclein assemblies combined with chronic-type inflammatory cues promote a neurotoxic microglial phenotype. J Neuroinflammation. 2024 Feb 21;21(1):54.

91. Dutta D, Jana M, Majumder M, Mondal S, Roy A, Pahan K. Selective targeting of the TLR2/MyD88/NF-κB pathway reduces α-synuclein spreading in vitro and in vivo. Nat Commun. 2021 Sep 10;12(1):5382.

92. Fellner L, Irschick R, Schanda K, Reindl M, Klimaschewski L, Poewe W, et al. Toll-like receptor 4 is required for α-synuclein dependent activation of microglia and astroglia. Glia. 2013 Mar;61(3):349–60.

93. Xia Y, Zhang G, Han C, Ma K, Guo X, Wan F, et al. Microglia as modulators of exosomal alpha-synuclein transmission. Cell Death Dis. 2019 Feb 20;10(3):1–15.

94. Guo M, Wang J, Zhao Y, Feng Y, Han S, Dong Q, et al. Microglial exosomes facilitate α-synuclein transmission in Parkinson's disease. Brain. 2020 May;143(5):1476–97.

95. Alberts B, Johnson A, Lewis J, Raff M, Roberts K, Walter P. Innate Immunity. In: Molecular Biology of the Cell 4th edition [Internet]. Garland Science; 2002 [cited 2024 Mar 26]. Available from: https://www.ncbi.nlm.nih.gov/books/NBK26846/

96. Furman D, Campisi J, Verdin E, Carrera-Bastos P, Targ S, Franceschi C, et al. Chronic inflammation in the etiology of disease across the life span. Nat Med. 2019 Dec;25(12):1822–32.

97. Heneka MT, Kummer MP, Latz E. Innate immune activation in neurodegenerative disease. Nat Rev Immunol. 2014 Jul;14(7):463–77.

98. Furman D, Chang J, Lartigue L, Bolen CR, Haddad F, Gaudilliere B, et al. Expression of specific inflammasome gene modules stratifies older individuals into two extreme clinical and immunological states. Nat Med. 2017 Feb;23(2):174–84.

99. Netea MG, Balkwill F, Chonchol M, Cominelli F, Donath MY, Giamarellos-Bourboulis EJ, et al. A guiding map for inflammation. Nat Immunol. 2017 Jul 19;18(8):826–31.

100. Slavich GM. Understanding inflammation, its regulation, and relevance for health: a top scientific and public priority. Brain Behav Immun. 2015 Mar;45:13–4.

101. Bennett JM, Reeves G, Billman GE, Sturmberg JP. Inflammation–Nature's Way to Efficiently Respond to All Types of Challenges: Implications for Understanding and Managing "the Epidemic" of Chronic Diseases. Front Med [Internet]. 2018 Nov 27 [cited 2024 Mar 11];5. Available from: https://www.frontiersin.org/articles/10.3389/fmed.2018.00316

102. Roth GA, Abate D, Abate KH, Abay SM, Abbafati C, Abbasi N, et al. Global, regional, and national age-sex-specific mortality for 282 causes of death in 195 countries and territories, 1980–2017: a systematic analysis for the Global Burden of Disease Study 2017. The Lancet. 2018 Nov 10;392(10159):1736–88.

103. Franchi L, Eigenbrod T, Muñoz-Planillo R, Nuñez G. The inflammasome: a caspase-1-activation platform that regulates immune responses and disease pathogenesis. Nat Immunol. 2009 Mar;10(3):241–7.

104. Tang D, Kang R, Coyne CB, Zeh HJ, Lotze MT. PAMPs and DAMPs: signal 0s that spur autophagy and immunity. Immunol Rev. 2012 Sep;249(1):158–75.

105. Li D, Wu M. Pattern recognition receptors in health and diseases. Signal Transduct Target Ther. 2021 Aug 4;6(1):1–24.

106. Lehnardt S. Innate immunity and neuroinflammation in the CNS: the role of microglia in Toll-like receptor-mediated neuronal injury. Glia. 2010 Feb;58(3):253–63.

107. Downes CE, Crack PJ. Neural injury following stroke: are Toll-like receptors the link between the immune system and the CNS? Br J Pharmacol. 2010 Aug;160(8):1872–88.

108. Gorina R, Santalucia T, Petegnief V, Ejarque-Ortiz A, Saura J, Planas AM. Astrocytes are very sensitive to develop innate immune responses to lipid-carried short interfering RNA. Glia. 2009 Jan 1;57(1):93–107.

109. de Alba E. Structure, interactions and self-assembly of ASC-dependent inflammasomes. Arch Biochem Biophys. 2019 Jul 30;670:15–31.

110. Kelley N, Jeltema D, Duan Y, He Y. The NLRP3 Inflammasome: An Overview of Mechanisms of Activation and Regulation. Int J Mol Sci. 2019 Jan;20(13):3328.

111. Swanson KV, Deng M, Ting JPY. The NLRP3 inflammasome: molecular activation and regulation to therapeutics. Nat Rev Immunol. 2019 Aug;19(8):477–89.

112. Freeman L, Guo H, David CN, Brickey WJ, Jha S, Ting JPY. NLR members NLRC4 and NLRP3 mediate sterile inflammasome activation in microglia and astrocytes. J Exp Med. 2017 Apr 12;214(5):1351–70.

113. Gustin A, Kirchmeyer M, Koncina E, Felten P, Losciuto S, Heurtaux T, et al. NLRP3 Inflammasome Is Expressed and Functional in Mouse Brain Microglia but Not in Astrocytes. PLOS ONE. 2015 Jun 19;10(6):e0130624.

114. Johann S, Heitzer M, Kanagaratnam M, Goswami A, Rizo T, Weis J, et al. NLRP3 inflammasome is expressed by astrocytes in the SOD1 mouse model of ALS and in human sporadic ALS patients. Glia. 2015;63(12):2260–73.

115. Guo H, Callaway JB, Ting JPY. Inflammasomes: mechanism of action, role in disease, and therapeutics. Nat Med. 2015 Jul;21(7):677–87.

116. He W ting, Wan H, Hu L, Chen P, Wang X, Huang Z, et al. Gasdermin D is an executor of pyroptosis and required for interleukin-1β secretion. Cell Res. 2015 Dec;25(12):1285–98.

117. Kawai T, Akira S. The role of pattern-recognition receptors in innate immunity: update on Toll-like receptors. Nat Immunol. 2010 May;11(5):373–84.

118. Hayden MS, Ghosh S. Signaling to NF-kappaB. Genes Dev. 2004 Sep 15;18(18):2195–224.

119. Kawai T, Akira S. Toll-like receptor downstream signaling. Arthritis Res Ther. 2004 Nov 30;7(1):12.

120. O'Neill LAJ, Bowie AG. The family of five: TIR-domain-containing adaptors in Toll-like receptor signalling. Nat Rev Immunol. 2007 May;7(5):353–64.

121. Bauernfeind FG, Horvath G, Stutz A, Alnemri ES, MacDonald K, Speert D, et al. Cutting edge: NF-kappaB activating pattern recognition and cytokine receptors license NLRP3 inflammasome activation by regulating NLRP3 expression. J Immunol Baltim Md 1950. 2009 Jul 15;183(2):787–91.

122. Yang Y, Wang H, Kouadir M, Song H, Shi F. Recent advances in the mechanisms of NLRP3 inflammasome activation and its inhibitors. Cell Death Dis. 2019 Feb 12;10(2):1–11.

123. Vanaja SK, Rathinam VAK, Fitzgerald KA. Mechanisms of inflammasome activation: recent advances and novel insights. Trends Cell Biol. 2015 May;25(5):308–15.

124. Lamkanfi M, Dixit VM. Mechanisms and functions of inflammasomes. Cell. 2014 May 22;157(5):1013–22.

125. Deczkowska A, Keren-Shaul H, Weiner A, Colonna M, Schwartz M, Amit I. Disease-Associated Microglia: A Universal Immune Sensor of Neurodegeneration. Cell. 2018 May 17;173(5):1073–81.

126. Hulse J, Bhaskar K. Crosstalk Between the NLRP3 Inflammasome/ASC Speck and Amyloid Protein Aggregates Drives Disease Progression in Alzheimer's and Parkinson's Disease. Front Mol Neurosci [Internet]. 2022 [cited 2022 Sep 23];15. Available from: https://www.frontiersin.org/articles/10.3389/fnmol.2022.805169

127. Hornung V, Bauernfeind F, Halle A, Samstad EO, Kono H, Rock KL, et al. Silica crystals and aluminum salts activate the NALP3 inflammasome through phagosomal destabilization. Nat Immunol. 2008 Aug;9(8):847–56.

128. Halle A, Hornung V, Petzold GC, Stewart CR, Monks BG, Reinheckel T, et al. The NALP3 inflammasome is involved in the innate immune response to amyloid-beta. Nat Immunol. 2008 Aug;9(8):857–65.

129. Zhou R, Yazdi AS, Menu P, Tschopp J. A role for mitochondria in NLRP3 inflammasome activation. Nature. 2011 Jan;469(7329):221–5.

130. Sorbara MT, Girardin SE. Mitochondrial ROS fuel the inflammasome. Cell Res. 2011 Apr;21(4):558–60.

131. Heid ME, Keyel PA, Kamga C, Shiva S, Watkins SC, Salter RD. Mitochondrial Reactive Oxygen Species Induces NLRP3-Dependent Lysosomal Damage and Inflammasome Activation. J Immunol. 2013 Nov 15;191(10):5230–8.

132. Wen H, Gris D, Lei Y, Jha S, Zhang L, Huang MTH, et al. Fatty acid–induced NLRP3-ASC inflammasome activation interferes with insulin signaling. Nat Immunol. 2011 May;12(5):408–15.

133. Anderson RM, Hadjichrysanthou C, Evans S, Wong MM. Why do so many clinical trials of therapies for Alzheimer's disease fail? The Lancet. 2017 Nov 25;390(10110):2327–9.

134. Dokholyan NV, Mohs RC, Bateman RJ. Challenges and progress in research, diagnostics, and therapeutics in Alzheimer's disease and related dementias. Alzheimers Dement Transl Res Clin Interv. 2022;8(1):e12330.

135. Dick MS, Sborgi L, Rühl S, Hiller S, Broz P. ASC filament formation serves as a signal amplification mechanism for inflammasomes. Nat Commun. 2016 Jun 22;7(1):11929.

136. Scheckel C, Aguzzi A. Prions, prionoids and protein misfolding disorders. Nat Rev Genet. 2018 Jul;19(7):405–18.

137. Franklin BS, Bossaller L, De Nardo D, Ratter JM, Stutz A, Engels G, et al. The adaptor ASC has extracellular and "prionoid" activities that propagate inflammation. Nat Immunol. 2014 Aug;15(8):727–37.

138. Baroja-Mazo A, Martín-Sánchez F, Gomez AI, Martínez CM, Amores-Iniesta J, Compan V, et al. The NLRP3 inflammasome is released as a particulate danger signal that amplifies the inflammatory response. Nat Immunol. 2014 Aug;15(8):738–48.

139. Franklin BS, Latz E, Schmidt FI. The intra- and extracellular functions of ASC specks. Immunol Rev. 2018;281(1):74–87.

140. Sahillioğlu AC, Özören N. Artificial Loading of ASC Specks with Cytosolic Antigens. PLOS ONE. 2015 Aug 10;10(8):e0134912.

141. Ben-Sasson SZ, Hogg A, Hu-Li J, Wingfield P, Chen X, Crank M, et al. IL-1 enhances expansion, effector function, tissue localization, and memory response of antigen-specific CD8 T cells. J Exp Med. 2013 Mar 11;210(3):491–502.

142. Lelouard H, Gatti E, Cappello F, Gresser O, Camosseto V, Pierre P. Transient aggregation of ubiquitinated proteins during dendritic cell maturation. Nature. 2002 May 9;417(6885):177–82.

143. Nicholson DW. Caspase structure, proteolytic substrates, and function during apoptotic cell death. Cell Death Differ. 1999 Nov;6(11):1028–42.

144. Martinon F, Tschopp J. Inflammatory caspases and inflammasomes: master switches of inflammation. Cell Death Differ. 2007 Jan;14(1):10–22.

145. McIlwain DR, Berger T, Mak TW. Caspase functions in cell death and disease. Cold Spring Harb Perspect Biol. 2013 Apr 1;5(4):a008656.

146. Black RA, Kronheim SR, Merriam JE, March CJ, Hopp TP. A pre-aspartate-specific protease from human leukocytes that cleaves pro-interleukin-1 beta. J Biol Chem. 1989 Apr 5;264(10):5323–6.

147. Martinon F, Tschopp J. Inflammatory caspases: linking an intracellular innate immune system to autoinflammatory diseases. Cell. 2004 May 28;117(5):561–74.

148. Dinarello CA. Immunological and inflammatory functions of the interleukin-1 family. Annu Rev Immunol. 2009;27:519–50.

149. Sims JE, Smith DE. The IL-1 family: regulators of immunity. Nat Rev Immunol. 2010 Feb;10(2):89–102.

150. Puren AJ, Fantuzzi G, Dinarello CA. Gene expression, synthesis, and secretion of interleukin 18 and interleukin 1β are differentially regulated in human blood mononuclear cells and mouse spleen cells. Proc Natl Acad Sci U S A. 1999 Mar 2;96(5):2256–61.

151. Mehta VB, Hart J, Wewers MD. ATP-stimulated release of interleukin (IL)-1beta and IL-18 requires priming by lipopolysaccharide and is independent of caspase-1 cleavage. J Biol Chem. 2001 Feb 9;276(6):3820–6.

152. Zhu Q, Kannegant TD. Distinct regulatory mechanisms control proinflammatory cytokines IL-18 and IL-1β. J Immunol Baltim Md 1950. 2017 Jun 1;198(11):4210–5.

153. Ihim SA, Abubakar SD, Zian Z, Sasaki T, Saffarioun M, Maleknia S, et al. Interleukin-18 cytokine in immunity, inflammation, and autoimmunity: Biological role in induction, regulation, and treatment. Front Immunol. 2022 Aug 11;13:919973.

154. Arend WP, Palmer G, Gabay C. IL-1, IL-18, and IL-33 families of cytokines. Immunol Rev. 2008 Jun;223:20–38.

155. Kaplanski G. Interleukin-18: Biological properties and role in disease pathogenesis. Immunol Rev. 2018 Jan;281(1):138–53.

156. Lopez-Castejon G, Brough D. Understanding the mechanism of IL-1β secretion. Cytokine Growth Factor Rev. 2011 Aug 1;22(4):189–95.

157. Rubartelli A, Cozzolino F, Talio M, Sitia R. A novel secretory pathway for interleukin-1 beta, a protein lacking a signal sequence. EMBO J. 1990 May;9(5):1503–10.

158. Matsushima K, Taguchi M, Kovacs EJ, Young HA, Oppenheim JJ. Intracellular localization of human monocyte associated interleukin 1 (IL 1) activity and release of biologically active IL 1 from monocytes by trypsin and plasmin. J Immunol Baltim Md 1950. 1986 Apr 15;136(8):2883–91.

159. Kudo S, Mizuno K, Hirai Y, Shimizu T. Clearance and tissue distribution of recombinant human interleukin 1 beta in rats. Cancer Res. 1990 Sep 15;50(18):5751–5.

160. Bianco F, Pravettoni E, Colombo A, Schenk U, Möller T, Matteoli M, et al. Astrocyte-derived ATP induces vesicle shedding and IL-1 beta release from microglia. J Immunol Baltim Md 1950. 2005 Jun 1;174(11):7268–77.

161. MacKenzie A, Wilson HL, Kiss-Toth E, Dower SK, North RA, Surprenant A. Rapid secretion of interleukin-1beta by microvesicle shedding. Immunity. 2001 Nov;15(5):825–35.

162. Qu Y, Franchi L, Nunez G, Dubyak GR. Nonclassical IL-1 beta secretion stimulated by P2X7 receptors is dependent on inflammasome activation and correlated with exosome release in murine macrophages. J Immunol Baltim Md 1950. 2007 Aug 1;179(3):1913–25.

163. Perregaux D, Gabel CA. Interleukin-1 beta maturation and release in response to ATP and nigericin. Evidence that potassium depletion mediated by these agents is a necessary and common feature of their activity. J Biol Chem. 1994 May 27;269(21):15195–203.

164. Hogquist KA, Nett MA, Unanue ER, Chaplin DD. Interleukin 1 is processed and released during apoptosis. Proc Natl Acad Sci U S A. 1991 Oct 1;88(19):8485–9.

165. Tapia VS, Daniels MJD, Palazón-Riquelme P, Dewhurst M, Luheshi NM, Rivers-Auty J, et al. The three cytokines IL-1β, IL-18, and IL-1α share related but distinct secretory routes. J Biol Chem. 2019 May 24;294(21):8325–35.

166. Ashkenazi A, Salvesen G. Regulated cell death: signaling and mechanisms. Annu Rev Cell Dev Biol. 2014;30:337–56.

167. Hu Y, Wang B, Li S, Yang S. Pyroptosis, and its Role in Central Nervous System Disease. J Mol Biol. 2022 Feb 28;434(4):167379.

168. Elmore S. Apoptosis: A Review of Programmed Cell Death. Toxicol Pathol. 2007;35(4):495–516.

169. Smale G, Nichols NR, Brady DR, Finch CE, Horton WE. Evidence for Apoptotic Cell Death in Alzheimer's Disease. Exp Neurol. 1995 Jun 1;133(2):225–30.

170. Mochizuki H, Goto K, Mori H, Mizuno Y. Histochemical detection of apoptosis in Parkinson's disease. J Neurol Sci. 1996 May 1;137(2):120–3.

171. Martin LJ. Neuronal Death in Amyotrophic Lateral Sclerosis Is Apoptosis: Possible Contribution of a Programmed Cell Death Mechanism. J Neuropathol Exp Neurol. 1999 May 1;58(5):459–71.

172. Cookson BT, Brennan MA. Pro-inflammatory programmed cell death. Trends Microbiol. 2001 Mar 1;9(3):113–4.

173. Tsuchiya K. Inflammasome-associated cell death: Pyroptosis, apoptosis, and physiological implications. Microbiol Immunol. 2020 Apr;64(4):252–69.

174. Yu P, Zhang X, Liu N, Tang L, Peng C, Chen X. Pyroptosis: mechanisms and diseases. Signal Transduct Target Ther. 2021 Mar 29;6(1):1–21.

175. Shi J, Zhao Y, Wang K, Shi X, Wang Y, Huang H, et al. Cleavage of GSDMD by inflammatory caspases determines pyroptotic cell death. Nature. 2015 Oct 29;526(7575):660–5.

176. Liu Z, Wang C, Yang J, Zhou B, Yang R, Ramachandran R, et al. Crystal Structures of the Full-Length Murine and Human Gasdermin D Reveal Mechanisms of Autoinhibition, Lipid Binding, and Oligomerization. Immunity. 2019 Jul 16;51(1):43-49.e4.

177. Kuang S, Zheng J, Yang H, Li S, Duan S, Shen Y, et al. Structure insight of GSDMD reveals the basis of GSDMD autoinhibition in cell pyroptosis. Proc Natl Acad Sci. 2017 Oct 3;114(40):10642–7.

178. Liu X, Zhang Z, Ruan J, Pan Y, Magupalli VG, Wu H, et al. Inflammasome-activated gasdermin D causes pyroptosis by forming membrane pores. Nature. 2016 Jul;535(7610):153–8.

179. Ding J, Wang K, Liu W, She Y, Sun Q, Shi J, et al. Pore-forming activity and structural autoinhibition of the gasdermin family. Nature. 2016 Jul;535(7610):111–6.

180. Aglietti RA, Dueber EC. Recent Insights into the Molecular Mechanisms Underlying Pyroptosis and Gasdermin Family Functions. Trends Immunol. 2017 Apr;38(4):261–71.

181. Sborgi L, Rühl S, Mulvihill E, Pipercevic J, Heilig R, Stahlberg H, et al. GSDMD membrane pore formation constitutes the mechanism of pyroptotic cell death. EMBO J. 2016 Aug 15;35(16):1766–78.

182. Kayagaki N, Kornfeld OS, Lee BL, Stowe IB, O'Rourke K, Li Q, et al. NINJ1 mediates plasma membrane rupture during lytic cell death. Nature. 2021 Mar;591(7848):131–6.

183. Matikainen S, Nyman TA, Cypryk W. Function and Regulation of Noncanonical Caspase-4/5/11 Inflammasome. J Immunol. 2020 Jun 15;204(12):3063–9.

184. Shi J, Zhao Y, Wang Y, Gao W, Ding J, Li P, et al. Inflammatory caspases are innate immune receptors for intracellular LPS. Nature. 2014 Oct;514(7521):187–92.

185. Man SM, Karki R, Kanneganti TD. Molecular mechanisms and functions of pyroptosis, inflammatory caspases and inflammasomes in infectious diseases. Immunol Rev. 2017;277(1):61–75.

186. McKenzie BA, Fernandes JP, Doan MAL, Schmitt LM, Branton WG, Power C. Activation of the executioner caspases-3 and-7 promotes microglial pyroptosis in models of multiple sclerosis. J Neuroinflammation. 2020;17(1).

187. Chen X, He W ting, Hu L, Li J, Fang Y, Wang X, et al. Pyroptosis is driven by non-selective gasdermin-D pore and its morphology is different from MLKL channel-mediated necroptosis. Cell Res. 2016 Sep;26(9):1007–20.

188. Fink SL, Cookson BT. Caspase-1-dependent pore formation during pyroptosis leads to osmotic lysis of infected host macrophages. Cell Microbiol. 2006 Nov;8(11):1812–25.

189. Fink SL, Cookson BT. Pillars Article: Caspase-1-dependent pore formation during pyroptosis leads to osmotic lysis of infected host macrophages. Cell Microbiol. 2006. 8: 1812-1825. J Immunol Baltim Md 1950. 2019 Apr 1;202(7):1913–26.

190. Bortner CD, Cidlowski JA. Apoptotic volume decrease and the incredible shrinking cell. Cell Death Differ. 2002 Dec 1;9(12):1307–10.

191. Bido S, Muggeo S, Massimino L, Marzi MJ, Giannelli SG, Melacini E, et al. Microglia-specific overexpression of α-synuclein leads to severe dopaminergic neurodegeneration by phagocytic exhaustion and oxidative toxicity. Nat Commun. 2021 Oct 29;12(1):6237.

192. Jiang S, Maphis NM, Binder J, Chisholm D, Weston L, Duran W, et al. Proteopathic tau primes and activates interleukin-1β via myeloid-cell-specific MyD88- and NLRP3-ASC-inflammasome pathway. Cell Rep. 2021 Sep 21;36(12):109720.

193. Friker LL, Scheiblich H, Hochheiser IV, Brinkschulte R, Riedel D, Latz E, et al. β-Amyloid Clustering around ASC Fibrils Boosts Its Toxicity in Microglia. Cell Rep. 2020 Mar 17;30(11):3743-3754.e6.

194. Chu Y, Hirst WD, Federoff HJ, Harms AS, Stoessl AJ, Kordower JH. Nigrostriatal tau pathology in parkinsonism and Parkinson's disease. Brain. 2024 Feb 1;147(2):444–57.

195. Lim EW, Aarsland D, Ffytche D, Taddei RN, van Wamelen DJ, Wan YM, et al. Amyloid-β and Parkinson's disease. J Neurol. 2019 Nov;266(11):2605–19.

196. Venegas C, Kumar S, Franklin BS, Dierkes T, Brinkschulte R, Tejera D, et al. Microglia-derived ASC specks cross-seed amyloid-β in Alzheimer's disease. Nature. 2017 Dec 20;552(7685):355–61.

197. Gordon R, Albornoz EA, Christie DC, Langley MR, Kumar V, Mantovani S, et al. Inflammasome inhibition prevents α-synuclein pathology and dopaminergic neurodegeneration in mice. Sci Transl Med. 2018 Oct 31;10(465):eaah4066.

198. Chatterjee K, Roy A, Banerjee R, Choudhury S, Mondal B, Halder S, et al. Inflammasome and α-synuclein in Parkinson's disease: A cross-sectional study. J Neuroimmunol. 2020 Jan 15;338:577089.

199. Wang W, Nguyen LTT, Burlak C, Chegini F, Guo F, Chataway T, et al. Caspase-1 causes truncation and aggregation of the Parkinson's disease-associated protein α-synuclein. Proc Natl Acad Sci. 2016 Aug 23;113(34):9587–92.

200. Zheng R, Yan Y, Dai S, Ruan Y, Chen Y, Hu C, et al. ASC specks exacerbate α-synuclein pathology via amplifying NLRP3 inflammasome activities. J Neuroinflammation. 2023 Feb 5;20:26.

201. Pagano G, Taylor KI, Anzures-Cabrera J, Marchesi M, Simuni T, Marek K, et al. Trial of Prasinezumab in Early-Stage Parkinson's Disease. N Engl J Med. 2022 Aug 4;387(5):421–32.

202. Lang AE, Siderowf AD, Macklin EA, Poewe W, Brooks DJ, Fernandez HH, et al. Trial of Cinpanemab in Early Parkinson's Disease. N Engl J Med. 2022 Aug 4;387(5):408–20.

203. Wen Q, Ma L, Luo W, Zhou MQ, He D, Lin Y, et al. Comparison of four methods for the purification and refolding of human interleukin-2-mouse granulocyte/macrophage colony-stimulating factor fusion protein. Biotechnol Appl Biochem. 2008 May;50(Pt 1):41–8.

204. Stine WB, Dahlgren KN, Krafft GA, LaDu MJ. In vitro characterization of conditions for amyloid-beta peptide oligomerization and fibrillogenesis. J Biol Chem. 2003 Mar 28;278(13):11612–22.

205. Vaikath N, Sudhakaran I, Abdi I, Gupta V, Majbour N, Ghanem S, et al. Structural and Biophysical Characterization of Stable Alpha-Synuclein Oligomers. Int J Mol Sci. 2022 Nov 23;23(23):14630.

206. Nagamoto-Combs K, Kulas J, Combs CK. A novel cell line from spontaneously immortalized murine microglia. J Neurosci Methods. 2014 Aug 15;233:187–98.

207. Chaiwut R, Kasinrerk W. Very low concentration of lipopolysaccharide can induce the production of various cytokines and chemokines in human primary monocytes. BMC Res Notes. 2022 Feb 10;15:42.

208. Paolicelli RC, Sierra A, Stevens B, Tremblay ME, Aguzzi A, Ajami B, et al. Microglia states and nomenclature: A field at its crossroads. Neuron. 2022 Nov 2;110(21):3458–83.

209. Stutz A, Horvath GL, Monks BG, Latz E. ASC speck formation as a readout for inflammasome activation. Methods Mol Biol Clifton NJ. 2013;1040:91–101.

210. Glück IM, Mathias GP, Strauss S, Rat V, Gialdini I, Ebert TS, et al. Nanoscale organization of the endogenous ASC speck. iScience. 2023 Dec 15;26(12):108382.

211. Amstad PA, Yu G, Johnson GL, Lee BW, Dhawan S, Phelps DJ. Detection of caspase activation in situ by fluorochrome-labeled caspase inhibitors. BioTechniques. 2001 Sep;31(3):608–10, 612, 614, passim.

212. Bedner E, Smolewski P, Amstad P, Darzynkiewicz Z. Activation of caspases measured in situ by binding of fluorochrome-labeled inhibitors of caspases (FLICA): correlation with DNA fragmentation. Exp Cell Res. 2000 Aug 25;259(1):308–13.

213. Nguyen U, Squaglia N, Boge A, Fung PA. The Simple Western™: a gel-free, blot-free, hands-free Western blotting reinvention. Nat Methods. 2011 Nov;8(11):v–vi.

214. Chen JQ, Heldman MR, Herrmann MA, Kedei N, Woo W, Blumberg PM, et al. Absolute quantitation of endogenous proteins with precision and accuracy using a capillary western system. Anal Biochem. 2013 Nov 1;442(1):97–103.

215. Wendimu MY, Hooks SB. Microglia Phenotypes in Aging and Neurodegenerative Diseases. Cells. 2022 Jun 30;11(13):2091.

216. Masumoto J, Taniguchi S, Ayukawa K, Sarvotham H, Kishino T, Niikawa N, et al. ASC, a Novel 22-kDa Protein, Aggregates during Apoptosis of Human Promyelocytic Leukemia HL-60 Cells *. J Biol Chem. 1999 Nov 26;274(48):33835–8.

217. Fernandes-Alnemri T, Wu J, Yu JW, Datta P, Miller B, Jankowski W, et al. The pyroptosome: a supramolecular assembly of ASC dimers mediating inflammatory cell death via caspase-1 activation. Cell Death Differ. 2007 Sep;14(9):1590–604.

218. Kagan JC, Magupalli VG, Wu H. SMOCs: supramolecular organizing centres that control innate immunity. Nat Rev Immunol. 2014 Dec;14(12):821–6.

219. Kagan JC. Signaling organelles of the innate immune system. Cell. 2012 Dec 7;151(6):1168–78.

220. Fan Z, Pan YT, Zhang ZY, Yang H, Yu SY, Zheng Y, et al. Systemic activation of NLRP3 inflammasome and plasma α-synuclein levels are correlated with motor severity and progression in Parkinson's disease. J Neuroinflammation [Internet]. 2020 [cited 2024 Jul 18];17. Available from: https://www.ncbi.nlm.nih.gov/pmc/articles/PMC6950934/

221. Jang A, Lee HJ, Suk JE, Jung JW, Kim KP, Lee SJ. Non-classical exocytosis of alpha-synuclein is sensitive to folding states and promoted under stress conditions. J Neurochem. 2010 Jun;113(5):1263–74.

222. Wang S, Yuan YH, Chen NH, Wang HB. The mechanisms of NLRP3 inflammasome/pyroptosis activation and their role in Parkinson's disease. Int Immunopharmacol. 2019 Feb;67:458–64.

223. Pike AF, Varanita T, Herrebout MAC, Plug BC, Kole J, Musters RJP, et al. α-Synuclein evokes NLRP3 inflammasome-mediated IL-1β secretion from primary human microglia. Glia. 2021 Jun;69(6):1413–28.

224. Zilka N, Kazmerova Z, Jadhav S, Neradil P, Madari A, Obetkova D, et al. Who fans the flames of Alzheimer's disease brains? Misfolded tau on the crossroad of neurodegenerative and inflammatory pathways. J Neuroinflammation. 2012 Mar 7;9(1):47.

225. Cotman CW, Poon WW, Rissman RA, Blurton-Jones M. The role of caspase cleavage of tau in Alzheimer disease neuropathology. J Neuropathol Exp Neurol. 2005 Feb;64(2):104–12.

226. Rizzi L, Grinberg LT. Exploring the significance of caspase-cleaved tau in tauopathies and as a complementary pathology to phospho-tau in Alzheimer's disease: implications for biomarker development and therapeutic targeting. Acta Neuropathol Commun. 2024 Feb 28;12(1):36.

227. Liu D, Huang Y. Protocol for in vivo and in vitro activation of NLRP3 inflammasome in mice using monosodium urate. STAR Protoc. 2023 Sep 7;4(3):102554.

228. Guo H, Ting JPY. Inflammasome assays in vitro and in mouse models. Curr Protoc Immunol. 2020 Dec;131(1):e107.

229. Liu T, Zhang L, Joo D, Sun SC. NF-κB signaling in inflammation. Signal Transduct Target Ther. 2017 Jul 14;2(1):1–9.

230. McKee CM, Coll RC. NLRP3 inflammasome priming: A riddle wrapped in a mystery inside an enigma. J Leukoc Biol. 2020 Sep;108(3):937–52.

231. Barker BR, Taxman DJ, Ting JPY. Cross-regulation between the IL-1β/IL-18 processing inflammasome and other inflammatory cytokines. Curr Opin Immunol. 2011 Oct;23(5):591–7.

232. Deng I, Corrigan F, Zhai G, Zhou XF, Bobrovskaya L. Lipopolysaccharide animal models of Parkinson's disease: Recent progress and relevance to clinical disease. Brain Behav Immun - Health. 2020 Mar 18;4:100060.

233. Brown GC. The endotoxin hypothesis of neurodegeneration. J Neuroinflammation. 2019 Sep 13;16:180.

234. Brown GC, Camacho M, Williams-Gray CH. The Endotoxin Hypothesis of Parkinson's Disease. Mov Disord. 2023;38(7):1143–55.

235. Henry CJ, Huang Y, Wynne AM, Godbout JP. Peripheral Lipopolysaccharide (LPS) challenge promotes microglial hyperactivity in aged mice that is associated with

exaggerated induction of both pro-inflammatory IL-1β and anti-inflammatory IL-10 cytokines. Brain Behav Immun. 2008 Sep 12;23(3):309.

236. Castaño A, Herrera AJ, Cano J, Machado A. Lipopolysaccharide intranigral injection induces inflammatory reaction and damage in nigrostriatal dopaminergic system. J Neurochem. 1998 Apr;70(4):1584–92.

237. Nadeau S, Rivest S. Glucocorticoids play a fundamental role in protecting the brain during innate immune response. J Neurosci Off J Soc Neurosci. 2003 Jul 2;23(13):5536–44.

238. Nadeau S, Rivest S. Endotoxemia prevents the cerebral inflammatory wave induced by intraparenchymal lipopolysaccharide injection: role of glucocorticoids and CD14. J Immunol Baltim Md 1950. 2002 Sep 15;169(6):3370–81.

239. Teissier T, Boulanger E, Cox LS. Interconnections between Inflammageing and Immunosenescence during Ageing. Cells. 2022 Jan 21;11(3):359.

240. Ferrucci L, Fabbri E. Inflammageing: chronic inflammation in ageing, cardiovascular disease, and frailty. Nat Rev Cardiol. 2018 Sep;15(9):505–22.

241. Zhang W, Xiao D, Mao Q, Xia H. Role of neuroinflammation in neurodegeneration development. Signal Transduct Target Ther. 2023 Jul 12;8(1):1–32.

242. Tan EK, Chao YX, West A, Chan LL, Poewe W, Jankovic J. Parkinson disease and the immune system - associations, mechanisms and therapeutics. Nat Rev Neurol. 2020 Jun;16(6):303–18.

243. Wang J, Zhang XN, Fang JN, Hua FF, Han JY, Yuan ZQ, et al. The mechanism behind activation of the Nod-like receptor family protein 3 inflammasome in Parkinson's disease. Neural Regen Res. 2021 Aug 30;17(4):898–904.

244. Brahadeeswaran S, Sivagurunathan N, Calivarathan L. Inflammasome Signaling in the Aging Brain and Age-Related Neurodegenerative Diseases. Mol Neurobiol. 2022 Apr;59(4):2288–304.

245. Heneka MT, McManus RM, Latz E. Inflammasome signalling in brain function and neurodegenerative disease. Nat Rev Neurosci. 2018 Oct;19(10):610–21.

246. Hoss F, Rodriguez-Alcazar JF, Latz E. Assembly and regulation of ASC specks. Cell Mol Life Sci. 2017 Apr 1;74(7):1211–29.

247. Wu H. Higher-Order Assemblies in a New Paradigm of Signal Transduction. Cell. 2013 Apr 11;153(2):287–92.

248. Wu H, Fuxreiter M. The Structure and Dynamics of Higher-Order Assemblies: Amyloids, Signalosomes, and Granules. Cell. 2016 May 19;165(5):1055–66.

249. Cheng J, Waite AL, Tkaczyk ER, Ke K, Richards N, Hunt AJ, et al. Kinetic properties of ASC protein aggregation in epithelial cells. J Cell Physiol. 2010;222(3):738–47.

250. Sester DP, Thygesen SJ, Sagulenko V, Vajjhala PR, Cridland JA, Vitak N, et al. A Novel Flow Cytometric Method To Assess Inflammasome Formation. J Immunol. 2015 Jan 1;194(1):455–62.

251. Loo YM, Gale M. Immune Signaling by RIG-I-like Receptors. Immunity. 2011 May 27;34(5):680–92.

252. Kuri P, Schieber NL, Thumberger T, Wittbrodt J, Schwab Y, Leptin M. Dynamics of in vivo ASC speck formation. J Cell Biol. 2017 Jul 12;216(9):2891–909.

253. Nagar A, DeMarco RA, Harton JA. Inflammasome and Caspase-1 Activity Characterization and Evaluation: An Imaging Flow Cytometer–Based Detection and Assessment of Inflammasome Specks and Caspase-1 Activation. J Immunol. 2019 Feb 1;202(3):1003–15.

254. Misawa T, Takahama M, Kozaki T, Lee H, Zou J, Saitoh T, et al. Microtubule-driven spatial arrangement of mitochondria promotes activation of the NLRP3 inflammasome. Nat Immunol. 2013 May;14(5):454–60.

255. Nagar A, Harton JA. Flow Imaging of the Inflammasome: Evaluating ASC Speck Characteristics and Caspase-1 Activity. In: Barteneva NS, Vorobjev IA, editors. Spectral and Imaging Cytometry: Methods and Protocols [Internet]. New York, NY: Springer US; 2023 [cited 2024 Jul 15]. p. 185–202. Available from: https://doi.org/10.1007/978-1-0716-3020-4_11

256. Bryan NB, Dorfleutner A, Rojanasakul Y, Stehlik C. Activation of inflammasomes requires intracellular redistribution of the apoptotic speck-like protein containing a caspase recruitment domain (ASC). J Immunol Baltim Md 1950. 2009 Mar 1;182(5):3173–82.

257. Walsh JG, Logue SE, Lüthi AU, Martin SJ. Caspase-1 Promiscuity Is Counterbalanced by Rapid Inactivation of Processed Enzyme. J Biol Chem. 2011 Sep 16;286(37):32513–24.

258. Elliott JM, Rouge L, Wiesmann C, Scheer JM. Crystal Structure of Procaspase-1 Zymogen Domain Reveals Insight into Inflammatory Caspase Autoactivation. J Biol Chem. 2009 Mar 6;284(10):6546–53.

259. Mantovani A, Dinarello CA, Molgora M, Garlanda C. Interleukin-1 and Related Cytokines in the Regulation of Inflammation and Immunity. Immunity. 2019 Apr 16;50(4):778–95.

260. Dinarello CA, van der Meer JWM. Treating inflammation by blocking interleukin-1 in humans. Semin Immunol. 2013 Dec 15;25(6):469–84.

261. Franchi L, Park JH, Shaw MH, Marina-Garcia N, Chen G, Kim YG, et al. Intracellular NOD-like receptors in innate immunity, infection and disease. Cell Microbiol. 2008;10(1):1–8.

262. Boraschi D, Tagliabue A. The interleukin-1 receptor family. Semin Immunol. 2013 Dec 15;25(6):394–407.

263. Salminen A, Ojala J, Suuronen T, Kaarniranta K, Kauppinen A. Amyloid-beta oligomers set fire to inflammasomes and induce Alzheimer's pathology. J Cell Mol Med. 2008 Dec;12(6A):2255–62.

264. Chakraborty S, Kaushik DK, Gupta M, Basu A. Inflammasome signaling at the heart of central nervous system pathology. J Neurosci Res. 2010 Jun;88(8):1615–31.

265. de Vries HE, Blom-Roosemalen MC, van Oosten M, de Boer AG, van Berkel TJ, Breimer DD, et al. The influence of cytokines on the integrity of the blood-brain barrier in vitro. J Neuroimmunol. 1996 Jan;64(1):37–43.

266. Gibson RM, Rothwell NJ, Le Feuvre RA. CNS injury: the role of the cytokine IL-1. Vet J Lond Engl 1997. 2004 Nov;168(3):230–7.

267. Shaftel SS, Carlson TJ, Olschowka JA, Kyrkanides S, Matousek SB, O'Banion MK. Chronic Interleukin-1β Expression in Mouse Brain Leads to Leukocyte Infiltration and Neutrophil-Independent Blood–Brain Barrier Permeability without Overt Neurodegeneration. J Neurosci. 2007 Aug 29;27(35):9301–9.

268. Deng J, Yu XQ, Wang PH. Inflammasome activation and Th17 responses. Mol Immunol. 2019 Mar;107:142–64.

269. Chung Y, Chang SH, Martinez GJ, Yang XO, Nurieva R, Kang HS, et al. Critical Regulation of Early Th17 Cell Differentiation by Interleukin-1 Signaling. Immunity. 2009 Apr 17;30(4):576–87.

270. Mills KHG, Dungan LS, Jones SA, Harris J. The role of inflammasome-derived IL-1 in driving IL-17 responses. J Leukoc Biol. 2013 Apr 1;93(4):489–97.

271. Meng G, Zhang F, Fuss I, Kitani A, Strober W. A mutation in the Nlrp3 gene causing inflammasome hyperactivation potentiates Th17 cell-dominant immune responses. Immunity. 2009 Jun 19;30(6):860–74.

272. Sommer A, Marxreiter F, Krach F, Fadler T, Grosch J, Maroni M, et al. Th17 Lymphocytes Induce Neuronal Cell Death in a Human iPSC-Based Model of Parkinson's Disease. Cell Stem Cell. 2018 Jul 5;23(1):123-131.e6.

273. Shi Y, Wei B, Li L, Wang B, Sun M. Th17 cells and inflammation in neurological disorders: Possible mechanisms of action. Front Immunol. 2022;13:932152.

274. Munder M, Mallo M, Eichmann K, Modolell M. Murine Macrophages Secrete Interferon γ upon Combined Stimulation with Interleukin (IL)-12 and IL-18: A Novel Pathway of Autocrine Macrophage Activation. J Exp Med. 1998 Jun 15;187(12):2103–8.

275. Volin MV, Koch AE. Interleukin-18: a mediator of inflammation and angiogenesis in rheumatoid arthritis. J Interferon Cytokine Res Off J Int Soc Interferon Cytokine Res. 2011 Oct;31(10):745–51.

276. Nakanishi K, Yoshimoto T, Tsutsui H, Okamura H. Interleukin-18 regulates both Th1 and Th2 responses. Annu Rev Immunol. 2001;19:423–74.

277. Nakanishi K. Unique Action of Interleukin-18 on T Cells and Other Immune Cells. Front Immunol. 2018 Apr 20;9:763.

278. Mohamed Asik R, Suganthy N, Aarifa MA, Kumar A, Szigeti K, Mathe D, et al. Alzheimer's Disease: A Molecular View of β-Amyloid Induced Morbific Events. Biomedicines. 2021 Sep 1;9(9):1126.

279. Olanow CW, Savolainen M, Chu Y, Halliday GM, Kordower JH. Temporal evolution of microglia and α-synuclein accumulation following foetal grafting in Parkinson's disease. Brain J Neurol. 2019 Jun 1;142(6):1690–700.

280. Mogi M, Harada M, Narabayashi H, Inagaki H, Minami M, Nagatsu T. Interleukin (IL)-1 beta, IL-2, IL-4, IL-6 and transforming growth factor-alpha levels are elevated in ventricular cerebrospinal fluid in juvenile parkinsonism and Parkinson's disease. Neurosci Lett. 1996 Jun 14;211(1):13–6.

281. Chen X, Hu Y, Cao Z, Liu Q, Cheng Y. Cerebrospinal Fluid Inflammatory Cytokine Aberrations in Alzheimer's Disease, Parkinson's Disease and Amyotrophic Lateral Sclerosis: A Systematic Review and Meta-Analysis. Front Immunol [Internet]. 2018 Sep 19 [cited 2024 Jul 18];9. Available from: https://www.frontiersin.org/journals/immunology/articles/10.3389/fimmu.2018.02122/full

282. Zhang P, Shao XY, Qi GJ, Chen Q, Bu LL, Chen LJ, et al. Cdk5-Dependent Activation of Neuronal Inflammasomes in Parkinson's Disease. Mov Disord Off J Mov Disord Soc. 2016 Mar;31(3):366–76.

283. Rothwell N. Interleukin-1 and neuronal injury: mechanisms, modification, and therapeutic potential. Brain Behav Immun. 2003 Jun;17(3):152–7.

284. McColl BW, Rothwell NJ, Allan SM. Systemic inflammatory stimulus potentiates the acute phase and CXC chemokine responses to experimental stroke and exacerbates brain damage via interleukin-1- and neutrophil-dependent mechanisms. J Neurosci Off J Soc Neurosci. 2007 Apr 18;27(16):4403–12.

285. Tehranian R, Andell-Jonsson S, Beni SM, Yatsiv I, Shohami E, Bartfai T, et al. Improved recovery and delayed cytokine induction after closed head injury in mice with central overexpression of the secreted isoform of the interleukin-1 receptor antagonist. J Neurotrauma. 2002 Aug;19(8):939–51.

286. Dinarello CA, Simon A, van der Meer JWM. Treating inflammation by blocking interleukin-1 in a broad spectrum of diseases. Nat Rev Drug Discov. 2012 Aug;11(8):633–52.

287. Bianchi ME. DAMPs, PAMPs and alarmins: all we need to know about danger. J Leukoc Biol. 2007 Jan;81(1):1–5.

288. Dinarello CA. Introduction to the interleukin-1 family of cytokines and receptors: Drivers of innate inflammation and acquired immunity. Immunol Rev. 2018 Jan;281(1):5–7.

289. Cicchese JM, Evans S, Hult C, Joslyn LR, Wessler T, Millar JA, et al. Dynamic balance of pro- and anti-inflammatory signals controls disease and limits pathology. Immunol Rev. 2018 Sep;285(1):147.

290. Cai M, Zhuang W, Lv E, Liu Z, Wang Y, Zhang W, et al. Kaemperfol alleviates pyroptosis and microglia-mediated neuroinflammation in Parkinson's disease via inhibiting p38MAPK/NF-κB signaling pathway. Neurochem Int. 2022 Jan;152:105221.

291. Zhang X, Zhang Y, Li R, Zhu L, Fu B, Yan T. Salidroside ameliorates Parkinson's disease by inhibiting NLRP3-dependent pyroptosis. Aging. 2020 May 19;12(10):9405–26.

292. Rui W, Li S, Xiao H, Xiao M, Shi J. Baicalein Attenuates Neuroinflammation by Inhibiting NLRP3/caspase-1/GSDMD Pathway in MPTP Induced Mice Model of Parkinson's Disease. Int J Neuropsychopharmacol. 2020 Aug 6;23(11):762–73.

293. Ma X, Hao J, Wu J, Li Y, Cai X, Zheng Y. Prussian Blue Nanozyme as a Pyroptosis Inhibitor Alleviates Neurodegeneration. Adv Mater. 2022;34(15):2106723.

294. Zhang X, Zhang Y, Wang B, Xie C, Wang J, Fang R, et al. Pyroptosis-mediator GSDMD promotes Parkinson's disease pathology via microglial activation and dopaminergic neuronal death. Brain Behav Immun. 2024 Jul 1;119:129–45.

295. Jakobs C, Bartok E, Kubarenko A, Bauernfeind F, Hornung V. Immunoblotting for active caspase-1. Methods Mol Biol Clifton NJ. 2013;1040:103–15.

296. Shi C, Cao P, Wang Y, Zhang Q, Zhang D, Wang Y, et al. PANoptosis: A Cell Death Characterized by Pyroptosis, Apoptosis, and Necroptosis. J Inflamm Res. 2023 Apr 12;16:1523–32.

297. Rajesh Y, Kanneganti TD. Innate Immune Cell Death in Neuroinflammation and Alzheimer's Disease. Cells. 2022 Jun 10;11(12):1885.

298. Conos SA, Lawlor KE, Vaux DL, Vince JE, Lindqvist LM. Cell death is not essential for caspase-1-mediated interleukin-1β activation and secretion. Cell Death Differ. 2016 Nov;23(11):1827–38.

299. Evavold CL, Ruan J, Tan Y, Xia S, Wu H, Kagan JC. The Pore-Forming Protein Gasdermin D Regulates Interleukin-1 Secretion from Living Macrophages. Immunity. 2018 Jan 16;48(1):35-44.e6.

300. Heilig R, Dick MS, Sborgi L, Meunier E, Hiller S, Broz P. The Gasdermin-D pore acts as a conduit for IL-1β secretion in mice. Eur J Immunol. 2018 Apr;48(4):584–92.

301. Lieberman J, Wu H, Kagan JC. Gasdermin D activity in inflammation and host defense. Sci Immunol. 2019 Sep 6;4(39):eaav1447.

302. Taabazuing CY, Okondo MC, Bachovchin DA. Pyroptosis and Apoptosis Pathways Engage in Bidirectional Crosstalk in Monocytes and Macrophages. Cell Chem Biol. 2017 Apr 20;24(4):507-514.e4.

303. Tsuchiya K, Nakajima S, Hosojima S, Thi Nguyen D, Hattori T, Manh Le T, et al. Caspase-1 initiates apoptosis in the absence of gasdermin D. Nat Commun. 2019 May 7;10(1):2091.

304. Rogers C, Fernandes-Alnemri T, Mayes L, Alnemri D, Cingolani G, Alnemri ES. Cleavage of DFNA5 by caspase-3 during apoptosis mediates progression to secondary necrotic/pyroptotic cell death. Nat Commun. 2017 Jan 3;8(1):14128.

305. Wolf AJ, Reyes CN, Liang W, Becker C, Shimada K, Wheeler ML, et al. Hexokinase Is an Innate Immune Receptor for the Detection of Bacterial Peptidoglycan. Cell. 2016 Jul 28;166(3):624–36.

306. Munawara U, Catanzaro M, Xu W, Tan C, Hirokawa K, Bosco N, et al. Hyperactivation of monocytes and macrophages in MCI patients contributes to the progression of Alzheimer's disease. Immun Ageing A. 2021 Jun 21;18(1):29.

307. Zanoni I, Tan Y, Di Gioia M, Broggi A, Ruan J, Shi J, et al. An endogenous caspase-11 ligand elicits interleukin-1 release from living dendritic cells. Science. 2016 Jun 3;352(6290):1232–6.

308. Dyck CH van, Swanson CJ, Aisen P, Bateman RJ, Chen C, Gee M, et al. Lecanemab in Early Alzheimer's Disease. N Engl J Med. 2023 Jan 4;388(1):9–21.

309. Lashuel HA. Rethinking protein aggregation and drug discovery in neurodegenerative diseases: Why we need to embrace complexity? Curr Opin Chem Biol. 2021 Oct 1;64:67–75.

310. Chen GY, Nuñez G. Sterile inflammation: sensing and reacting to damage. Nat Rev Immunol. 2010 Dec;10(12):826–37.

311. Otani K, Shichita T. Cerebral sterile inflammation in neurodegenerative diseases. Inflamm Regen. 2020 Dec 8;40(1):28.

312. Zahid A, Li B, Kombe AJK, Jin T, Tao J. Pharmacological Inhibitors of the NLRP3 Inflammasome. Front Immunol [Internet]. 2019 Oct 25 [cited 2024 Jul 22];10. Available from: https://www.frontiersin.org/journals/immunology/articles/10.3389/fimmu.2019.02538/full

313. Zhang X, Wang Z, Zheng Y, Yu Q, Zeng M, Bai L, et al. Inhibitors of the NLRP3 inflammasome pathway as promising therapeutic candidates for inflammatory diseases (Review). Int J Mol Med. 2023 Mar 21;51(4):35.

314. Soriano-Teruel PM, García-Laínez G, Marco-Salvador M, Pardo J, Arias M, DeFord C, et al. Identification of an ASC oligomerization inhibitor for the treatment of inflammatory diseases. Cell Death Dis. 2021 Dec 13;12(12):1–11.

315. Chen C, Zhou Y, Ning X, Li S, Xue D, Wei C, et al. Directly targeting ASC by lonidamine alleviates inflammasome-driven diseases. J Neuroinflammation. 2022 Dec 28;19:315.

316. Geng XL, Jiang YS, Zhao CN, Zhang ZZ, Liu YL, Ding PJ. Serum PYCARD may become a new diagnostic marker for rheumatoid arthritis patients. Eur J Med Res. 2024 Apr 4;29(1):218.

317. Quick JD, Silva C, Wong JH, Lim KL, Reynolds R, Barron AM, et al. Lysosomal acidification dysfunction in microglia: an emerging pathogenic mechanism of neuroinflammation and neurodegeneration. J Neuroinflammation. 2023 Aug 5;20(1):185.

318. Jiang P, Gan M, Yen SH, McLean PJ, Dickson DW. Impaired endo-lysosomal membrane integrity accelerates the seeding progression of α-synuclein aggregates. Sci Rep. 2017 Aug 9;7:7690.

319. Freeman D, Cedillos R, Choyke S, Lukic Z, McGuire K, Marvin S, et al. Alpha-Synuclein Induces Lysosomal Rupture and Cathepsin Dependent Reactive Oxygen Species Following Endocytosis. PLoS ONE. 2013 Apr 25;8(4):e62143.

320. Chen KW, Groß CJ, Sotomayor FV, Stacey KJ, Tschopp J, Sweet MJ, et al. The neutrophil NLRC4 inflammasome selectively promotes IL-1β maturation without pyroptosis during acute Salmonella challenge. Cell Rep. 2014 Jul 24;8(2):570–82.

321. Yu TG, Cha JS, Kim G, Sohn YK, Yoo Y, Kim U, et al. Oligomeric states of ASC specks regulate inflammatory responses by inflammasome in the extracellular space. Cell Death Discov. 2023 Apr 29;9(1):1–11.

322. Anderson FL, von Herrmann KM, Andrew AS, Kuras YI, Young AL, Scherzer CR, et al. Plasma-borne indicators of inflammasome activity in Parkinson's disease patients. NPJ Park Dis. 2021 Jan 4;7(1):2.

323. Prather ER, Gavrilin MA, Wewers MD. The central inflammasome adaptor protein ASC activates the inflammasome after transition from a soluble to an insoluble state. J Biol Chem [Internet]. 2022 Jun 1 [cited 2024 Jul 15];298(6). Available from: https://www.jbc.org/article/S0021-9258(22)00464-1/abstract

324. Mestas J, Hughes CCW. Of Mice and Not Men: Differences between Mouse and Human Immunology. J Immunol. 2004 Mar 1;172(5):2731–8.

325. Råberg L, Sim D, Read AF. Disentangling genetic variation for resistance and tolerance to infectious diseases in animals. Science. 2007 Nov 2;318(5851):812–4.

326. Schneider DS, Ayres JS. Two ways to survive infection: what resistance and tolerance can teach us about treating infectious diseases. Nat Rev Immunol. 2008 Nov;8(11):889–95.

327. Warren HS, Fitting C, Hoff E, Adib-Conquy M, Beasley-Topliffe L, Tesini B, et al. Resilience to bacterial infection: difference between species could be due to proteins in serum. J Infect Dis. 2010 Jan 15;201(2):223–32.

328. Mizrachi M, Diamond B. Impact of microglia isolation and culture methodology on transcriptional profile and function. J Neuroinflammation. 2024 Apr 8;21(1):87.

329. Yaqubi M, Groh AMR, Dorion MF, Afanasiev E, Luo JXX, Hashemi H, et al. Analysis of the microglia transcriptome across the human lifespan using single cell RNA sequencing. J Neuroinflammation. 2023 May 30;20:132.

330. Abud EM, Ramirez RN, Martinez ES, Healy LM, Nguyen CHH, Newman SA, et al. iPSC-Derived Human Microglia-like Cells to Study Neurological Diseases. Neuron. 2017 Apr 19;94(2):278-293.e9.

331. Muffat J, Li Y, Yuan B, Mitalipova M, Omer A, Corcoran S, et al. Efficient derivation of microglia-like cells from human pluripotent stem cells. Nat Med. 2016 Nov;22(11):1358–67.

332. Teo F, Kok CYL, Tan MJ, Je HS. Human pluripotent stem cell (hPSC)-derived microglia for the study of brain disorders. A comprehensive review of existing protocols. IBRO Neurosci Rep. 2024 Jun;16:497–508.

333. Ingber DE. Human organs-on-chips for disease modelling, drug development and personalized medicine. Nat Rev Genet. 2022 Aug;23(8):467–91.

334. Parkinson Canada [Internet]. [cited 2024 May 20]. Parkinson's Disease. Available from: https://www.parkinson.ca/about-parkinsons/

335. Kouli A, Torsney KM, Kuan WL. Parkinson's Disease: Etiology, Neuropathology, and Pathogenesis. In: Stoker TB, Greenland JC, editors. Parkinson's Disease: Pathogenesis and Clinical Aspects [Internet]. Brisbane (AU): Codon Publications; 2018 [cited 2024 Jul 30]. Available from: http://www.ncbi.nlm.nih.gov/books/NBK536722/

8. APPENDIX

Figure S1. Localization of cell-derived ASC specks in ASC-αSyn complex-treated cells.

3D projection movies and representative 63x magnification images of microglia treated with ASC-αSyn complexes revealing intracellular and extracellular ASC specks localization with respect to F-actin. *Arrowheads show ASC specks, which are ~1 µm in size. Yellow arrowhead points to the ASC speck shown in Figure 11, highlighting its intracellular localization. Scale bars, 20 and 50 µm.

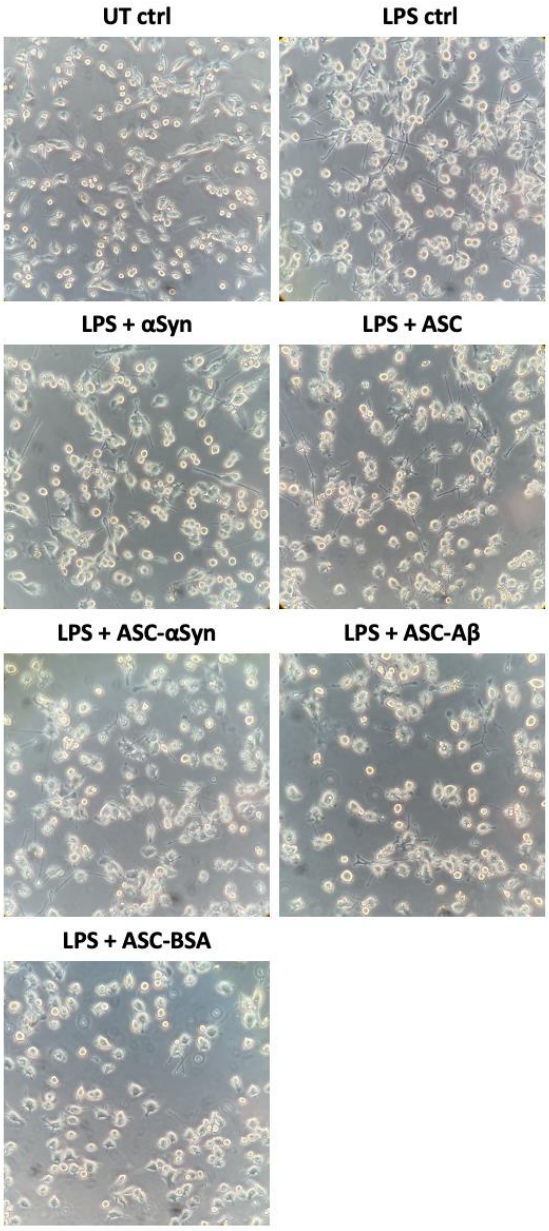

Figure S2. Microglia display morphological changes upon various inflammasome inducers.

Phase contrast micrographs of mouse SIM-A9 microglia after 3 h exposure of 100 ng/ml LPS followed by 24 h exposure of ASC, αSyn, or ASC-αSyn complexes. UT cells display small cell bodies with some cells with branched processes. Treatment with LPS transforms microglia to appear ramified with long branched processes, potentially to scan the microenvironment for extracellular dangers. Addition of a second inducer after LPS treatment, such as ASC and/or αSyn, activates microglia into more of an “amoeboid” phenotype, where such cells are spherical in shape, have larger cell bodies and lack abundant processes. Images were taken at 20x magnification using the Leica DMIL microscope.

Table 2. List of primary antibodies used in this study.

Antibody	Reference	Host/Clonality	Application/Dilution
NLRP3 [Cryo-2]	AdipoGen AG-20B-0014-C100	Mouse monoclonal	ICC: 1:100 IB: 1:1,000 Simple Western: 1:100
ASC [AL177]	AdipoGen AG-25B-0006-C100	Rabbit polyclonal	ICC: 1:100 IB: 1:1,000
Caspase-1 [Casper-1]	Adipogen AG-20B-0042	Mouse monoclonal	IB: 1:1,000 Simple Western: 1:100
GSDMD [EPR19828]	Abcam ab209845	Rabbit monoclonal	IB: 1:1,000 Simple Western: 1:100
Iba-1	Fujifilm Wako 019-19741	Rabbit polyclonal	ICC: 1:500
CD68 [RM1031]	Abcam ab303565	Rabbit polyclonal	ICC: 1:100
MAP2 [HM-2]	Sigma-Aldrich M4403	Mouse monoclonal	ICC: 1:250
GFAP	Dako Z0334	Rabbit polyclonal	ICC: 1:250
αSyn [LB 509]	Abcam ab27766	Mouse monoclonal	IB: 1:1,000
actin-HRP [AC-15]	Sigma A3854	Mouse monoclonal	Simple Western: 1:500

Table 3. List of secondary antibodies used in this study.

Antibody	Reference	Form	Application/Dilution
Goat anti-mouse	Invitrogen A-11029	Alexa Fluor™ 488-conjugated	ICC: 1:500
Goat anti-rabbit	Invitrogen A-11008	Alexa Fluor™ 488-conjugated	ICC: 1:500
Goat anti-rabbit	Sigma A0545	HRP-conjugated	IB: 1:10,000
Rabbit anti-mouse	Sigma A9044	HRP-conjugated	IB: 1:7,500